University of Nevada, Reno

A Model Evaluation of a Non-potable Reuse Facility and a Potable Reuse Design

A thesis submitted in partial fulfillment of the requirements for the degree of Master of Science in Civil and Environmental Engineering

by

Carson Nikkel

Dr. Eric A. Marchand/Thesis Advisor

December 2013

University of Nevada, Reno
Statewide • Worldwide

THE GRADUATE SCHOOL

We recommend that the thesis
prepared under our supervision by

CARSON T. NIKKEL

entitled

A Model Evaluation Of A Non-potable Reuse Facility And A Potable Reuse Design

be accepted in partial fulfillment of the
requirements for the degree of

MASTER OF SCIENCE

Eric A. Marchand, Advisor

Keith E. Dennett, Committee Member

Jeffrey Lacombe, Graduate School Representative

Marsha H. Read, Ph. D., Dean, Graduate School

December, 2013

Abstract

Since the widespread construction of wastewater facilities in the United States beginning in the 1970s, treatment technology has advanced slowly. Small changes have been adapted throughout the years; however, the layout of a typical wastewater treatment facility has remained the same. The common design is becoming dated, though. Concerns about diminishing supplies of freshwater have generated support for the adaptation of both potable and non-potable water reuse facilities. This study sought to further understand both types of water reuse.

The first phase of the study examined the non-potable reuse systems at South Truckee Meadows Water Reclamation Facility (STMWRF) in Reno, NV. Due to elevated nutrient concentrations in the effluent from the facility, the storage of non-potable reuse water in nearby Huffaker Hills Reservoir was leading to seasonal algal populations. These algal populations were responsible for problems with the non-potable reuse water. As part of the study, effluent from the facility was collected, analyzed, and used to create a computer simulation of the facility's unit processes. From this simulation, new aeration cycles were developed for the oxidation ditches at STMWRF to decrease nutrient concentrations and reduce future algal populations in the reservoir.

The second phase of the project proposed an innovative potable reuse system that could replace the current systems in use at STMWRF or other similar water reuse facilities. The proposed low-energy, high-effluent quality reuse system combined recent technologies in the wastewater field, including forward osmosis, membrane distillation,

anaerobic membrane bioreactors, SHARON and ANAMMOX, and struvite precipitation. These unit processes form a mutualistic relationship that reduces the normally high cost of potable reuse through various resource recovery systems. The proposed potable reuse system was modeled using computer simulations, and then compared to the current treatment capabilities and operating conditions at STMWRF. The simulations demonstrated that the proposed potable reuse system operated on a similar monthly budget, with the majority of influent wastewater being discharged as a high-quality potable effluent. A smaller portion of the influent was then discharged as a non-potable effluent. The quality of the non-potable effluent was determined to be similar to STMWRF's current non-potable effluent. Overall, the proposed system demonstrated the plausibility of using potable reuse systems in the near future.

Acknowledgements

This thesis and the research that it is based on was made possible by the help and support of many people. I would first like to thank my family (Keith, Dianne, Ashley and Scott) for helping me along the way. I would like to thank Dr. Eric Marchand for his continued assistance and support throughout the entire project. I would like to thank my research assistant, Ashley Kaiser, for many hours of her life spent sampling and testing. Additionally, I would like to thank Viktoriya Weirauch, Peter Benchetler, and Emily Cole for their assistance in the lab. I would also like to acknowledge the help from Washoe County, including Shawnee Dunagan, John Hulett, Rick Warner, John Buzzone, and the plant operators at South Truckee Meadows Water Reclamation Facility. Lastly, I would like to thank Dr. Keith Dennett and Dr. Jeff LaCombe for their service on my committee, as well as Dr. Amy Childress and Dr. Andrea Achilli for their guidance on the second phase of the project.

Table of Contents

List of Figures

List of Tables

Chapter 1 Introduction

Wastewater treatment in the United States has remained relatively unchanged for the past 40 years. Common practice for wastewater facilities is to treat influent wastewater to specified regulatory standards, and then discharge the effluent into a natural system (river, lake, or aquifer). Recently, reuse facilities have become popular as they allow treated wastewater to be used for practical purposes. Reuse may be divided among two categories: non-potable and potable. Non-potable reuse diverts some (or all) treated wastewater from the facility to applications that do not require potable water, such as irrigation. The main advantage of non-potable reuse is that the water demands on upstream water treatment facilities are typically reduced. In addition, treated wastewater often contains elevated concentrations of both nitrogen and phosphorus, which are valuable nutrients in agriculture applications. The second type of reuse, potable, requires that wastewater be treated sufficiently so that it is safe for human consumption. Potable reuse, though, faces two strong criticisms. First, potable reuse is more expensive due to increased treatment requirements. Secondly, the public generally perceives reuse water as unacceptable for direct consumption. Despite these negatives, potable reuse offers a future to communities around the world that are facing water scarcity.

Locally, the South Truckee Meadows Water Reclamation Facility (STMWRF) practices non-potable water reuse, storing treated wastewater in the Huffaker Hills Reservoir. During summer (when the water demand is high), the reservoir is used to

supply non-potable water for irrigation and water amenities. Recently, the effluent from the facility has exhibited variances in water quality, leading to increased nutrient concentrations in the reuse water. When the reuse water is stored in the reservoir, sunlight combines with excess nitrogen and phosphorus to promote large algal blooms. These algae are responsible for problems in the reuse distribution system, such as clogged valves and irrigation equipment.

In order to address the water quality issues associated with non-potable reuse systems at STMWRF, this study employed computer modeling to evaluate the performance of the facility. Through the development of a model, operating conditions at the facility could be altered in an effort to reduce effluent nutrient concentrations in the reuse water, and therefore potentially limit algal growth in the reservoir.

In addition to examining the current status of non-potable reuse at STMWRF, the study also considered potable water reuse, and what systems would be required to change the reuse systems at STMWRF (or other similar facilities) from non-potable to potable. The focus of the second part of the study was to address the main concerns about potable reuse by reducing the cost of potable treatment while maintaining a high quality effluent. Funding was obtained from the WateReuse Foundation to investigate a potable reuse design proposed by the research team. The proposed system combined recent treatment technologies, including forward osmosis, membrane distillation, an anaerobic membrane bioreactor, SHARON/ANAMMOX, and struvite precipitation in a mutualistic relationship. In this proposed design, water initially enters the system through forward osmosis (Figure 1-1).

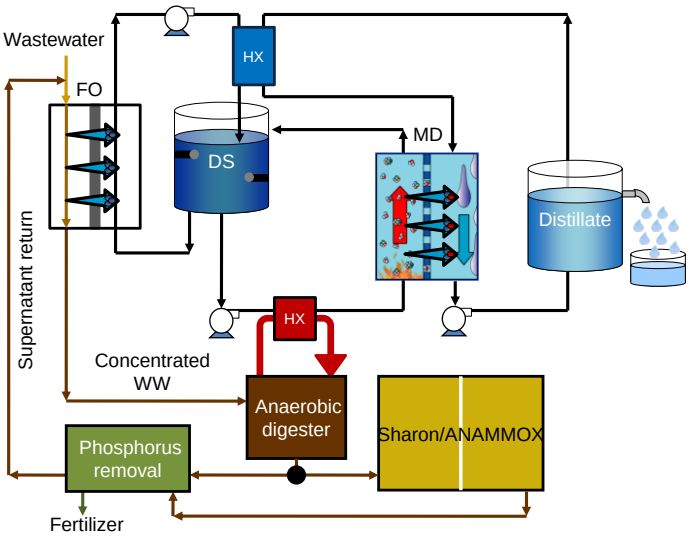

Figure 1-1: Proposed design for potable water reuse facility

Forward osmosis (FO) serves as a preconcentration step, as clean water in the influent wastewater diffuses across the forward osmosis membrane into the draw solution. The draw solution contains an inorganic solute that is used to maintain osmotic pressure, fueling the process. The draw solution then flows through membrane distillation (MD), a thermally-driven separation step that extracts clean water from the solute. This also serves to maintain the concentration of the solute in the draw solution. Water that did not diffuse across the forward osmosis membrane flows into an anaerobic membrane bioreactor (AnMBR). The AnMBR serves to remove organics and inorganics (excluding nitrogen and phosphorus) from the system. The AnMBR also produces methane biogas, which may be used to fuel the thermally-driven MD process. After passing through the AnMBR, water flows into SHARON and ANAMMOX reactors, which are responsible for removing nitrogen from the system. Finally, struvite

precipitation is used to remove phosphorus. Struvite is a common fertilizer, that could potentially be sold to offset facility operating costs. Remaining water is recycled into the influent, and the process continues. The large majority of influent water is discharged from the system through MD as clean, potable water. A small portion of water is discharged from the system after struvite precipitation as a non-potable effluent.

The proposed potable reuse system was modeled using the same methods as in the first part of the study. The model allowed comparisons of both treatment cost and effluent quality between the current non-potable reuse systems and the designed potable reuse system.

Chapter 2 Literature Review

2.1 What is an Oxidation Ditch?

An oxidation ditch is a cyclical treatment reactor that facilitates multiple treatment methods at once. Whereas larger wastewater treatment plants typically operate multiple individual treatment processes (aeration basins, nitrification, denitrification, and phosphorus removal), an oxidation ditch allows these different processes to be combined in a single system. This is advantageous for smaller treatment facilities as the system is much less complex than larger facilities, reducing operation and maintenance costs [1]. Additionally, the oxidation ditch design provides further advantages. Aeration naturally provides mixing to the system. Influent wastewater is diluted by a factor of up to 30 times, as the flow in the ditch is far greater than the influent flow. This gives the system resistance to shock loading (spikes in influent concentrations) [2]. STMWRF uses two 1.59 million gallon (MG) oxidation ditches to handle influent flows ranging from 3 to 4 million gallons per day (Table 2-1).

Table 2-1: Characteristics of oxidation ditches at STMWRF[a]

Volume (each, MG)	Depth (ft)	Aeration	# of Aeration Grids per Ditch	Mixer Type	# of Mixers per Ditch
1.6	14	Fine-bubble membrane panels	7	Submerged Propellers	3

[a] Data for STMWRF provided by Washoe County [3].

Conceptually, the basis for the treatment capabilities of an oxidation ditch are rooted in its maintenance of two distinct treatment zones: an aerobic zone and an anoxic zone. The aerobic zone maintains elevated concentrations of dissolved oxygen (DO), such that oxygen can act as the electron acceptor in the degradation reactions of influent organic compounds and ammonium (electron donors). The elimination of organic compounds occurs through three main processes: 1) the transformation of these organic species into carbon dioxide, 2) the synthesis of organics into new cells, and 3) the degradation of cells into carbon dioxide. These reactions are performed by aerobic heterotrophic bacteria, governed by the following stoichiometry [2]:

$$C_XO_YH_ZN_AS_B \text{ (Organics)} + O_2 + \text{nutrients} \rightarrow CO_2 + NH_3 + C_5H_7NO_2 \text{ (New Cells)}$$

$$C_5H_7NO_2 + 5\ O_2 \rightarrow 5\ CO_2 + 2\ H_2O + NH_3 + \text{energy}$$

The second reaction in the aerobic zone reaction, nitrification by aerobic autotrophic bacteria, is similarly a two-step reaction. The first step is the oxidation of ammonium (NH_4^+) to nitrite (NO_2^-) by nitroso-bacteria:

$$2\ NH_4^+ + 3\ O_2 \rightarrow 2\ NO_2^- + 4\ H^+ + 2\ H_2O$$

The second step transforms the newly formed nitrite into nitrate (NO_3^-) through further oxidation by nitro-bacteria:

$$2\ NO_2^- + O_2 \rightarrow 2\ NO_3^-$$

DO for the aerobic zone is generally provided by air diffusers located at the bottom of the oxidation ditch. As water leaves the aerobic zone and oxygen is no longer being supplied, DO concentrations quickly decrease. This marks the beginning of the anoxic zone. In the anoxic zone, nitrate becomes the dominant electron acceptor,

allowing denitrification to occur. The process of denitrification involves five transformation steps, in which nitrate is reduced to nitrite, then nitric oxide (NO), nitrous oxide (N_2O), and finally nitrogen gas (N_2). As the final product is a gas, the nitrogen volatilizes from the water into the atmosphere, thus removing nitrogen from the water. Denitrification is facilitated by heterotrophic bacteria. The stoichiometric reaction for the process is [2]:

$$C_{10}H_{19}O_3N + 10\ NO_3^- \rightarrow 5\ N_2 + 10\ CO_2 + 3\ H_2O + NH_3 + 10\ OH^-$$

The last contaminant of concern in the treatment process is phosphorus. Phosphorus is removed from the system through uptake into biomass. As water is discharged from the oxidation ditch, it enters a clarifier, in which the mixed liquor suspended solids (MLSS) are settled out. The settled solids take two different paths after the clarifier. A large majority of the solids are returned to the oxidation ditch as return activated sludge (RAS) in order to continue treatment. A small amount of the solids are removed from the process as waste activated sludge (WAS). The wasted sludge serves as the mechanism for phosphorus removal from the system, with phosphorus being responsible for nearly 3% of the dry weight of cells in the WAS [4]. This process can be enhanced by the inclusion of an anaerobic zone during treatment. In the process termed enhanced biological phosphorus removal (EBPR), phosphorus-accumulating organisms are conditioned to uptake additional phosphorus by cycling them between an aerobic/anoxic zone and an anaerobic zone. In the aerobic/anoxic zone, conditioned bacteria uptake additional phosphorus in preparation for the upcoming anaerobic zone. Once in the anaerobic zone, these bacteria use the stored

phosphorus for energy, thereby releasing orthophosphate (PO_4^{3-}). In a properly designed and operated system, the continued growth of bacteria serves to uptake more phosphorus in the aerobic zone than was released in the anaerobic zone. As STMWRF has no designed anaerobic zones, it was initially assumed that EBPR does not occur. However, as the current aeration cycles include hours without aeration, it is highly likely that anaerobic zones develop within the system. As water is discharged from these anaerobic zones, bacteria would release phosphorus for energy in this zone, possibly explaining elevated concentrations of phosphorus in the effluent [2].

The physical layout of STMWRF consists of two oxidation ditches designed as mirror images of each other (Figure 2-1). Influent wastewater and RAS are pumped into the ditches right before submerged banana blade propellers, which mix the incoming flow with the existing flow in the ditch. Water in the northern ditch flows counterclockwise, and water in the southern ditch flows clockwise. Shortly after mixing, water enters the aerobic zone. Blowers are responsible for maintaining concentrations of dissolved oxygen. After the aerobic zone, water flows into the anoxic zones. The anoxic zones are much larger than the aerobic zones. Approximately 1/3rd of the way through the anoxic zone, water is removed from the system through the effluent. Effluent water flows to the MLSS splitter, which sends flow either to the secondary clarifiers, or to the RAS/WAS pumping structure. Water remaining in the ditch passes the mixers again, where influent flow is introduced. The process repeats continually.

Figure 2-1: Location of aerobic/anoxic zones at STWMRF (Google, 2013)

2.2 Nutrient Availability and the Growth of Algae

Algae are photosynthetic autotrophic eukaryotes present in most water systems. There are different types of algae, varying from unicellular to multicellular [2]. The chemical formula describing the biomass of algae varies depending on their type. However, the average stoichiometric formula for algae is $C_{124}N_{16}S_{1.3}P$ [5]. As algae are

autotrophs, they are able to fix carbon from inorganic sources, such bicarbonate (HCO_3^-) or carbon dioxide (CO_2). Therefore, carbon is rarely a limiting nutrient in their production. The stoichiometric ratio of nitrogen to phosphorus in algal biomass generally varies between 7:1 and 25:1; thus, the demand for nitrogen in their synthesis greatly outweighs the demand for phosphorus [6].

The available chemical forms of nitrogen and phosphorus can influence both the growth and sustenance of algal populations. Algae with sufficient access to ammonium (NH_4^+) were shown to have 30% increased growth rates over populations with access to other forms of nitrogen, as well as having higher photosynthetic capacity and increased biomass [7]. In addition, algal populations were responsible for near 100% removal of available ammonium in pond testing [8]. In terms of phosphorus uptake, orthophosphate was shown to be the preferable form for algae, with a near 90% removal rate in the same pond testing [8]. Therefore, reducing effluent discharges of ammonium and orthophosphate into receiving waters can hinder the growth of algal populations.

2.3 Forward Osmosis

Osmosis is the transfer of water across a semi-permeable membrane. The driving force behind osmosis is the difference in osmotic pressure between the solutions on either side of the membrane. High osmotic pressure is generated by a high solute concentration, with the required solute being an ion (usually with low-molecular weight). During osmosis, water naturally diffuses across the membrane towards the side with the higher osmotic pressure (known as the draw solution). Since the

membrane is semi-permeable, it is capable of rejecting nearly all ion transfer across the membrane, preventing the majority of the draw solute from diffusing across the membrane. Therefore, the process can continue as long as the osmotic pressure differences remain [18].

Forward osmosis can be applied to wastewater applications as a preconcentration step to further treatment. Influent wastewater (the feed) is passed over the dense side of the membrane, inducing flow across the membrane to the draw solution (which has a higher osmotic pressure than the influent wastewater). As the membrane is only semi-permeable, the rejection rate of contaminants in the wastewater is extremely high, allowing only clean water to pass through the membrane. The result of this water flux across the membrane is a more concentrated wastewater (as the volume of water has been reduced, but the mass of contaminants remains the same), and the creation of a more dilute draw solution (as the volume of water has increased, but the mass of draw solute remains the same). In order prevent dilution of the draw solute, which would then reduce the osmotic pressure in the draw solution, the water added must be removed by another mechanism [9]. In the proposed design, membrane distillation is used to maintain the draw solute concentration, in addition to producing potable water.

The literature review of forward osmosis focused on eight parameters: membrane material, characteristics of the feed solution, temperature, characteristics of the draw solution, ionic strength of the draw solution, reverse solute flux, steady-state flux, and water recovery (Table 2-2). The review yielded a large amount of information;

however, particular attention was paid to applications involving wastewater as a feed solution. Many studies selected distilled water as a feed solution (which can help characterize flux and reverse solute flux of a chosen membrane), yet does not aid in modeling efforts for the proposed design in the second phase of this project [14,18,20,21,24]. Among the studies that used wastewater-related feed solutions (primary or secondary effluent, activated sludge, digester centrate, synthetic wastewater), the membrane that was consistently used was the Hydration Technology® cellulose triacetate cartridge membrane [13,17,26-31]. Most of the selected studies used sodium chloride (NaCl) as the draw solute [10,11,13,14,16,17,19-24,26-31]. This choice was due to the fact that NaCl results in a high flux across the membrane. On the other hand, NaCl also has a high reverse solute flux across the membrane [10,11,20,21,23,26,27,31]. Reverse solute flux represents the flow of draw solute across the membrane from the draw solution to the influent stream. This presents a significant issue in the design, as the system is conceptually based using a recycling approach. Solutes that travel across the membrane would end up effluent, which would then return to the influent through the recycle flow. The increased solute concentration on the feed side of the membrane would reduce the osmotic pressure across the membrane, leading to lower flux and water recovery. Additionally, high salt content could irreversibly damage microbial colonies in the anaerobic bioreactor, the SHARON process, and in the ANAMMOX reactor.

In order to mitigate this issue, the proposed system would require a solute with low reverse salt flux. The literature review discovered several different studies that

used magnesium chloride ($MgCl_2$) as the draw solute [18,21,25]. This solute was shown to have slightly lower fluxes across the membrane, coupled with much lower reverse solute fluxes. Furthermore, magnesium is required for struvite precipitation, and would therefore be consumed naturally by the proposed system (also reducing chemical input costs later in the treatment process). However, chloride would still accumulate in the system, and could lead to overall performance problems. This issue required that a non-potable effluent stream (a waste stream) be included in the system. The literature review suggested an ionic strength for magnesium chloride within the range of 2.0 to 5.0 M.

The two remaining parameters were temperature and percent water recovery. Suitable temperatures reported in the literature varied between 20° and 25°C, which were (in most cases), the ambient temperatures in the labs where the studies were conducted [10-18,20-24,25-31]. Water recovery represents one of the most important values, as it dictates all flow balances for the system. This value represents a volumetric ratio of the amount of water recovered through the membrane relative to the total influent wastewater. There were not many studies with information concerning water recovery; however, several investigations reported values ranging between 50-70% [19,28,30]. Therefore, the model was evaluated within this range to determine the effectiveness of the forward osmosis process.

Table 2-2: Model parameters for forward osmosis[b]

Membrane Material	Flux (L/m^2h)	Reverse Solute Flux (g/m^2h)	Draw Solution	Solute Ionic Strength (M)	Water Recovery
HTI-CTA	2.7-12.9	0.15*Flux	$MgCl_2$	2.0 – 5.0	50 - 70%

[b] References for data ranges are (10-31).

2.4 Membrane Distillation

Membrane distillation (MD) uses a porous hydrophobic membrane to facilitate the transfer of clean water from a feed solution to a distillate stream. The chosen type of MD for the proposed design was direct contact membrane distillation (DCMD). In DCMD, the feed stream (containing a non-volatile solute) is heated and then brought into contact with the membrane, with the distillate (also known as the permeate) stream on the other side of the membrane containing cold water. Water vapor then passes across the membrane and reconstitutes in the cold distillate stream, creating flux across the membrane. As long as the feed solution contains no volatile solutes, the system produces clean water [46]. Coupled with the forward osmosis process, the design retains a method to re-concentrate the draw solute and produce a potable effluent from influent wastewater. In addition, removing water from the draw solution that was added during forward osmosis (FO) returns the concentration in the draw solute to its original value. This mutually beneficial relationship between FO and MD prevents the need to add additional draw solute and allows FO to operate at stable fluxes over longer periods of time.

The advantage of using DCMD is that it only requires energy for heating the draw solution and for maintaining correct water velocities near the membrane (by pumping) [46]. Of the two, heating the draw stream is generally the largest energy requirement. However, a low-grade heat stream is all that is required to maintain the correct draw solution temperatures. As the design of the potable reuse system relies on resource recovery systems to reduce costs, the necessary energy for this heat stream could potentially be provided by captured methane in the anaerobic membrane bioreactor (AnMBR).

The literature review for DCMD focused on nine parameters: membrane material and morphology, temperature of the permeate and draw solution, composition and ionic strength of the draw solution, flux, water recovery, and salt rejection (Table 2-3). Membrane material was almost always polyvinylidene fluoride (PVDF), polytetrafluoroethylene (PTFE), polypropylene (PP), or some combination of the three [30,33-52]. The most popular morphologies studied were either flat-sheet membranes or hollow-fiber membranes, with both resulting in similar fluxes [30,33-35,37-52]. Permeate temperatures tended to be near ambient (17.5° – 23°C) so as to prevent unnecessary energy costs to heat (or cool) the permeate stream [30,33-41,43,45-51]. The draw solution temperatures, however, fluctuated more widely. Temperatures as low as 30°C were reported, as well as temperatures reaching 128°C [30,33-52]. Low temperatures result in relatively low flux values, while extremely high temperatures lead to decreasing salt rejection values (as the solute would begin to volatilize along with the water). Acceptable temperatures for the draw solution were determined to fall

within the range of 40° to 80°C. The draw solution was almost always NaCl with an ionic strength near 1.0 M [30,33,34,36-52]. The ionic strength of the solution seemed to have little to no effect on flux values. The application of magnesium chloride as a draw solute is a relatively new concept, so no studies had been conducted to determine its rejection in DCMD. However, as long as the draw solute is not volatile, it will not pass through the semi-permeable membrane; therefore, magnesium chloride was chosen as the solute. Flux also had a wide range of reported values, from about 2 to 93 L/m^2h for draw solutions containing salts [30,33-52]. The vast majority of values fell with the range of 10 to 80 L/m^2h. As with FO, water recovery is an important parameter, since it relates to the percentage of the draw solution flow that could be recovered as pure water. Few studies provided this information, giving a range of 80 to 95% water recovery [30,35]. Salt rejection was always reported as extremely high (>95%), with most studies reporting rejection near 100% [36-39,44,47,48,51].

Table 2-3: Model parameters for membrane distillation[c]

Permeate Temperature (°C)	Draw Temperature (°C)	Draw Solution	Ionic STR of Draw (M)	Flux (L/m^2h)	Water Recovery %	Salt Rejection %
17.5 – 23	40 – 80	$MgCl_2$	2.0 – 5.0	10 – 80	80 – 95	>95

[c] References for data ranges are (30, 33-52)

2.5 Anaerobic Membrane Bioreactor

The two components of an anaerobic membrane bioreactor (AnMBR) are the bioreactor and membrane filtration system. Typical bioreactors are supplied with oxygen, allowing for aerobic reactions to degrade organic substrates present in the wastewater [63]. In anaerobic bioreactors, external electron acceptors are not supplied. This results in a rapid depletion of natural electron acceptors in the water (dissolved oxygen, nitrate, and ferric iron). At this point, fermentation and hydrolysis become the dominant reactions, degrading the substrates using intermediate electron acceptors [63]. Eventually, the organics in the water are released as CH_4 (methane gas). Anaerobic bioreactors are characterized by much higher mixed-liquor suspended solids (MLSS) concentrations compared to their aerobic counterparts, with values typically ranging between 10 and 80 g/L [53,54,56,63].

The second aspect of the AnMBR is the membrane filtration. In membrane filtration, vacuum pressure is used to generate flux across a membrane. Microfiltration or ultrafiltration membranes are usually selected based on required effluent and flux values. A smaller pore size in the membrane will result in lower flux values, but a higher quality effluent. A significant issue associated with this process is membrane fouling. Filtering water with high organic content typically results in several types of fouling, which can serve to reduce the water flux across the membrane and decrease effluent quality [62]. Periodically relaxing the membrane, scouring it with gas, or cleaning it in a weak acid can return flux values to near initial values [62].

In the proposed potable reuse system, the AnMBR serves two main purposes: 1) removal of chemical oxygen demand (COD) and 2) production of methane biogas (Table 2-4). COD is a quantitative measurement of the organic strength of the wastewater. This measurement excludes nitrogen species, but includes toxic and non-biodegradable organics that may be unavailable to microorganisms. Therefore, removing COD reduces the "strength" of the wastewater, leaving only specific nutrients (nitrogen and phosphorus species) to be removed. Since the reactor is anaerobic, methane biogas is produced as a result of fermentation. Capturing this biogas is important to the design, as this biogas will provide the energy required to increase the draw solution temperature in the DCMD process.

Using an AnMBR has other distinct advantages. Large energy savings are offered over aerobic membrane bioreactors, as energy-intensive blowers are not required to aerate the reactor. AnMBRs typically have a solids retention time (SRT) of 60 days or more [53-56,61,63]. Some have infinite SRTs, meaning that solids are never removed from the reactor [57,59,60,62]. A direct effect of a long SRT is low sludge production. With infinite SRTs, sludge is not removed from the reactor, resulting in no sludge production. Removal, dewatering, and transport of sludge are expensive processes.. Having little to no sludge production offers significant savings to a wastewater treatment facility.

AnMBRs can be designed with a variety of different reactor configurations. This diversity leads to a variety of operating conditions and process controls. Therefore, the parameters selected for consideration in the literature review, were type of wastewater

treated, type of reactor, volume of reactor, temperature, hydraulic retention time (HRT), solids retention time (SRT), biogas production, concentration of solids in the reactor, influent COD, influent total suspended solids (TSS), effluent COD, COD removal efficiency, and membrane flux. In the proposed design, the forward osmosis step concentrates incoming wastewater, and then AnMBR treats the high strength wastewater. Studies that similarly treated high-strength wastewater were chosen for comparison, including municipal wastewater, brewery wastewater, and sludge [53-63]. The most popular reactor configurations were continuous-stirred tank reactors (CSTRs) and upflow anaerobic sludge blankets (UASBs) [56,63]. Some systems used a two-stage design, placing the membrane in a separate reactor that was only fed supernatant from the bioreactor [57,58,60]. These “sidestream” configurations reduced the rate of fouling on the membrane. Reactor volume was monitored to determine if measured values were constant across laboratory, pilot, and full-scale studies. The smallest reactor was just 1 liter, while the largest was 200,000 liters [55,63]. Both reactors returned similar results (in terms of COD removal), as did reactors with intermediate volumes. Temperature was an important parameter, as some reactors were heated up to 35 °C [54,63]. As the second part of the project stresses conservation of energy resources, systems that operated at ambient temperature were given additional consideration. Systems operated at temperatures between 15 and 35 °C reported similar COD removal values, suggesting that the proposed bioreactor would not require heating [53-63].

The remaining parameters were considered more important, as they dictated how the computer model was run. The HRT was variable with values reported in the range of 2 to 480 hours without general consensus [53-63]. The SRT tended to be long (>100 days), with the longer SRTs returning higher COD removal efficiencies [53-63]. Data for biogas production was rarely available in the literature, yet reported values were typically near 0.25 L CH_4 / g COD [54,56-58,60]. MLSS concentrations for the systems studied were usually within the range of 5 to 30 g/L [54,56-58,60,61,63]. The influent COD for high strength wastewaters were approximately 1.0 g COD/L or higher, which were suitable concentrations for the wastewater modeled in the proposed design [54,55,58,59,63]. The feed TSS varied, with values generally above 0.25 g/L [54,60-63]. The effluent COD was consistently reported at minimal values, usually below 0.1 g/L [53,54,58,59,63]. These values directly affected the COD removal efficiency, which was almost always greater than 90% [56-58,60,63]. Finally, membrane flux was rarely reported. Steady state values fell within 5 to 8 L/m^2h [53-55,57-62].

Table 2-4: Model parameters for anaerobic membrane bioreactor[d]

Temperature (°C)	HRT (hours)	SRT (days)	Biogas Prod. (L CH_4 / g COD)	MLSS Conc. (g/L)
17.5 – 23	40 – 80	> 60	0.20 – 0.30	5 - 30

Feed COD (g/L)	Feed TSS (g/L)	Effluent COD (g/L)	COD Removal Efficiency %	Flux (L/m^2h)
>1	0.25 – 3	<0.1	> 80	5 - 8

[d] References for data ranges are (53 - 63).

2.6 SHARON and ANAMMOX

SHARON and ANAMMOX represent recent advancements in wastewater treatment. Whereas conventional treatment uses nitrification followed by denitrification to remove nitrogen, recent literature has reported a new methodology [64]. In a domestic wastewater influent, nitrogen exists as both organic nitrogen and ammonium. After initial treatment (using either aerobic or anaerobic reactors), this nitrogen is converted almost completely to ammonium (NH_4^+). In treatment facilities designed for nitrogen removal, the ammonium is used by autotrophs as an electron donor, oxidized to nitrite (NO_2^-) and then nitrate (NO_3^-) through the process of nitrification [64]. The SHARON (single reactor high-yield ammonium removal over nitrite) process is known as partial nitrification. In this process, a short SRT is used to prevent full conversion of ammonium to nitrite. Additionally, oxygen is limited to prevent any conversion of nitrite to nitrate. The target result of SHARON is an even molar ratio of ammonium to nitrite. The equation describing SHARON is as follows [64]:

$$NH_4^+ + 1.5\ O_2 \rightarrow NO_2^- + H_2O + 2\ H^+$$

In the ANAMMOX process (anaerobic ammonium oxidation), the available ammonium is used as an electron donor, while nitrite is used as an electron acceptor. Conventional treatment of nitrate (denitrification) requires an additional electron donor to be used in this step, usually by the addition of methanol or acetate [64]. The nitrogen is released from the ANAMMOX process as nitrogen gas. The equation describing the ANAMMOX process is as follows [64]:

$$NH_4^+ + 1.32\ NO_2^- + 0.066\ HCO_3^- + 0.13\ H^+ \rightarrow 1.02\ N_2 + 0.26\ NO_3^- +$$

$$0.66\ CH_2O_{0.5}N_{0.15} + 2.03\ H_2O$$

SHARON and ANAMMOX serve one purpose: the removal of nitrogen. The advantage of using these treatment processes is due to the reduction in treatment costs, as using SHARON and ANAMMOX eliminates the need for an expensive external electron acceptor. In conventional treatment of nitrate (denitrification), this external electron acceptor is typically either methanol or acetate [64]. Current research into the SHARON process is somewhat sparse, with only four studies found that were specific to the SHARON process. The ANAMMOX process has been studied more thoroughly, with a greater wealth of information available. A few studies combined both processes, therefore making it difficult to find specific data for each process.

The SHARON process had 8 parameters that were considered important for the modeling of the proposed system: type of reactor, reactor volume, temperature, HRT, SRT, dissolved oxygen (DO) in the reactor, nitrogen loading rate, and effluent molar ratio between nitrite and ammonium (Table 2-5). All the reactors found in the literature were CSTRs [64-68]. The research returned a wide spectrum of reactor volumes, with a range between 2 liters and 2,100 liters [64-68]. Therefore, during modeling, volume was varied as required. Temperatures studied ranged between 19° C to 35° C, with better molar ratios occurring at higher temperatures [64-68]. Due to this, the SHARON reactor may require heating; however, in the proposed design, the SHARON reactor could be used as a heat sink for membrane distillation to reduce treatment costs. Almost all of the HRTs fell within 24 to 36 hours, while the SRT was consistently the

same as the HRT due to the CSTR configuration [64,65,68]. Dissolved oxygen levels were always less than 3 mg/L [64-68]. Nitrogen loading rates ranged between 0.1 and 3.3 kg $N/m^{3*}d$, suggesting the SHARON process can handle a wide range of loading rates [64-68]. Effluent molar ratios between NO_2^- and NH_4^+ were generally reported near 1.0 [64-68].

Table 2-5: Model parameters for SHARON process[e]

Reactor Type	Temperature (°C)	HRT (hours)	SRT	DO (mg/L)	N Load (kg N/m^3*d)	NO_2^-:NH_4^+
CSTR	19 – 35	4.8 – 36	Same as HRT	< 3.0	0.1 – 3.3	1

[e] References for data ranges are (64 - 68)

The ANAMMOX process had nine specific parameters that were considered for modeling: type of reactor, reactor volume, temperature, HRT, nitrogen loading rate, nitrogen removal rate, specific nitrification rate, nitrogen removal percentage, and molar ratio between nitrogen and ammonium, nitrite, and nitrate (Table 2-6). Over 10 different reactor configurations were used in various studies with sequencing batch reactors (SBRs) displaying the best performance [64,70-75]. However, the final system design could potentially use one of the other reactor configurations. Reactor volume was highly variable, with reactors as small as 0.2 L up to 70,000 L, without clear trends concerning size and nitrogen removal efficiencies [64, 70-75]. Most ANAMMOX reactors were operated at 35° C, with only a few studies operating below 25° C [64,70-75]. These studies had promising results, providing evidence that the reactor may not require heating. HRT values changed markedly due to the diversity in reactor type, with most

HRTs under 48 hours [64,70-75]. Nitrogen loading rates and removal rates can be better summarized by the nitrogen removal percentage; however, some loading rates were relatively high (>15 g N / L*d) with similarly elevated removal rates [64,70,73,74]. This information suggests that the ANAMMOX process can handle the concentrated waste that is expected in the proposed system. Specific nitrification rates (SNR) were mostly between 0.15 and 1.15 g N / g VSS*d [64,73]. Nitrogen removal percentages were at or above 70% [64,71,73]. Finally, the molar reaction ratio between ammonium, nitrite, and nitrate was consistently reported to be near 1.0 : 1.2 : 0.2 [64,71].

Table 2-6: Model parameters for ANAMMOX[f]

Reactor Type	Temperature (°C)	HRT (hours)	SNR (g N/ g VSS*d)	N Removal (%)	Rxn N Ratio (NH_4^+:NO_2^- :NO_3^-)
SBR	22 – 35	< 48	0.15 – 1.15	> 70	1 : 1.2 : 0.2

[f] References for data ranges are (64, 70 - 75).

2.7 Struvite Precipitation

Struvite precipitation is an alternative method to remove phosphorus from wastewater. Historically, phosphorus has unintentionally precipitated in wastewater treatment facilities as struvite ($MgNH_4PO_4$*6 H_2O). Precipitated struvite is generally considered a nuisance. Struvite solidifies in pipes and valves, reducing the effective diameter and increasing head losses. However, struvite is a suitable fertilizer since it contains ammonium and orthophosphate. Phosphorus can effectively be forced to

precipitate as struvite, and then sold as fertilizer to offset energy and chemical costs [89].

Promoting the precipitation of struvite requires two reactor conditions: an elevated pH and the addition of magnesium [76]. The pH must be kept at 9 or below, though, as ammonium will change speciation to ammonia, and volatilize out of the system (thereby retarding struvite formation). Elevating the pH in struvite reactors is usually accomplished by one of two methods: aerating the system to strip carbon dioxide (CO_2) or adding sodium hydroxide (NaOH). Magnesium is almost always added as magnesium chloride [76,78-90].

Due to the recent emergence of struvite precipitation as a positive, research on the process is somewhat sparse. Ten parameters were determined to be important to the operation of a struvite reactor: influent wastewater composition, reactor type, reactor volume, pH, temperature, HRT, molar ration of Mg:P, total phosphorus removal, total nitrogen removal, and chemical additions (Table 2-7). As the initial FO process in the proposed system concentrates the contaminants in the influent, a high concentration of phosphorus is expected in the struvite reactor. Therefore, research focused on applications that included high phosphorus concentrations (swine wastewater and digester effluents). The typical reactors used in struvite precipitation are CSTRs, SBRs, or what was deemed as “crystallization reactors” [76-90]. Again, the reactor size was highly variable and can likely accommodate the scope of this project. The pH was consistently between 8 and 9, with an average near 8.5 [76,77,79-86,88,90]. Temperatures varied from 0° to 30° C, with the highest removal rates reported at, or

slightly below, 20° C [76-90]. The HRT was found to be 4 hours or less, with mixing as a viable method to reduce HRT and still maintain high precipitation rates [76-78,81,83,85-90]. The molar ratio of Mg:P was 1:1 in struvite, and a value of 1 was reported consistently with high phosphorus removal rates [76-83,87-90]. A molar ratio up to 1.5 also seemed to be acceptable; however, this could lead to excessive magnesium in the system. The total phosphorus removal for SBR systems was reportedly 88% or higher [77,80,82-85,88]. The total nitrogen removal for the SBRs was similarly elevated at 80% or better [83-86]. The systems studied used magnesium chloride to induce struvite precipitation. The pH was adjusted through air stripping or the addition of sodium hydroxide.

Table 2-7: Model parameters for struvite precipitation[g]

Reactor Type	pH	Temperature (°C)	HRT (hours)	Mg:P molar ratio	Total P Removal (%)	Total N Removal (%)	Additon of:
CSTR/SBR	8 – 9	14.5 – 25	< 4.0	1:1	> 88	> 80	$MgCl_2$

[g] References for data ranges are (76 - 90).

Chapter 3 Research Goals and Objectives

Currently, the treated effluent from STMWRF is stored in Huffaker Hills Reservoir and then later used seasonally as non-potable reuse water primarily for irrigation. Due to elevated concentrations of nitrogen and phosphorus in the effluent, algal growth in the reservoir has been significant enough to affect the quality of the reuse water in recent years. The primary objective of the first part of this study was to develop and calibrate a computer model of STMWRF. Using the model, new operating parameters were then proposed for the facility in an effort to reduce effluent nitrogen and phosphorus concentrations.

For the second phase of this study, the primary objective was to develop a computer model used to design and predict the performance of a potable reuse treatment design. The model would allow comparison with actual facilities, using the current configuration of STMWRF as the reference facility. The potable reuse treatment system was developed under the premise of a low energy, high quality effluent facility. Specifically, the feasibility of the potable reuse facility could be compared in terms of energy costs and effluent quality to the performance of the current configuration of STMWRF. Through these comparisons, the feasibility of the potable reuse system could be determined.

Chapter 4 Materials and Methods

The first phase of the project required the development of a computer simulation of STMWRF. The development of the model required samples from the facility to test for influent and effluent concentrations of ammonium, orthophosphate, nitrate, and nitrite. From this collected data, the model could be constructed. The second phase similarly required the construction of a model; however, the second model did not require any sampling be conducted.

4.1 Collection of On-site Data

4.1.1 Sampling the Oxidation Ditch

In order to develop the computer model of STMWRF, data from the facility had to be collected using on-site testing and monitoring. The influent sampling point was chosen to be at the headworks, as it allowed for easy sampling. The effluent sampling location was chosen to be at the mixed liquor suspended solids (MLSS) splitter box (Figure 2-1, 4-1). It was decided that three days worth of data would provide sufficient information to build the model. For each day, data needed to be collected at hourly intervals. A Teledyne Isco 3700 full-size portable sampler (Lincoln, NE) was set up at each sampling point, and allowed to run for one day (Figure 4-2). The samplers contained 24 individual 500 mL glass sample containers, and a computer control system allowed samples to be taken at hourly intervals. Samples were collected using a peristaltic pump connected to vinyl tubing that was placed in the appropriate sampling location. The units were set to collect 100 mL samples. Both ice and mercuric chloride

($HgCl_2$) were used to prevent sample degradation before testing. Ice was used to retard the kinetics of reactions that would degrade the sample (Figure 4-3). Mercuric chloride was dosed to a concentration of 1 g/L to inhibit any microbial activity in the samples, which would further alter the composition of the samples [91].

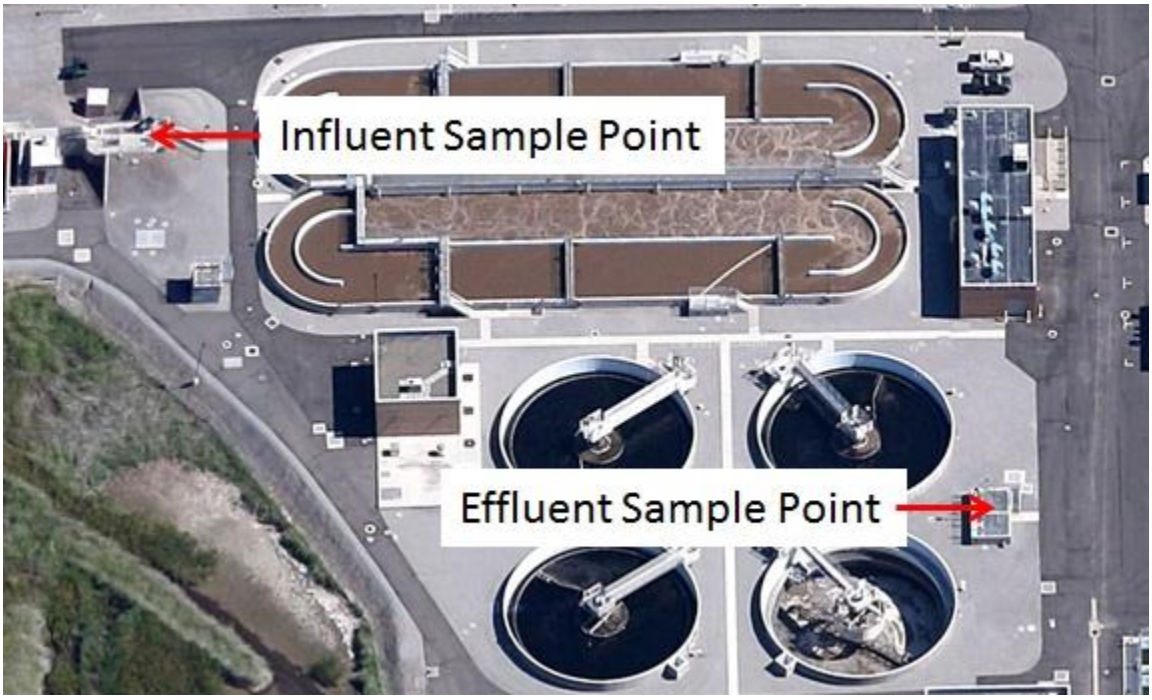

Figure 4-1: Location of influent and effluent sample points (Google, 2013)

Figure 4-2: Example of Teledyne Isco Sampler

Figure 4-3: Preparation of ISCO for sampling

4.1.2 Flow, Aeration, and RAS Recycle

In addition to water quality tests for the influent and effluent, information about facility operation was required to develop the computer model. STMWRF is equipped with a Supervisory Control and Data Acquisition (SCADA) system, which collected real-time facility operation data. Data that were important to the development of the model included total flow rate into the facility and individual flow rates into each of the two oxidation ditches (calculated using 15 minute averages provided by the SCADA system). Return activated sludge (RAS) and waste activated sludge (WAS) flow rates were also required, as well as oxygen supply rates to the oxidation ditch. The supply rates were set by the plant operators, and correspond to air flow rates provided to the diffusers in the bottom of each of the oxidation ditches. The values were set in terms of standard cubic feet per minute (scfm).

4.2 Sample Analyses

4.2.1 Nutrient Analysis

Ammonium, orthophosphate, nitrate, and nitrite were analyzed using a Lachat Quikchem 8500 Ion Analyzer with Automated Sampler (Lachat Instruments, Loveland, CO). The methods used include Quikchem methods 10-107-06-2-J (ammonium), 10-115-01-1-V (orthophosphate), and 10-107-04-01-A (nitrate + nitrite). Samples were tested within 48 hours of initial sampling in order to ensure limited transformation or loss of compounds of interest.

4.2.1.1 Ammonium

Quikchem method 10-107-06-2-J was used to determine the concentration of total ammonium. When ammonium was heated in the presence of salicylate and hypochlorite within an alkaline phosphate buffer, free ammonium was converted to monochloramine and an emerald green color is produced and monitored by a photodiode at a wavelength of 630 nm. Sodium nitroprusside was added to intensify the color. Photodiode voltage peak areas for known standards were measured and a calibration curve was developed relating time-integrated voltage to concentration. The voltage peak areas from the samples were then compared to the calibration curve to determine the concentration. This method was appropriate for ammonium concentrations ranging from 0.30 to 30 mg N/L.

4.2.1.2 Nitrate and Nitrite

Quikchem method 10-107-04-01-A was used to determine the combined concentration of nitrate and nitrite. When nitrite diazontizes with sulfanilamide and couples with N-(1-napthyl)ethlyendiamine dihydrochloride, a water-soluble magenta dye was produced which was monitored at a wavelength of 520 nm. A copperized cadmium column was used to reduce nitrate to nitrite. When the column was included in the system, the measured concentration consisted of only nitrite. Therefore, the nitrate concentration was determined by subtracting the “column off” value from the “column on” value. This method was appropriate for nitrite concentrations ranging from 0.2 to 20 mg N/L.

4.2.1.3 Orthophosphate

Quikchem method 10-115-01-1-V was used to determine the concentration of orthophosphate. When orthophosphate reacted with ammonium molybdate and antimony potassium tartrate under acidic conditions, a complex was formed and then that complex was reduced with ascorbic acid to form a blue complex which was monitored at a wavelength of 880 nm. A calibration curve was developed for different concentrations.

For each method, a five-point calibration curve was developed at the beginning of each run. Also, three check standards were included in each run, and as long as these check standards were measured within 10% of their actual value, the run was continued. Generally, the ammonium checks measured within 0-5% of their actual value. Orthophosphate and nitrate + nitrite checks were less accurate measuring within 2.5 – 10%.

4.2.2 COD Analysis

Chemical oxygen demand (COD) was measured using the Ampule Method as described by Standard Methods [92]. COD is a quantitative measure of the amount of oxygen required to oxidize matter in the sample (both organic and inorganic compounds). The Ampule Method uses premixed vials in which samples are added and then heated at 120° C for 2 hours. The main oxidizing agent in the premixed vials is dichromate, with silver sulfate used as a catalyst. The amount of dichromate consumed by the sample represents the amount of COD in the sample, which can be measured using a spectrophotometer. Dichromate oxidizes COD in the sample, with the chromate

being reduced to an oxidation state of +3 from +6, which alters the color of the sample from orange to green. By creating a standard curve using predetermined concentrations of COD, samples with unknown concentrations of COD can be measured [92].

4.3 Computer Modeling

The computer modeling software used throughout the project was the *BioWin* Wastewater Simulation Module Version 3.1 (EnviroSim Associates Ltd., Hamilton, Ontario, Canada). The software allows calibration of the model space using actual facility operating conditions. The process of modeling began by integrating the unit processes of the wastewater plant into the modeling environment. Once the wastewater unit processes were included, boundary conditions were generated by placing influent and effluent structures. Structures and recycle networks were connected using simple pipes. Unit processes were matched to their real-world counterparts in terms of volumes, depths, and surface areas.

After the plant was constructed in the model space, the calibration of the model began. The first step of calibration was adjusting the influent in the model to match the actual influent. The purpose of the calibration was to make adjustments within the model so that the predicted effluent flows and concentrations match the actual effluent. A flow balance was performed to verity the stability of the model. It indicated whether or not the modeled system allowed proper flows paths such that no water was accumulating in a reactor, and that no reactors were drying out. After the flow balance was completed, the model was run using a “steady-state” approach. The steady-state

model did not use the time varying data that was entered into the model. Instead, it used averages of the data. The purpose of running the steady-state model was to act as another "check" on the model to ensure that all the connected processes were interacting correctly. Secondly, it also created a benchmark for the model that was useful for assessing the non-steady state (dynamic) model. After the steady-state model was completed, the next step was to run the dynamic model which operated over longer periods of time. This part of the processes integrated the unsteady-state data into the model, and similarly produced unsteady-state data. At this point, the output from the model was compared to the effluent of the facility to determine proper calibration of the model. Kinetic and stoichiometric data could then be altered within the model to calibrate the model. Once the predicted effluent from the model matched the effluent from the facility, the calibration step was complete. Predictive modeling was then performed allowing the user to evaluate the facility under different operating conditions. Using an iterative approach, the performance of the facility can be optimized using the model. The optimized operating parameters could then be implemented at the real facility, in an attempt to further validate performance of the model.

4.4 Statistical Analyses

The data were compiled and analyzed in Microsoft's Excel 2010. The program allowed manipulation and conversion of data, as well as producing all data plots. The program was also used in all statistical analyses of the data.

Chapter 5 Results and Discussion

5.1 Overview

There were two primary goals of this research. The first was to propose a new operating strategy at STMWRF to reduce effluent ammonium and orthophosphate concentrations. The second was to determine the feasibility of implementing a potable water reuse facility at STMWRF. In order to achieve both of these goals, a computer model of both the existing facility at STMWRF and the proposed potable reuse facility were created.

5.2 STMWRF Influent and Effluent Testing

A large volume of data was used to develop the model of STMWRF. The majority of the operational data were available from the SCADA system at the facility. However, the model required influent nitrogen, phosphorus, and COD. Effluent data were also required to ensure that the model was properly calibrated. Water quality data were collected from the facility on three separate occasions, with each round of testing beginning on a Thursday morning and ending on a Friday morning. All of the tests were performed during the month of April in 2013. One data set was discarded due to an equipment malfunction with the Lachat Quikchem 8500. The malfunction forced the samples to sit beyond the analysis window of 48 hours, reducing the integrity of the data. Therefore, the first set and second set of data were used in the construction of the model. The reason that two data sets were necessary was because the first set was needed to initially calibrate the model, and the second set was then needed to validate

the model. In terms of the data itself, larger influent flows and concentrations were expected in the morning and the early evening. The reason for these increases is due to the common work schedule, which has people most active in terms of water use at these two times of the day.

An additional consideration was the fact that the treatment performance of the two oxidation ditches were expected to be different. As it was not possible to individually sample the effluent for each oxidation ditch, testing instead occurred at the combined effluent of the two ditches. Therefore, the reported effluent concentrations represent the combined treatment capabilities of the two ditches.

5.2.1 Influent and Effluent Ammonium

The influent concentrations of ammonium at STMWRF were typical of low to medium strength wastewaters and were within the range of 12-25 mg NH_4^+-N/L (Figure 5-1) [2]. The average influent concentration for the first set of data (24 samples) was 11.2 ± 3.7 mg NH_4^+-N/L. The second set of data was characterized by higher influent ammonium concentrations, with an average influent concentration of 18.2 ± 4.5 mg NH_4^+-N/L. However, one of the main advantages of the oxidation ditch design is its resistance to shock loading, and therefore the effluents were expected to be similar. The average discharge for the first set was 6.0 ± 1.0 mg NH_4^+-N/L, and the average for the second set was 5.2 ± 1.8 mg NH_4^+-N/L, demonstrating that the effluent for the two sets were relatively similar (Figure 5-2).

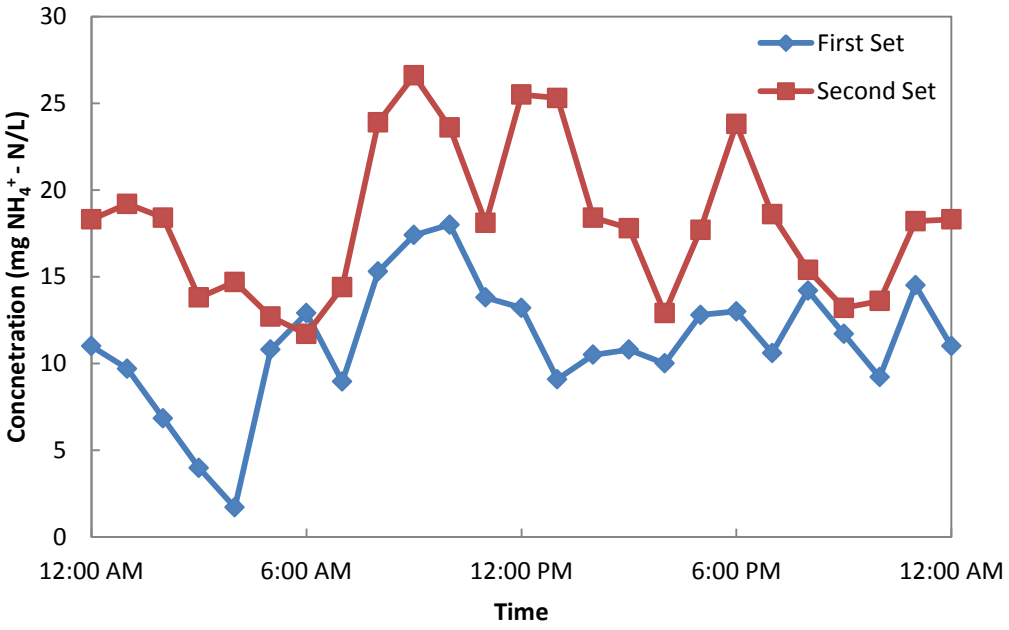

Figure 5-1: Influent ammonium concentrations at STMWRF.

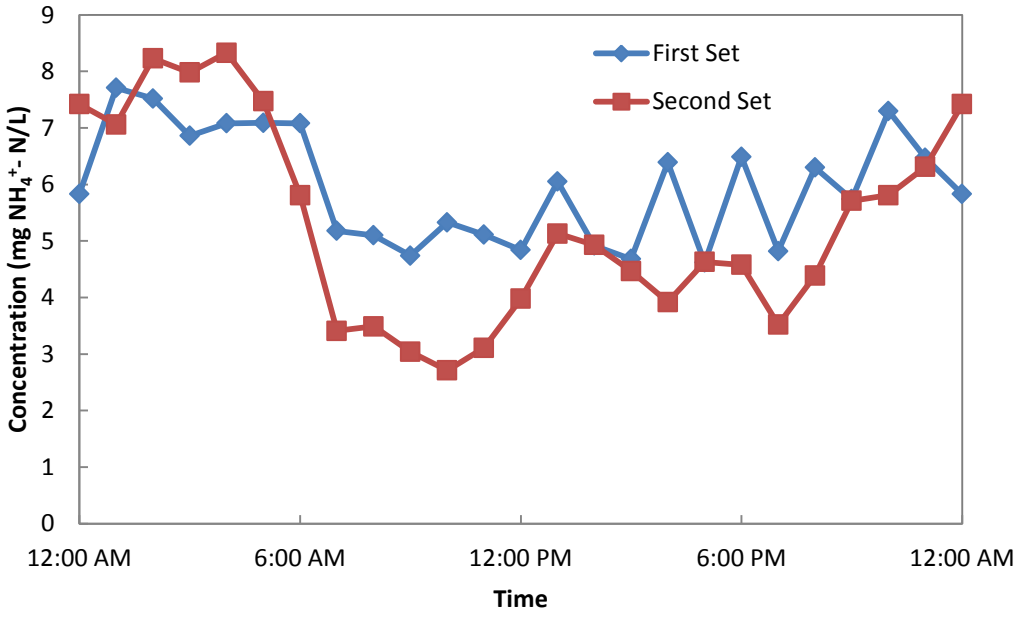

Figure 5-2: Effluent ammonium concentrations at STMWRF.

5.2.2 Influent and Effluent Nitrate + Nitrite

Most influent nitrogen at wastewater plants is either bound as organic nitrogen or as ammonium. However, the influent was also tested for nitrate and nitrite, as these compounds can show up if industrial or agricultural effluents are responsible for some portion of the wastewater influent. Nitrate and nitrite (a combined value) were found at minimal concentrations in the influent (Figure 5-3). The influent concentrations for both days of sampling were much closer than those of ammonium, with the first set maintaining an average of 0.45 ± 0.57 mg NO_3^--N + NO_2^--N/L, and the second set an average of 0.45 ± 0.46 mg NO_3^--N + NO_2^--N/L. There was a considerable spike in influent concentrations late in the day during both days. Typical domestic wastewater influents contain little to no nitrate or nitrite, so these elevated concentrations were somewhat abnormal [2]. Concentrations in the effluent were expected to be higher than those in the influent, due to the conversion of ammonium to nitrate + nitrite in the oxidation ditches. This assumption was proven true, even though effluent concentrations were at or near zero throughout a large part of the day (Figure 5-4). The first set of data had an average effluent concentration of 0.55 ± 0.85 mg NO_3^--N + NO_2^--N/L. The second set of data demonstrated much higher effluent concentrations, with an average of 1.5 ± 2.1 mg NO_3^--N + NO_2^--N/L. Examining the data showed that concentrations for both sets would rapidly rise during the late morning, before quickly dropping again. This was thought to be due to the aeration scheme in the oxidation ditches.

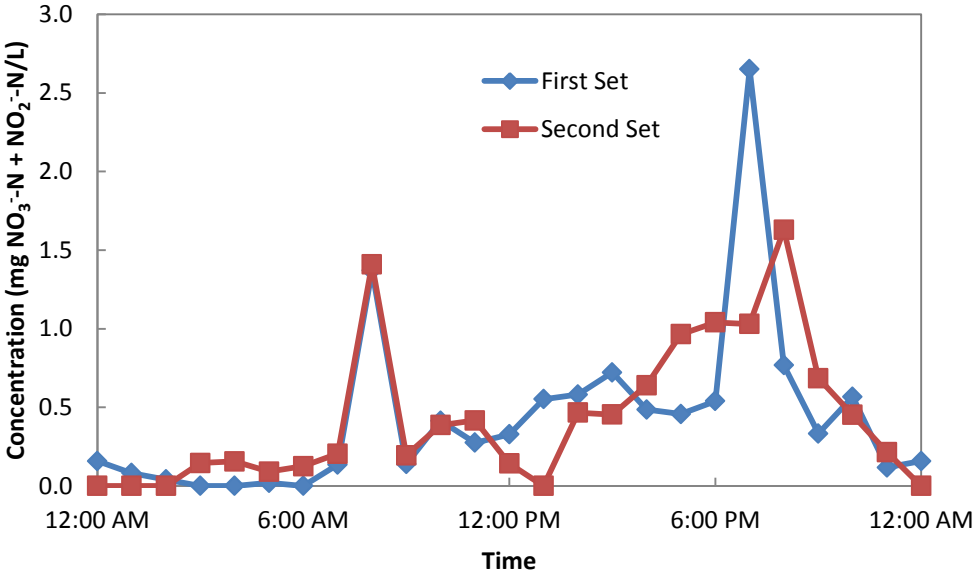

Figure 5-3: Influent nitrate + nitrite concentrations at STMWRF.

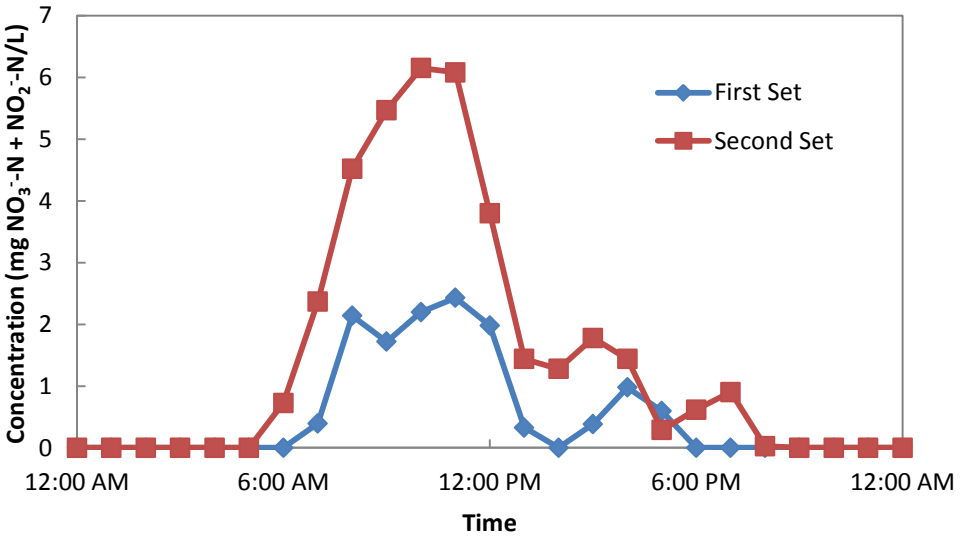

Figure 5-4: Effluent nitrate + nitrite concentrations at STMWRF.

5.2.3 Influent and Effluent Orthophosphate

High concentrations of orthophosphate were not expected in the influent. The data confirmed these expectations, with the first set of data having an average

concentration of 2.5 ± 0.6 mg PO_4^{3-} - P/L, and the second set having an average concentration of 2.5 ± 0.7 mg PO_4^{3-} - P/L (Figure 5-5). These concentrations of orthophosphate in the influent were typical of a low strength wastewater, as the average concentrations were less than 4 mg PO_4^{3-} - P/L [2]. The effluent concentrations were highly variable, with large peaks in both the early morning and late night that correlated well with low effluent flows from the facility (Figure 5-6). The average effluent concentration for the first data set were 2.2 ± 2.05 mg PO_4^{3-} - P/L, with the second set slightly higher with an average concentration of 2.8 ± 2.9 mg PO_4^{3-} - P/L . As indicated by the large standard deviation, the time series data for effluent phosphorus from the plant was highly irregular.

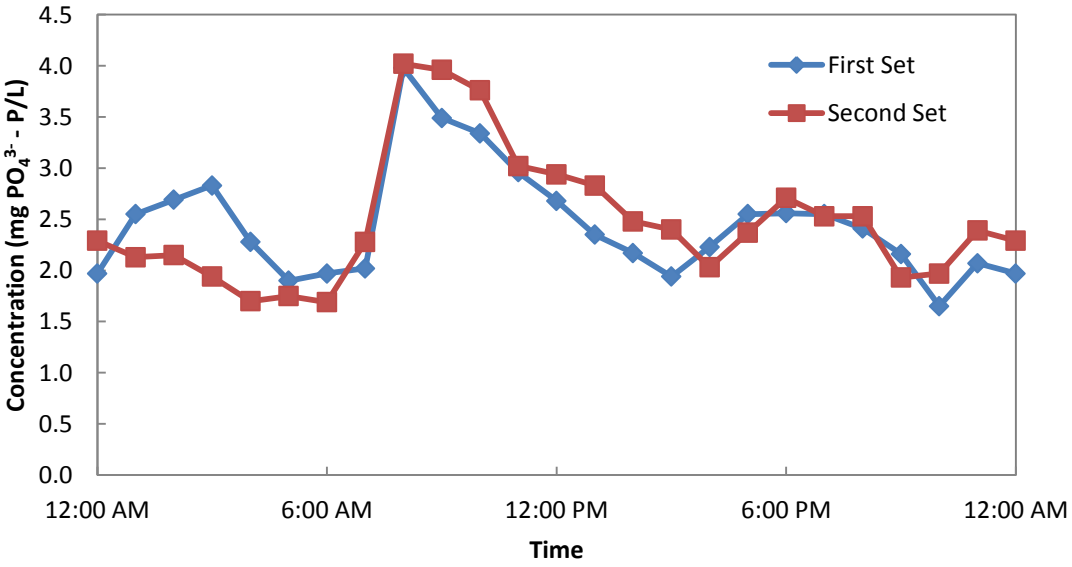

Figure 5-5: Influent orthophosphate concentrations at STMWRF.

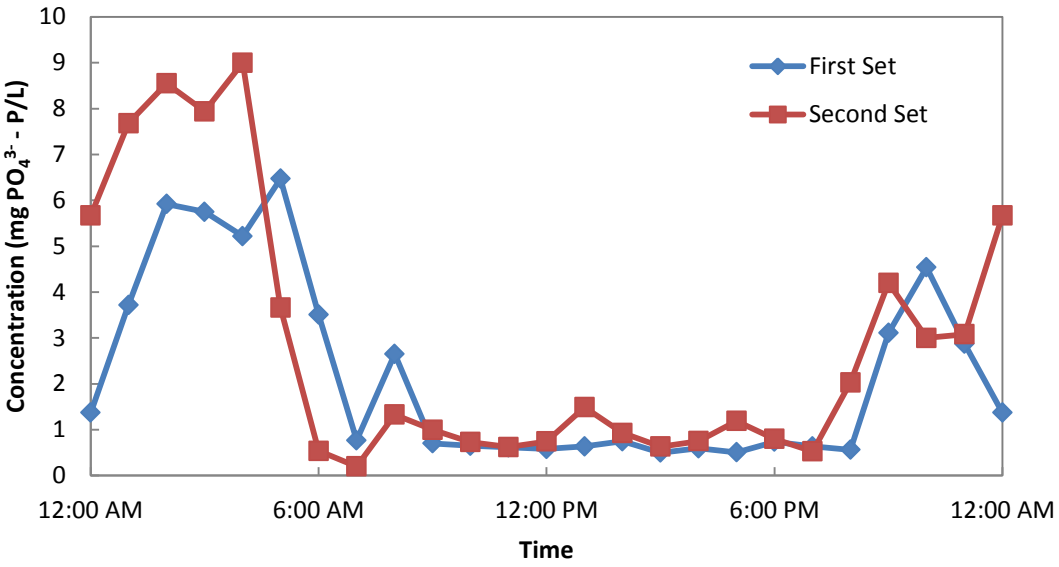

Figure 5-6: Effluent orthophosphate concentrations at STMWRF.

5.2.4 Influent and Effluent Carbonaceous Oxygen Demand

COD tests were also conducted on both the influent and effluent. COD is generally used to gauge the strength of a wastewater, with higher COD values corresponding to a more concentrated wastewater. The influent COD fell within ranges typical of a low strength domestic wastewater, with an average influent COD concentration of 178 ± 154 mg COD/L for the first data set, and 203 ± 50 mg COD/L for the second set (Figure 5-7). Both days had similar values, with small spikes in influent concentration that differentiated the two days. The effluent values were more closely matched, with an average effluent COD concentration of 49 ± 11 mg COD/L for the first set, and 46 ± 11 mg COD/L for the second set (Figure 5-8). It is important to note that the effluent test values do not represent the effluent values for the facility as a whole,

as further removal of COD may occur after the sample point used in this study. For the tested nutrients, though, concentrations are unlikely to change beyond the effluent sampling point. The overall removal efficiency for the second data set was much higher, with an average removal efficiency of 76% ± 7%. The first data set was more varied, with an average removal efficiency of 61% ± 20%.

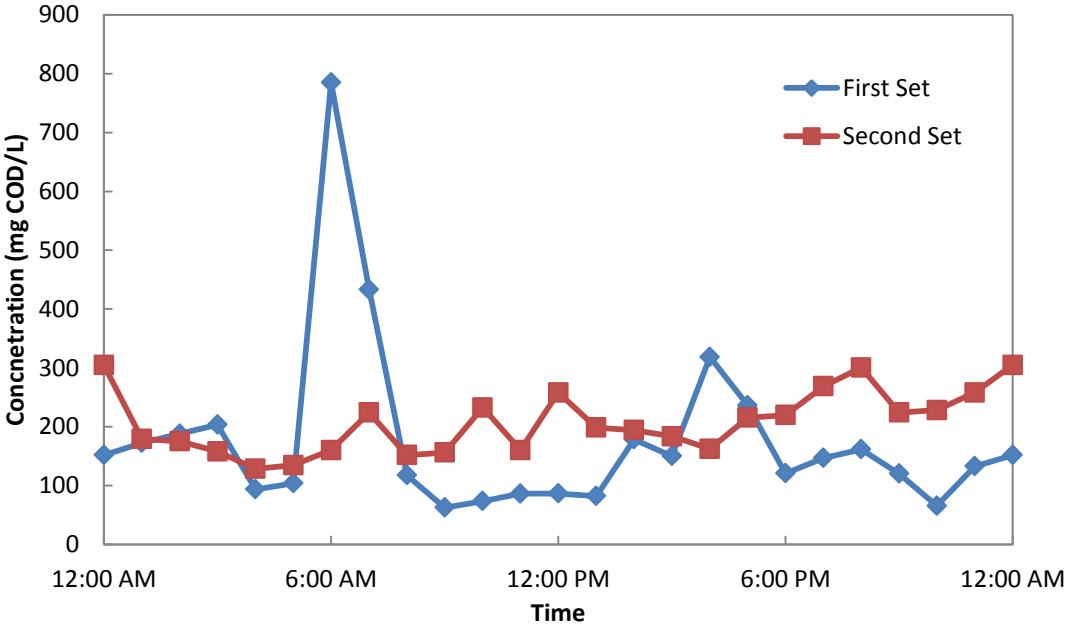

Figure 5-7: Influent COD concentrations at STMWRF.

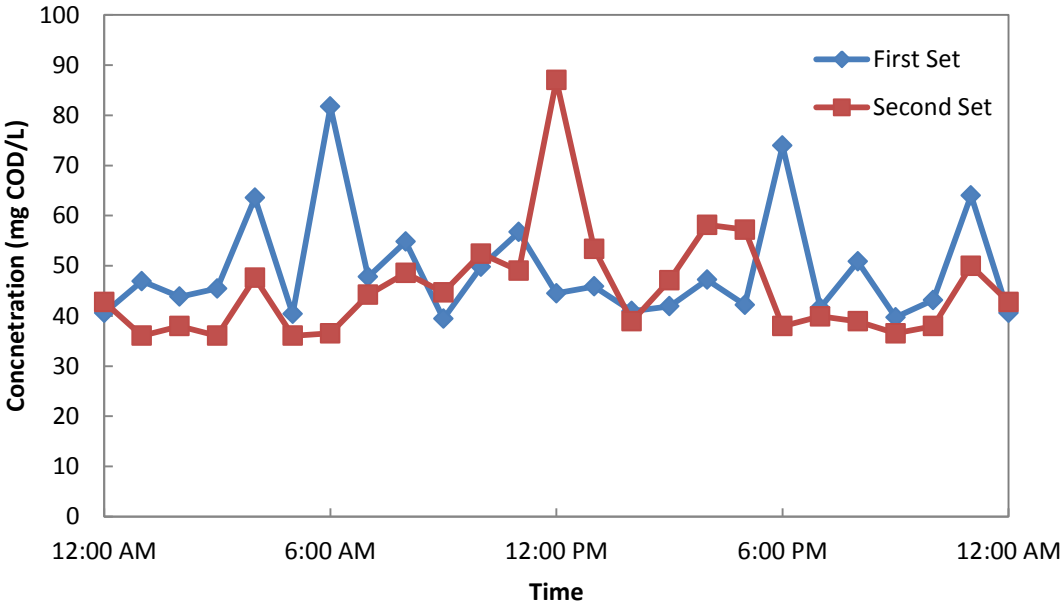

Figure 5-8: Effluent COD concentrations at STMWRF.

5.3 Model of Operating Conditions at STMWRF

Once the analysis of the influent and effluent water quality was completed, the modeling stage began. The second set of data was used to calibrate the model, though the first set would have worked as well. The water quality data was combined with the data gathered from the SCADA system at STMWRF (Table 5-1). The *BioWin* model included the construction of the physical plant in the model space (Figure 5-9, 5-10). In the model, the oxidation ditch was not represented as a single unit. Instead, the ditch was divided into 6 different reactors, with the aerobic and anoxic zones being equally represented by 3 reactors each (Table 5-2). There are two oxidation ditches at STMWRF; therefore, the model included a total of 12 reactors (with each set of 6 placed

in parallel). The total volume of each parallel set of 6 reactors was equal to the total volume of one oxidation ditch. The four secondary clarifiers located at STMWRF were only represented as one clarifier in the model since clarifier performance was not part of the study. It was important to include at least one clarifier, though, as clarifiers are responsible for the RAS flow that combines with the influent to the oxidation ditches and the WAS flow which is important for determining the solids retention time. The model did not include the final treatment processes used at STMWRF (namely filtration and disinfection). Since these final treatment processes have little to no effect on the nutrients of concern, their exclusion did not affect the ability of the model to simulate the performance of the facility.

Table 5-1: Example of SCADA data used for modeling[h]

Time	Influent Flow (MGD – 15 min. avg.)	Ditch 1 Air Flow (scfm)	Ditch 2 Air Flow (scfm)
8:30 AM	3.12	1,736	3,290
9:30 AM	4.27	1,676	3,283
10:30 AM	4.75	1,635	3,149
11:30 AM	4.62	1,590	3,073
12:30 PM	4.44	0	0
1:30 PM	4.15	0	0
2:30 PM	3.93	1,619	2,855
3:30 PM	3.68	1,590	2,855
4:30 PM	3.54	0	0
5:30 PM	3.47	1,602	2,768
6:30 PM	3.53	1,592	2,828
7:30 PM	3.82	1,622	2,929
8:30 PM	4.26	0	0
9:30 PM	4.66	1,722	2,951
10:30 PM	4.90	1,689	3,073
11:30 PM	4.72	1,705	3,104
12:30 AM	4.10	0	0
1:30 AM	3.36	0	0
2:30 AM	2.75	989	1,178
3:30 AM	2.26	0	0
4:30 AM	2.02	1,012	1,184
5:30 AM	1.91	1,841	3,409
6:30 AM	1.91	1,821	3,432
7:30 AM	2.32	1,781	3,404

[h] Data for STMWRF provided by Washoe County [3]

Figure 5-9: Overview of STMWRF (Google, 2013)

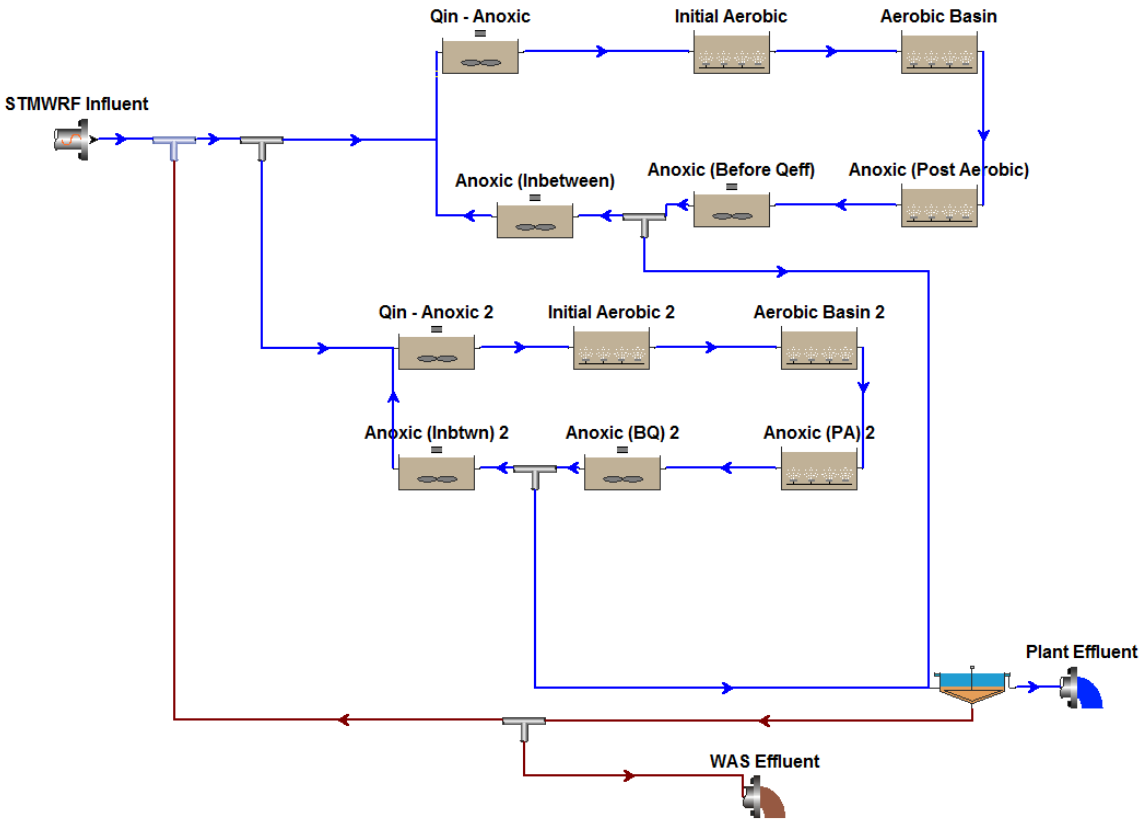

Figure 5-10: Representation of STMWRF oxidation ditches and secondary clarifier in *BioWin*

Table 5-2: Physical characteristics of sub-reactors

	Volume (MG)	Water Depth (ft)	Surface Area (ft^2)
Qin – Anoxic	0.337	13	3,460
Initial Aerobic	0.109	13	1,125
Aerobic Basin	0.539	13	5,547
Anoxic (Post Aerobic)	0.068	13	698
Anoxic (Before Qeff)	0.183	13	1,886
Anoxic (In between)	0.349	13	3,588

With the mock facility built within the model, the calibration of the model began. Influent flow and concentrations were adjusted to match the data gathered from sampling, as well as operating parameters (such as aeration and recycle rates) [3]. Then the model was continually altered until the characteristics of the effluent predicted by the model were consistent with the effluent from the actual facility. The process of calibration consisted of changing kinetic and stoichiometric parameters used within the model. The *BioWin* model was based on studies into wastewater characterization and activated sludge modeling by WERF (Water Environment Research Foundation, Alexandria, VA). Using the equations developed by WERF, influent and operating conditions are input in the model, and then these equations are used to predict the concentrations for the different constituents throughout the treatment system. As many of these equations require iterative solutions, the process of modeling a facility could be extremely difficult. Within these equations are various coefficients which describe the reactions in the treatment process, including kinetic and stoichiometric data. Not all treatment facilities are the same, though, and either data type can vary depending on factors such as the microbial community in the bioreactor. The calibration of the STMWRF model focused on altering kinetic values from their defaults (as set by WERF) to values that aptly describe the treatment processes at STMWRF (Table 5-3).

Table 5-3: Examples of default and calibrated kinetic coefficients in *BioWin*

	Default Value	Calibrated Value
AOB Max Specific Growth Rate (1/d)	0.9	1.5
AOB Aerobic Decay Rate (1/d)	0.17	0.07
AOB Substrate (NH_4^+) half saturation (mg N/L)	0.7	0.45
NOB Max Specific Growth Rate (1/d)	0.7	0.6
ANAMMOX Aerobic Decay Rate (1/d)	0.019	0.024
OHO Aerobic Decay Rate (1/d)	0.62	0.60
OHO Max Specific Growth Rate (1/d)	3.2	3.5
PAO Sequestration Rate (1/d)	6	10
PAO Anaerobic Decay Rate (1/d)	0.04	0.0095

The desired data from the model (hourly values over a 24-hour period) made the modeling process more complicated than initially anticipated. Given the resources available, exactly matching effluent concentrations provided at every given hour with the model became too time-intensive and unrealistic. Therefore, the model was instead calibrated using mass discharge instead of concentrations. Using mass discharge meant that the model facility had to discharge the same weight (in pounds) of nutrients as the actual facility did. This approach allowed the effluent concentrations to differ slightly between the model and actual facility throughout the day. The final values compared were pounds of nitrogen and phosphorus discharged each day.

The nutrients of concern were ammonium, orthophosphate, and the combined amount of nitrate and nitrite. These nutrients were used in the calibration of the model. Ammonium represented the greatest nutrient mass discharged from the facility (Figure 5-11). Part of the reason the model had to be completed using mass discharge was due to the erratic characteristics of the effluent from the oxidation ditches at STMWRF. Whereas an oxidation ditch is generally assumed to have a relatively stable effluent, the effluent from STMWRF was observed to spike and drop rapidly. The reason for the unstable effluent was most likely due to the aeration schedule used at the facility (Table 5-1). In the aeration schedule, there were multiple hours when the air was shutoff. During these periods, the aerobic zone disappeared within the reactor, promoting the growth of the anoxic zone, and likely inducing anaerobic zones to appear. This lack of air resulted in spikes in the effluent concentrations of ammonium, and drops in the concentrations of nitrate + nitrite. The timing of these off-cycles was determined by facility operators, and the rationale for the chosen cycles was not investigated. The model was unable to replicate the same magnitude of changes in its effluent concentrations; however, it was able to predict similar mass discharge over a 24 hour period (Table 5-4).

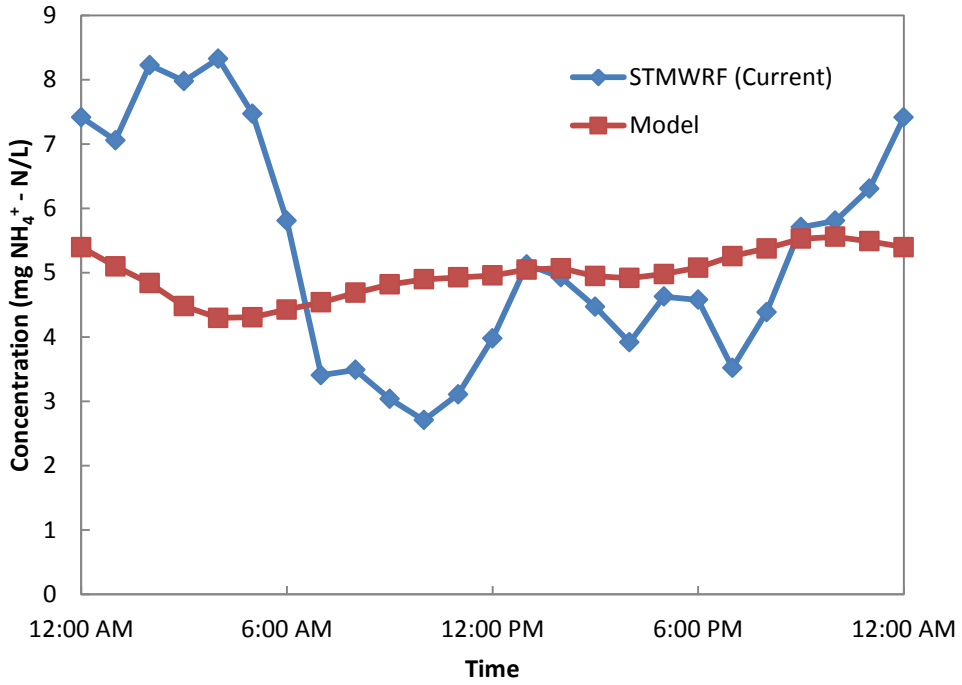

Figure 5-11: Effluent mass discharge of ammonium.

Table 5-4: Comparison of mass discharge of ammonium.

	STMWRF (Current)	Model	Difference
Mass Discharge (lbs N/day)	149.6	149.6	0.0

Orthophosphate was the next nutrient of concern. The facility data exhibited high effluent concentrations in the early morning hours, with concentrations severely spiking again in the late night hours. The model could not replicate such trends, and instead followed a dampened and more gradual trend (Figure 5-12). Whereas the ammonium mass discharge between the model and facility had no difference, there was a slight difference in discharge rates for orthophosphate. A margin of 0.6 lbs P/day existed between the discharge predicted by the model and the actual facility (Table 5-5).

The reason for this discrepancy was related to the method used to calibrate the model. Once one parameter was altered, the modeling exercise continued with varying the next parameter. Unfortunately, in a wastewater treatment facility, a number of the parameters are closely related. Values cannot be "fixed"; attempting to change the discharge of one constituent will inadvertently change another. Therefore, a small difference always remained with either ammonium or orthophosphate, and eventually the final model still retained a minor difference in the total mass discharge for orthophosphate.

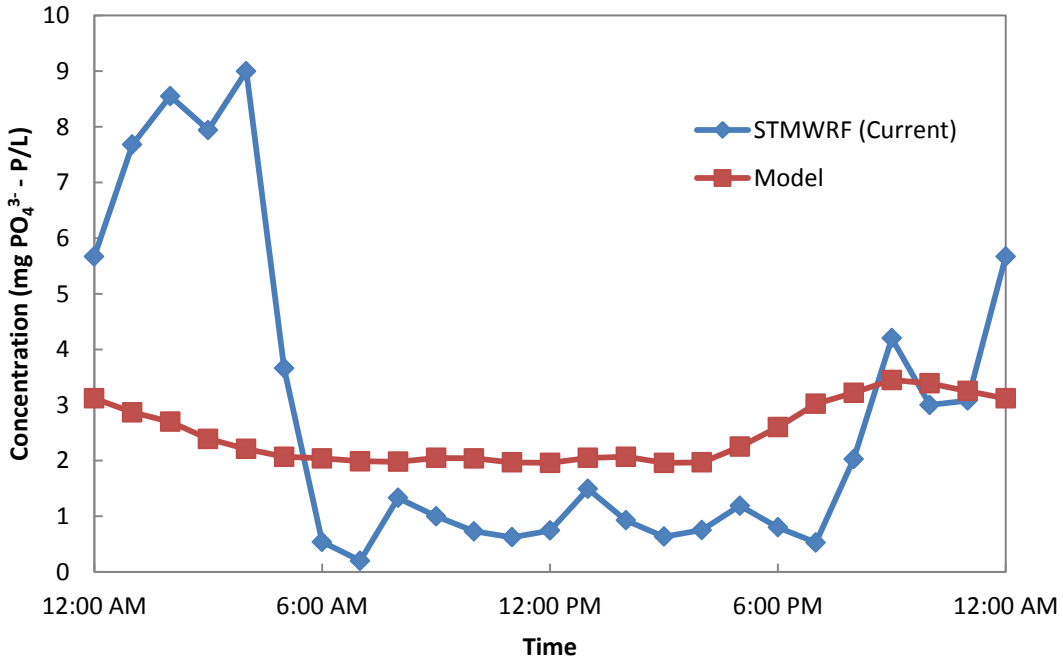

Figure 5-12: Effluent mass discharge of orthophosphate.

Table 5-5: Comparison of mass discharge of orthophosphate.

	STMWRF (Current)	Model	Difference
Mass Discharge (lbs P/day)	74.8	74.2	0.6

The last nutrient of concern was the combined concentration of nitrate and nitrite. Nitrate and nitrite were treated as a combined value, as both the laboratory testing procedures and modeling produced combined values. Unlike orthophosphate and ammonium, the model could not be calibrated sufficiently to attain the same mass discharge as the facility (Figure 5-13). For unclear reasons, STMWRF routinely experienced a large peak discharge of nitrate and nitrite in the late morning hours. The model was able to maintain a similar peak, though the magnitude was 56% lower. Due to this peak export of nitrate + nitrite, the model could not accurately mimic the mass discharge observed at the facility (Table 5-6). It is believed that this magnitude of the peak was possibly an infrequent occurrence, as the first day of testing produced a similar spike of smaller magnitude, with concentrations much closer to those that the model was producing. Therefore, despite the difference in mass discharge, it was determined that the model's output was acceptable, and would be suitable during later predictive modeling.

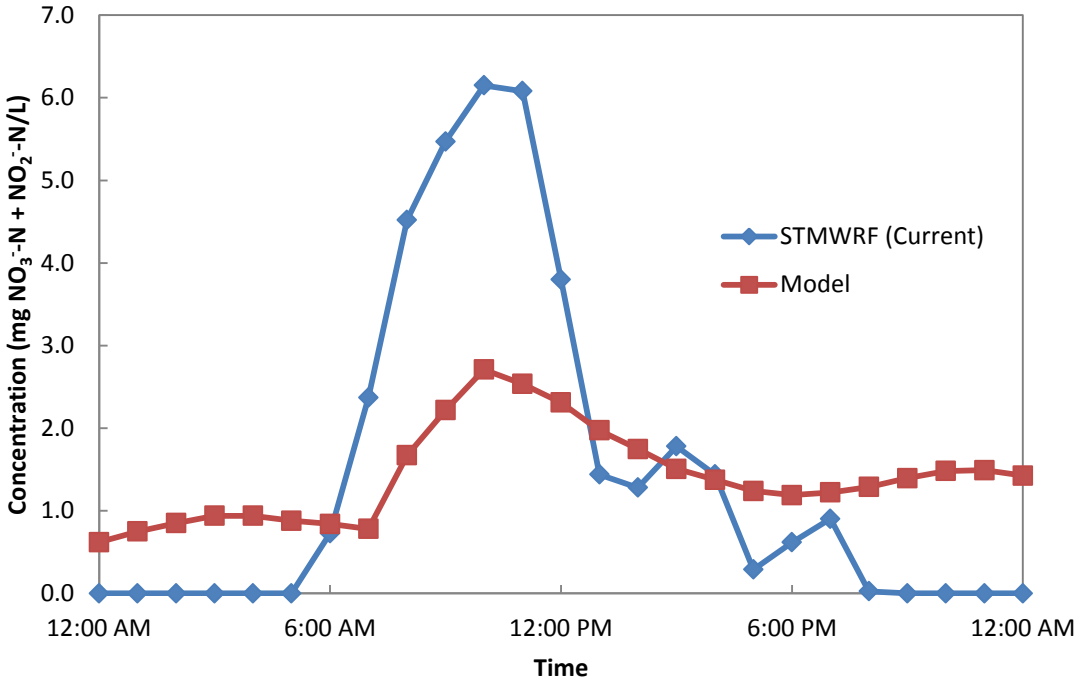

Figure 5-13: Effluent mass discharge of nitrate + nitrite.

Table 5-6: Comparison of mass discharge of nitrate + nitrite.

	STMWRF (Current)	Model	Difference
Mass Discharge (lbs N/day)	49.6	39.1	10.5

Additionally, influent data and operating conditions from the first set of data were input into the model. The model was constructed using the second set of data, and therefore it was not expected that model effluent concentrations would closely match the actual effluent concentrations from the first set of data. As expected, there was a relatively large difference between the predicted concentrations in the effluent and the actual concentrations in the effluent (Table 5-7). The average total concentration of nitrogen in the predicted effluent was 4.3 ± 0.3 mg N/L, whereas the

actual effluent concentration was 6.5 ± 0.9 mg N/L. For phosphorus, the predicted average effluent concentration was 3.6 ± 0.1 mg P/L, and the actual effluent concentration was 2.2 ± 2.1 mg P/L. The reason for this discrepancy was complex, as the facility was operating differently during the first data set, with different aeration and recycle rates when compared with the second data set. An iterative process of recalibrating the kinetic and stoichiometric values within the model while using the first and second sets of data would allow the predicted effluent concentrations to converge with the actual effluent concentrations. This iterative process would require additional time, and was considered unnecessary at this point in time. The model was constructed as a predictive tool to understand expected changes in the facility as a result of operational adjustments, and did not need to perfectly predict effluent concentrations for multiple sets of data.

Table 5-7: Comparison of mass discharges for the first data set.

	STMWRF (Current)	Model	Difference
Mass Discharge (lbs N/day)	207	140	67
Mass Discharge (lbs P/day)	59	114	58

5.4 Predictive Modeling

The next step was to experiment with operating parameters at STMWRF to find a solution to their discharge issues. As discussed, the facility operates with an on/off aeration schedule, with about 7 hours throughout the day not receiving any air (Table 5-1). The method of improving the effluent from the facility was to adjust the aeration

cycles in the oxidation ditches. In general, oxidation ditches are designed to have constant aeration; therefore, altering aeration reduces their efficiency. Since the blowers used to aerate the ditches are controlled by the operators, incorporating a new aeration cycle is a relatively easy task. Other possible adjustments to facility operation are either more difficult or expensive to implement, and would not likely have as significant of an effect on the effluent as adjusting the aeration system. These other possible changes include adjusting recycle rates or introducing new unit processes to the system. Additionally, ammonium and orthophosphate concentrations are strongly correlated to aeration. Since oxygen is the electron acceptor in the transformation reaction for ammonium, additional aeration would likely result in further reductions in ammonium concentrations [2]. For phosphorus, additional aeration would reduce the likelihood of anaerobic zones developing. Anaerobic zones are responsible for conditioning organisms in the reactor to uptake additional phosphorus. As this is the method through which phosphorus is currently removed at STMWRF, the additional air would reduce phosphorus removal [2]. Therefore, proposed adjustments to the aeration cycles were specified at the onset of the study based on the theoretical basis of oxidation ditch operation.

Each oxidation ditch at the facility currently operates under a different aeration schedule (Figure 5-14). The only difference between the two schedules is the volume of air diffused into each ditch. The diffusers in oxidation ditch #2 are in need of repair due to tears in some of the membrane diffusers. This repair is scheduled to occur in the fall of 2013. These tears result in coarse bubbles being produced (instead of fine bubbles),

which do not transfer oxygen as efficiently into the water [2]. Therefore, aeration has to be increased to ensure the same amount of oxygen is being supplied to the ditch. Other than the difference in air flow, the timing of on-off cycles is consistent between the two ditches. The maximum air flow rate for oxidation ditch #1 is slightly above 1,800 scfm (Figure 5-15). Oxidation ditch #2 has a maximum air flow rate that is nearly double, related to the inefficiency of its diffusers (Figure 5-16). When the diffusers are replaced in the oxidation ditch #2, it is expected that the air flow rate will be identical to that used in oxidation ditch #1.

Figure 5-14: Configuration of oxidation ditches (Google, 2013)

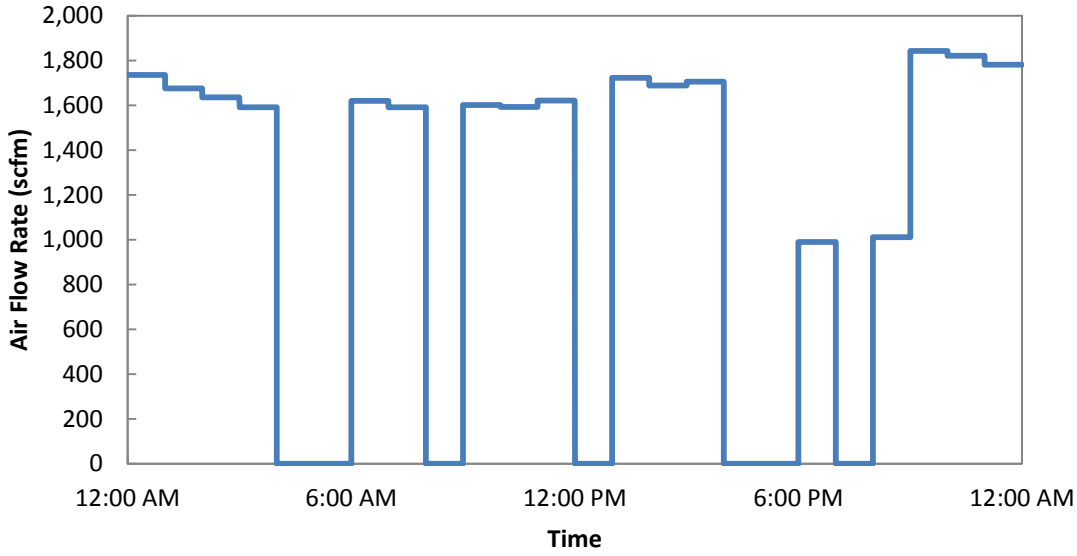

Figure 5-15: Aeration cycle for oxidation ditch #1 at STMWRF.

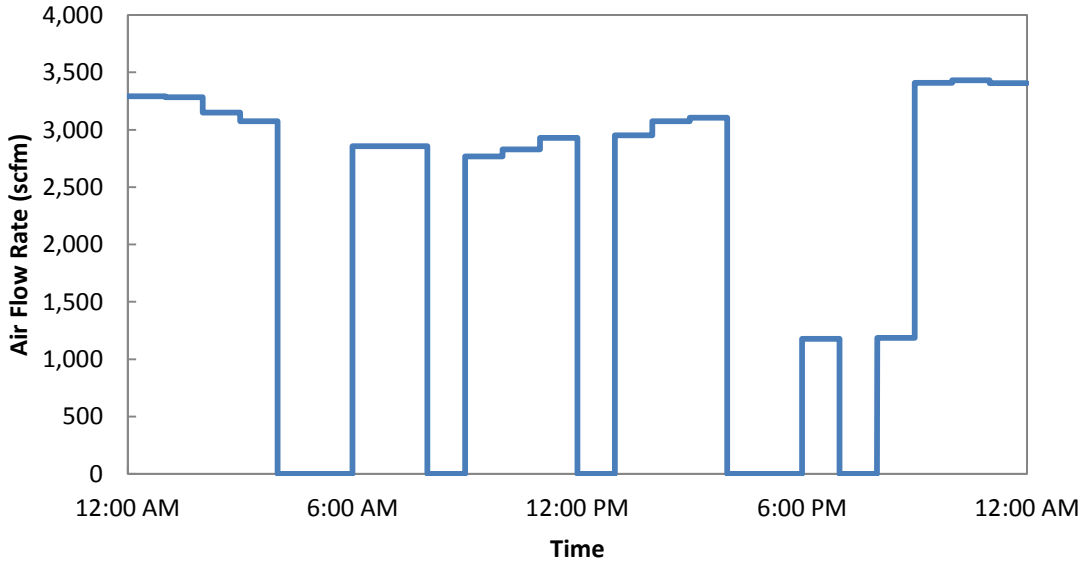

Figure 5-16: Aeration cycle for oxidation ditch #2 at STMWRF.

The initial adjustments made in the model were to incorporate continuous aeration. After this initial change, an iterative approach was used to generate an

optimized aeration scheme (OAS). The iterative approach took advantage of the ability to modify a single hour of aeration in each ditch. The aeration at each hour was individually either increased or decreased in small increments (50 scfm). Then the model was run for a period of time (approximately 25 days) to ensure stability. After this model run, the three nutrients of concern were examined to determine the effects of the modified aeration. Each hour was then further adjusted in an attempt to minimize effluent concentrations of ammonium, orthophosphate, and nitrate + nitrite. After the entire day had been optimized using this process, the method continued to ensure the stability of the approach. It is important to note that the new proposed aeration schemes were not statistically optimized. The use of the word "optimized" corresponds to a rough optimization, with values developed through non-computation methods. True optimization would require an iterative solver seeded within the model, which was not used.

5.5 Proposed Modifications to Improve Effluent Quality

The new aeration cycle proposed for the model had much lower maximum flow rates than the current cycles. Oxidation ditch #1 and oxidation ditch #2 both used the same general aeration cycle, except with different scales to accommodate the inefficient diffuser panels in oxidation ditch #2. The new proposed aeration cycle for oxidation ditch #1 had a maximum air flow of approximately 1,600 scfm (Figure 5-17). For oxidation ditch #2, the new proposed aeration cycle provided a maximum air flow of 2,800 scfm (Figure 5-18). Even though continuous aeration is recommended, the total

air added to each ditch every day remains close to the current amounts, with less than a 3% increase in total air added to each oxidation ditch (Table 5-8).

The new proposed aeration scheme was based on matching the variations in influent ammonium concentrations at the facility. As influent ammonium increased, the amount of air that should be supplied to the ditches was correspondingly increased. A comparison of influent ammonium concentrations for the first data set with aeration in oxidation ditch #1 demonstrates a reasonable correlation (Figure 5-19). However, parameters such as orthophosphate and influent flow did not correlate well.

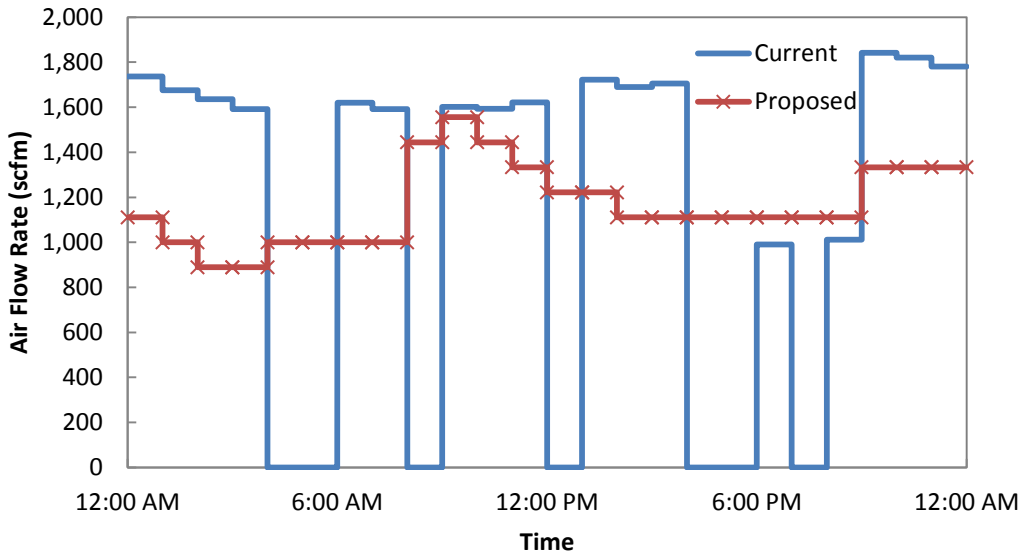

Figure 5-17: Proposed new aeration cycle for the first oxidation ditch at STMWRF.

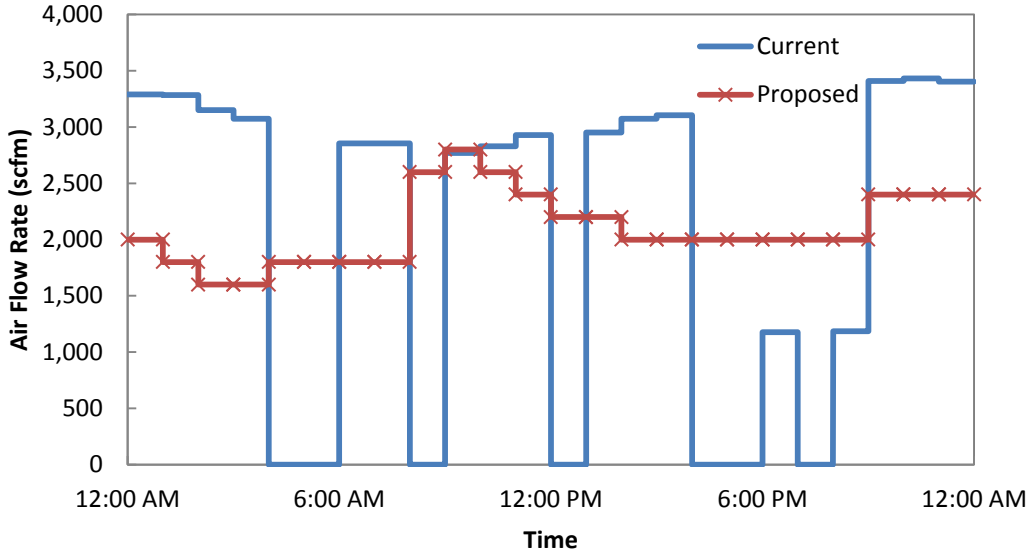

Figure 5-18: Proposed new aeration cycle for the second oxidation ditch at STMWRF.

Table 5-8: Comparison of total air supplied to oxidation ditches.

	Current Aeration (ft^3/day)	Proposed Aeration (ft^3/day)	Change
Ditch 1	39.2×10^7	40.2×10^7	+2.4%
Ditch 2	70.2×10^7	72.3×10^7	+2.9%

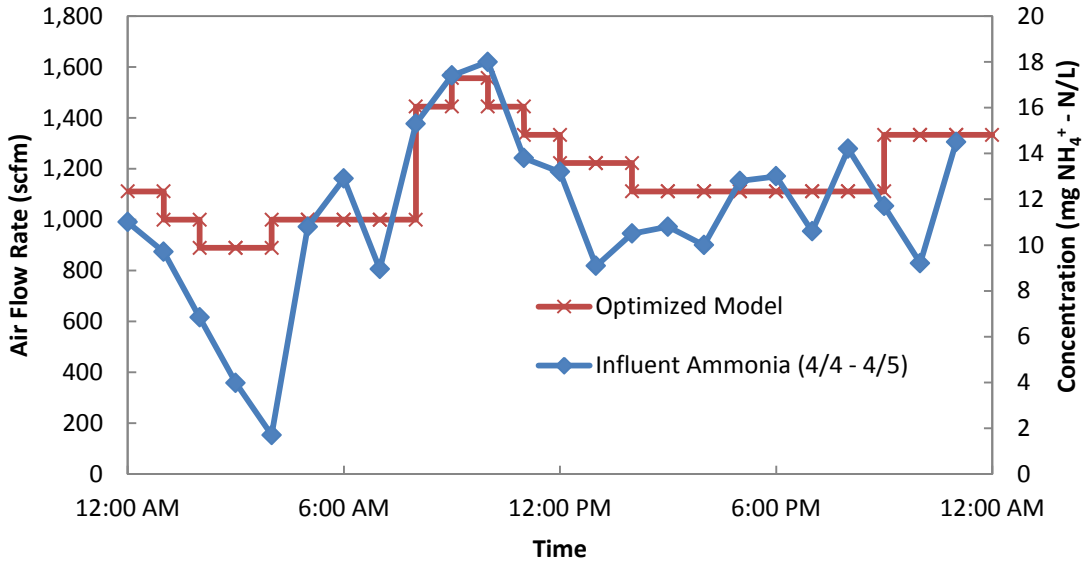

Figure 5-19: Correlation between proposed aeration cycle and influent ammonium.

As the purpose of the new aeration scheme was to reduce the effluent concentrations of ammonium, orthophosphate, and nitrate + nitrite, it is important to compare the performance of the system using the proposed aeration scheme with the current aeration scheme, in order to determine the effects on mass discharge from the system.

5.5.1 Ammonium Discharge using Optimized Aeration Scheme (OAS)

The effects of continuous aeration on ammonium concentrations can clearly be seen by the overall decrease in effluent concentrations of ammonium throughout the day (Figure 5-20). Whereas the modeled effluent concentration during the on-off aeration scheme remained between 4 mg/L and 6 mg/L with an average of 5.0 ± 0.4 mg NH_4^+-N/L, the predicted new effluent concentrations were between 3 mg/L and 4 mg/L with an average of 3.4 ± 0.34 mg NH_4^+-N/L. The effectiveness of the new aeration

scheme was also gauged using the mass discharge approach (Table 5-9). The new mass discharge rate eliminated nearly 50 pounds of additional nitrogen per day being discharged into Huffaker Hills Reservoir.

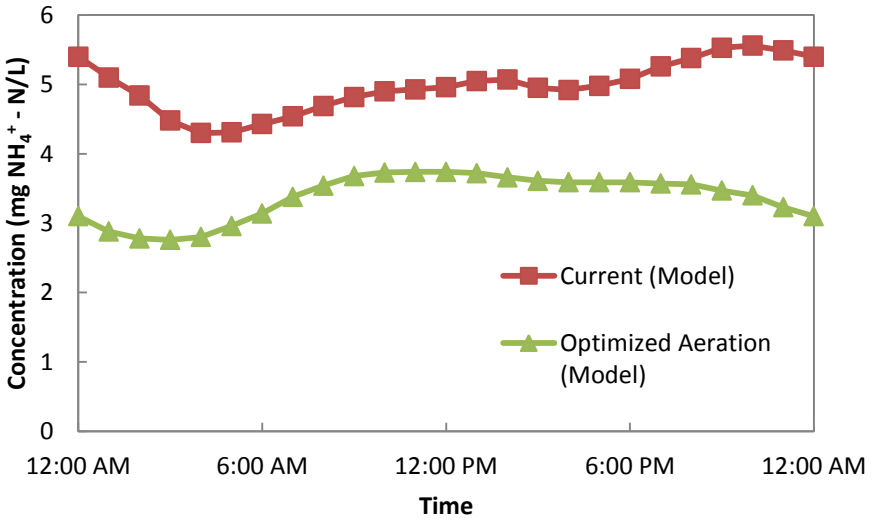

Figure 5-20: Effluent concentration of ammonium using different aeration schemes.

Table 5-9: Variations in ammonium discharge using different aeration schemes.

Current Mass Discharge (lbs N/day)	New Mass Discharge (lbs N/day)	Change in Mass Discharge
149.6	102.1	-32%

5.5.2 Orthophosphate Discharge using OAS

Orthophosphate was the next nutrient examined using the proposed new aeration scheme. In general, orthophosphate was determined to have a negative correlation with increased aeration. Due to this, the optimization of the model required careful adjustment so as to keep concentrations of both nitrogen and phosphorus in

check (as aeration needed to be increased to decrease ammonium). The proposed new aeration scheme had a less dramatic effect on the effluent concentrations of orthophosphate than it did with the effluent concentrations of ammonium (Figure 5-21). The most noticeable effect was the disappearance of a peak in orthophosphate concentrations in both the morning and evening. Throughout the midday, the concentration slightly increased over the current aeration scheme. The predicted new average effluent concentration using the proposed aeration scheme was 2.1 ± 0.2 mg PO_4^{3-} - P/L, whereas the current model average was 2.4 ± 0.5 mg PO_4^{3-} - P/L for the current aeration scheme. Overall, mass discharge was predicted to decrease by 9.9 pounds of phosphorus per day (Table 5-10).

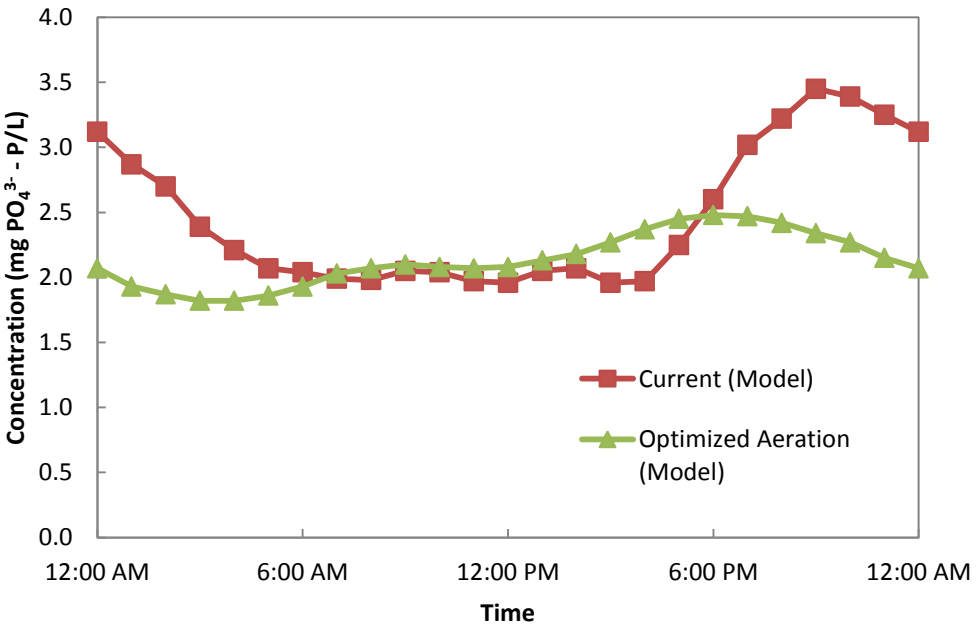

Figure 5-21: Effluent concentration of orthophosphate using different aeration schemes.

Table 5-10: Variations in orthophosphate discharge using different aeration schemes.

Current Mass Discharge (lbs P/day)	New Mass Discharge (lbs P/day)	Change in Mass Discharge
74.2	64.3	-14%

5.5.3 Impact of OAS on Effluent Nitrate + Nitritevi

Even if the discharge of ammonium exhibited a large decrease, a corresponding increase in nitrate and nitrite would negate the benefits, since algae in the can still grow using nitrate or nitrite as a nitrogen source. In general, increasing aeration will increase effluent concentrations of nitrate + nitrite, since the increase in the concentration of dissolved oxygen from aeration would decrease the size of the anoxic zone in the oxidation ditches. It is in the anoxic zone that nitrate and nitrite are transformed to nitrogen gas, and therefore removed from the system. However, by eliminating the periods without aeration, combined with overall reductions in aeration, the concentrations of nitrate + nitrite were predicted to be reduced (Figure 5-22). Concentrations were expected to remain relatively stable through the early hours, while the peaks originally observed throughout the remainder of the day were not expected to occur. The new predicted average effluent concentration was 0.7 ± 0.1 mg NO_3^--N + NO_2^--N/L, compared with model of the current system having an average of 1.4 ± 0.4 mg NO_3^--N + NO_2^--N/L. The result was a projected decrease of nearly 20 pounds of nitrogen per day (Table 5-11).

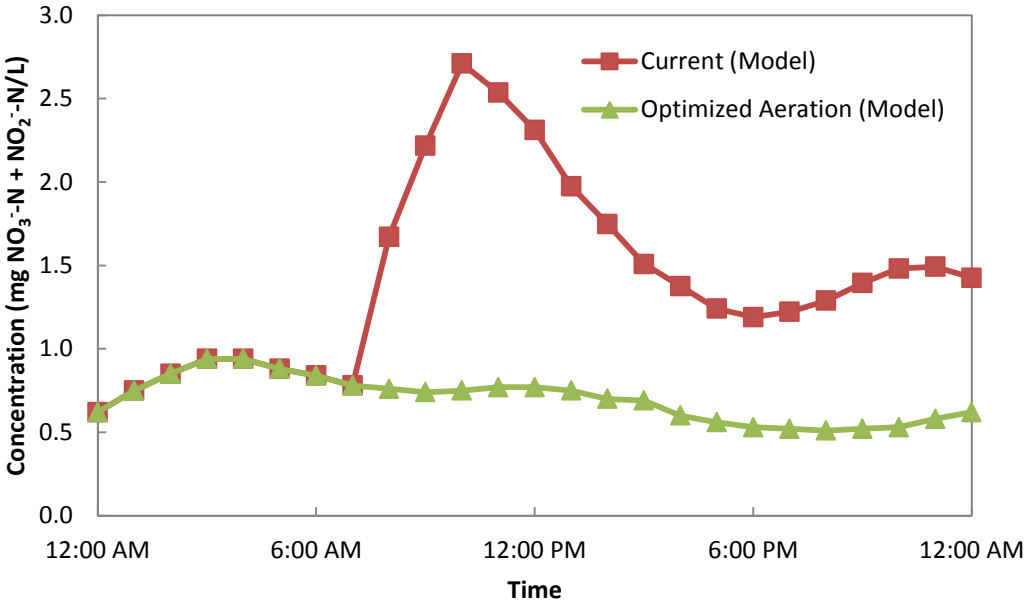

Figure 5-22: Effluent concentration of nitrate + nitrite using different aeration schemes.

Table 5-11: Variations in nitrate + nitrite discharge using different aeration schemes.

Current Mass Discharge (lbs N/day)	New Mass Discharge (lbs N/day)	Change in Mass Discharge
39.1	20.2	-48%

5.5.4 Summary of OAS

The proposed changes in aeration would likely result in small cost increases due to an increase in the total air supplied to the two oxidation ditches. The chief benefit of the proposed modified operational strategy is that the loadings of nitrogen and phosphorus to the reservoir are expected to decrease by nearly 70 pounds per day and almost 10 pounds per day, respectively. Based on typical nitrogen to phosphorus ratios of 16:1, nitrogen is the limiting nutrient to algal growth in the reservoir [5]. Reducing

the effluent concentration of the limiting nutrient will likely have a dramatic effect on the quantity of algae within the reservoir. Based on the generic formula for algae of $C_{124}N_{16}S_{1.3}P$, the maximum possible reduction in algal mass in the reservoir by this removal of nitrogen is 530 pounds per day [5]. The reduction in orthophosphate could also result in a lower mass of algae. The proposed optimized aeration scheme represents the best aeration scheme in terms of reductions in ammonium, orthophosphate, and nitrate + nitrite when compared to current effluent discharges of these compounds.

5.6 Comparison of Optimized Aeration with Alternative Aeration Cycles

To provide comparison with the optimized aeration model, two other aeration scenarios were modeled. The first was an increase in aeration above the optimized model, and the second was a decrease in aeration below the optimized model. By testing multiple aeration schemes, the results should enable Washoe County engineers to develop a suitable aeration schedule.

5.6.1 Increase in Aeration over Optimized Model

During the first alternative aeration model, the aeration cycles proposed in the optimized model were increased by 20% (Figure 5-23, 5-24). Increasing aeration generally has a positive effect on effluent ammonium, and a negative effect on effluent orthophosphate and nitrate + nitrite.

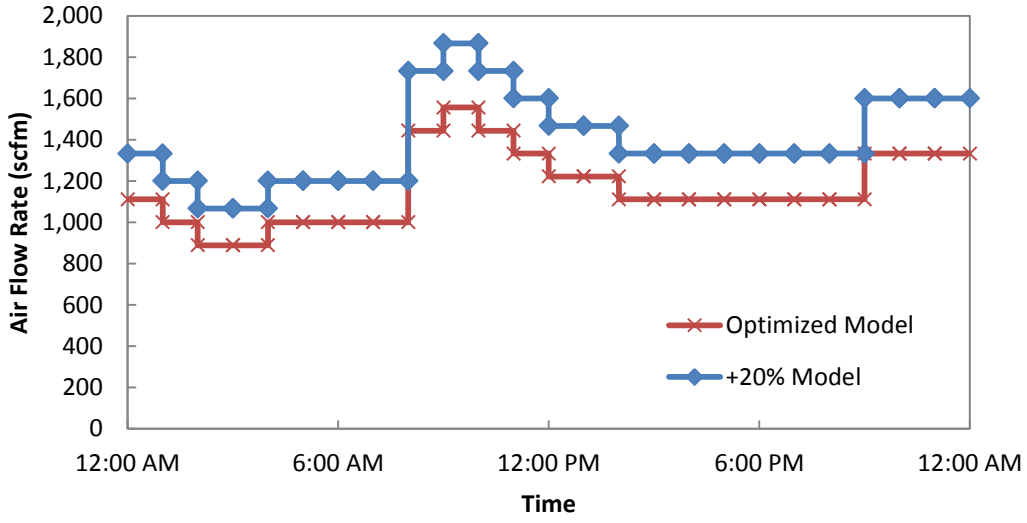

Figure 5-23: Increased aeration cycle for oxidation ditch #1 at STMWRF.

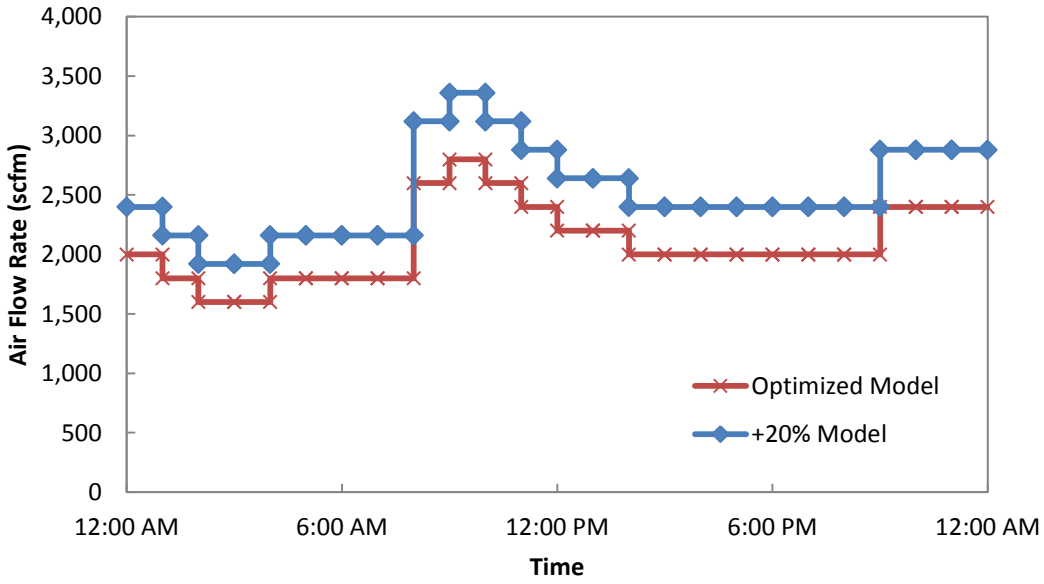

Figure 5-24: Increased aeration cycle for oxidation ditch #2 at STMWRF.

5.6.1.1 Impact of Increased Aeration on Effluent Ammonium

The most noticeable result of increased aeration was a projected drop in ammonium (Figure 5-25). Since the bacteria that perform ammonium oxidation require

oxygen, increasing aeration was expected to decrease the effluent concentrations of ammonium. The average effluent concentration was expected to drop significantly, from an average of 5.0 ± 0.4 mg NH_4^+-N/L with current aeration to 1.6 ± 0.3 mg NH_4^+-N/L. The total mass discharged was also expected to drop, with a predicted decrease in nitrogen discharged of almost 100 pounds per day compared to the current aeration strategy (Table 5-12).

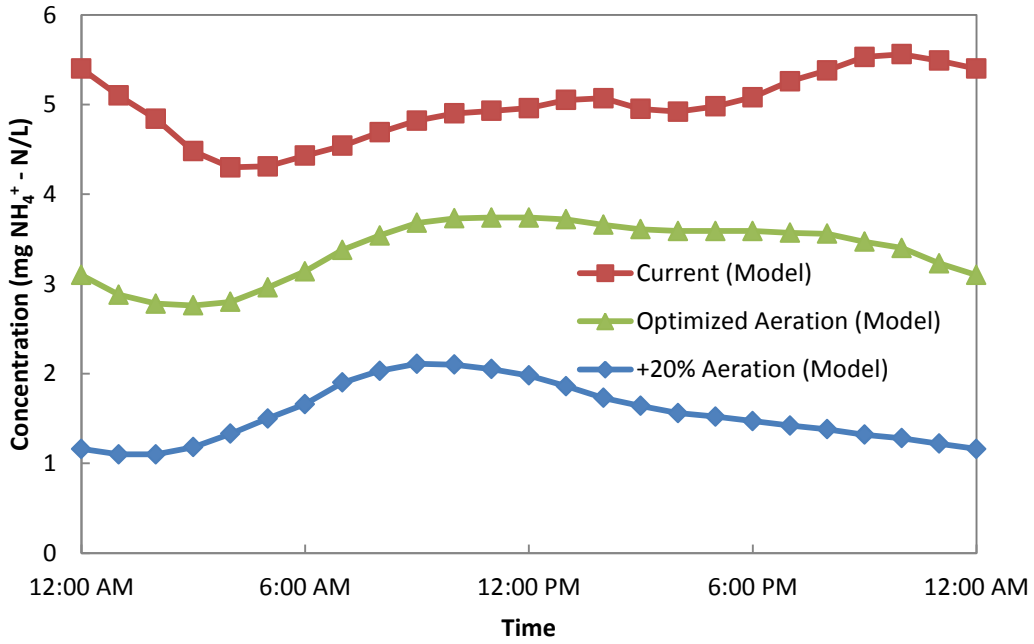

Figure 5-25: Effluent concentration of ammonium using increased aeration scheme.

Table 5-12: Variations in ammonium discharge using increased aeration scheme.

Current Mass Discharge (lbs N/day)	+20% Aeration Mass Discharge (lbs N/day)	Change in Mass Discharge
149.6	46.8	-69%

5.6.1.2 Impact of Increased Aeration on Orthophosphate

Whereas the increased aeration was expected to have a positive impact on effluent ammonium concentrations, the opposite was anticipated for orthophosphate. The increased aeration likely caused any anaerobic zones in the ditches to disappear, which resulted in less orthophosphate uptake by microorganisms in the reactors. Therefore, average effluent concentrations of orthophosphate were expected to increase from 2.4 ± 0.5 mg PO_4^{3-} - P/L to 2.8 ± 0.2 mg PO_4^{3-} - P/L (Figure 5-26). This predicted increase lead to slightly over 10 additional pounds per day of phosphorus being discharged in comparison with current facility conditions (Table 5-13).

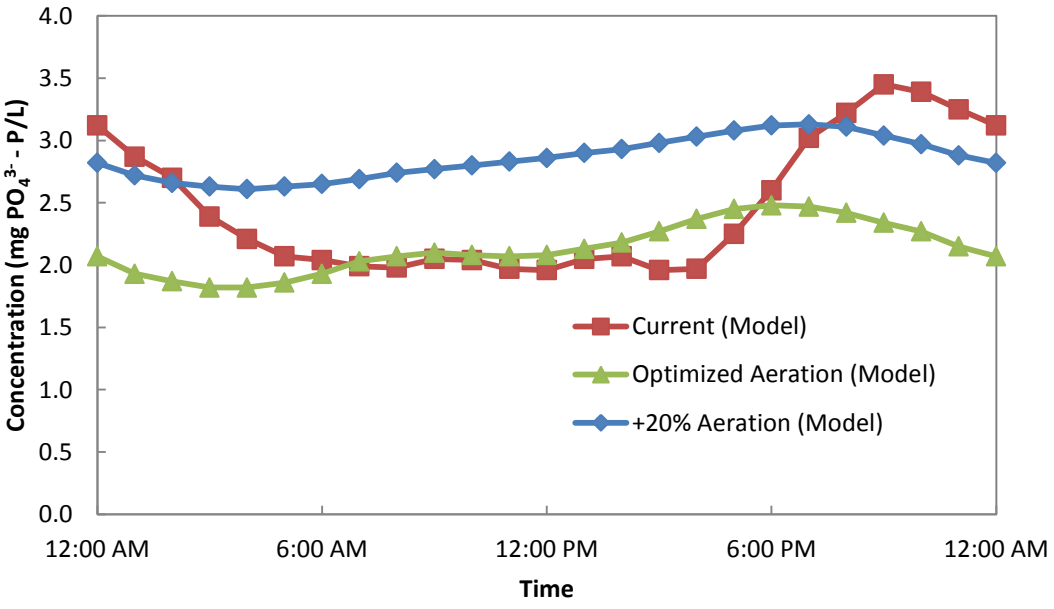

Figure 5-26: Effluent concentration of orthophosphate using increased aeration scheme.

Table 5-13: Variations in orthophosphate discharge using increased aeration scheme.

Current Mass Discharge (lbs P/day)	+20% Aeration Mass Discharge (lbs P/day)	Change in Mass Discharge
74.2	85.7	+15%

5.6.1.3 Impact of Increased Aeration on Nitrate + Nitrite

The effects of increased aeration on predicted effluent concentrations of nitrate and nitrite was similar to effects on orthophosphate. In general, nitrate and nitrite concentrations were expected to increase (Figure 5-27). As aeration increases, the size of anoxic zones in the ditches decrease, due to higher concentrations of dissolved oxygen entering the anoxic zones. Therefore, smaller effective anoxic zones would correspondingly result in less conversion of nitrate and nitrite into nitrogen gas. However, the average predicted effluent concentration of nitrate + nitrite remained similar, as the average effluent concentrations was 1.4 ± 0.4 mg NO_3^--N + NO_2^--N/L with current aeration, and 1.4 ± 0.2 mg NO_3^--N + NO_2^--N/L with the increased aeration scheme. The effect on the total mass discharge of nitrate + nitrite was small, with nearly 2 pounds of additional nitrate + nitrite nitrogen per day compared to the current model (Table 5-14).

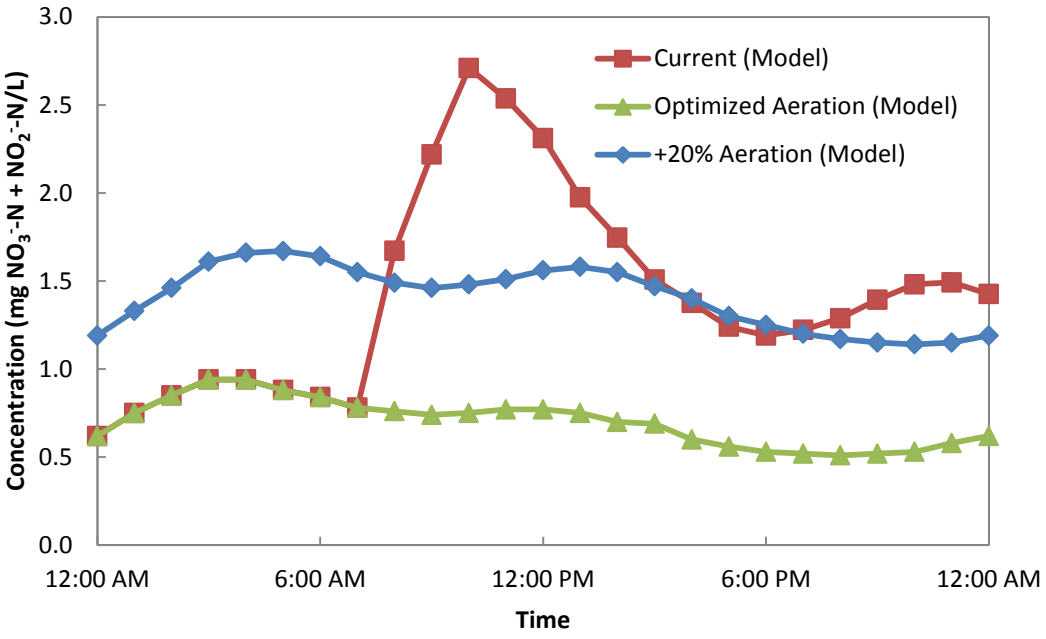

Figure 5-27: Effluent concentration of nitrate + nitrite using increased aeration scheme.

Table 5-14: Variations in nitrate + nitrite discharge using increased aeration scheme.

Current Mass Discharge (lbs N/day)	+20% Aeration Mass Discharge (lbs N/day)	Change in Mass Discharge
39.1	41.2	+5.3%

5.6.1.4 Summary of Increased Aeration Scheme

Overall, the increased aeration alternative could possibly provide STMWRF with a better approach to reduce algal growth in Huffaker Hills Reservoir than the optimized aeration strategy. Since nitrogen is the limiting nutrient in algal production in effluent from STMWRF, the ability to further reduce the total mass of nitrogen discharge could greatly reduce algal populations in the reservoir. The predicted increases in both nitrate

+ nitrite and phosphorus are relatively small and are clearly overshadowed by the large predicted drop for effluent ammonium concentrations. The mass of effluent nitrogen was expected to decrease by 100 pounds per day, while the mass of effluent phosphorus would increase by 11 pounds per day. In this scenario, nitrogen remains the limiting nutrient to algal production. A reduction of 100 pounds of nitrogen per day could potentially reduce algal mass in Huffaker Hills Reservoir by 802 pounds per day. Overall, the +20% aeration alternative has distinctive advantages to the facility should the Washoe County engineers and plant operators choose to adopt it.

5.6.2 Decrease in Aeration over Optimized Model

During the second alternative aeration, the aeration cycles proposed in the optimized model were decreased by 20% (Figure 5-28, 5-29). Decreasing aeration was expected to have an opposite response compared with the +20% model. General expectations were an increase in the mass discharge of ammonium in the effluent, and decreases in the mass discharges of orthophosphate and nitrate + nitrite in the effluent.

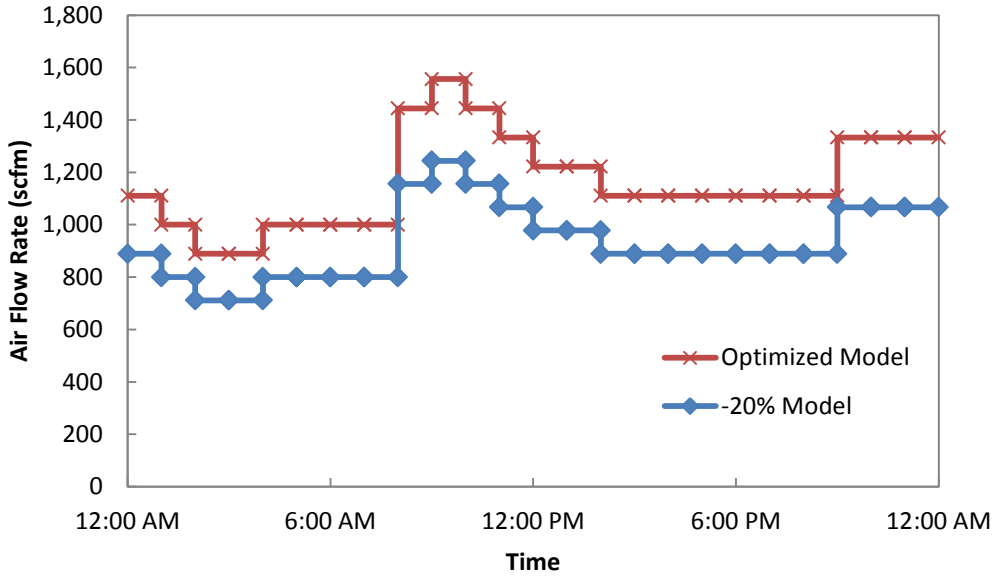

Figure 5-28: Decreased aeration cycle for the first oxidation ditch at STMWRF.

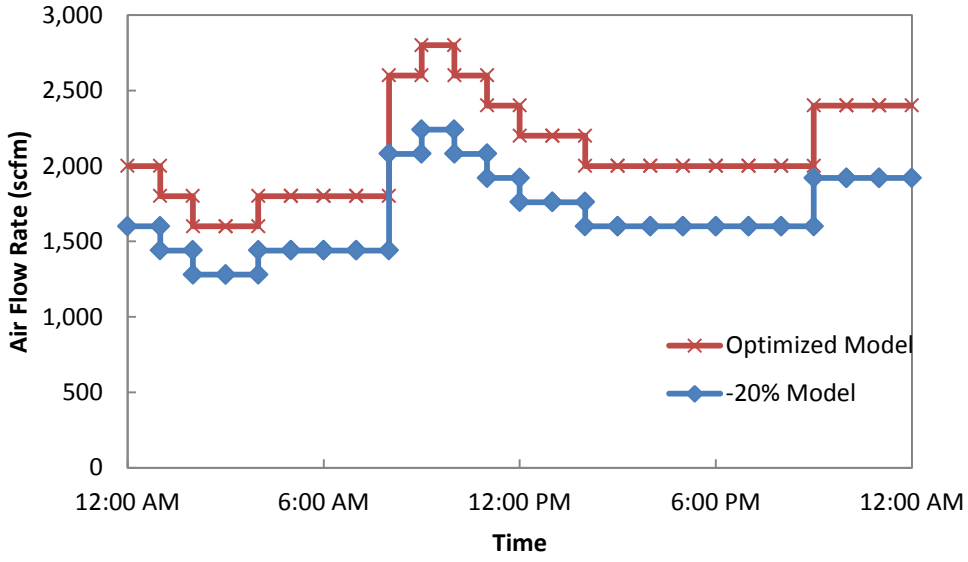

Figure 5-29: Decreased aeration cycle for the second oxidation ditch at STMWRF.

5.6.2.1 Impact of Decreased Aeration on Effluent Ammonium

As oxygen is required to convert ammonium to nitrate in the aerobic zone of the oxidation ditch, a decrease in the amount of oxygen supplied was expected to limit this

step from completely occurring. Therefore, an increase in ammonium in the effluent was expected (Figure 5-30). The average ammonium concentration in the effluent was drastically elevated, to an average of 9.0 ± 0.4 NH_4^+-N/L, up from the current model average of 6.2 ± 2.0 mg NH_4^+-N/L. The mass discharge increased as well, adding more than 100 additional pounds of nitrogen per day to the effluent (Table 5-15).

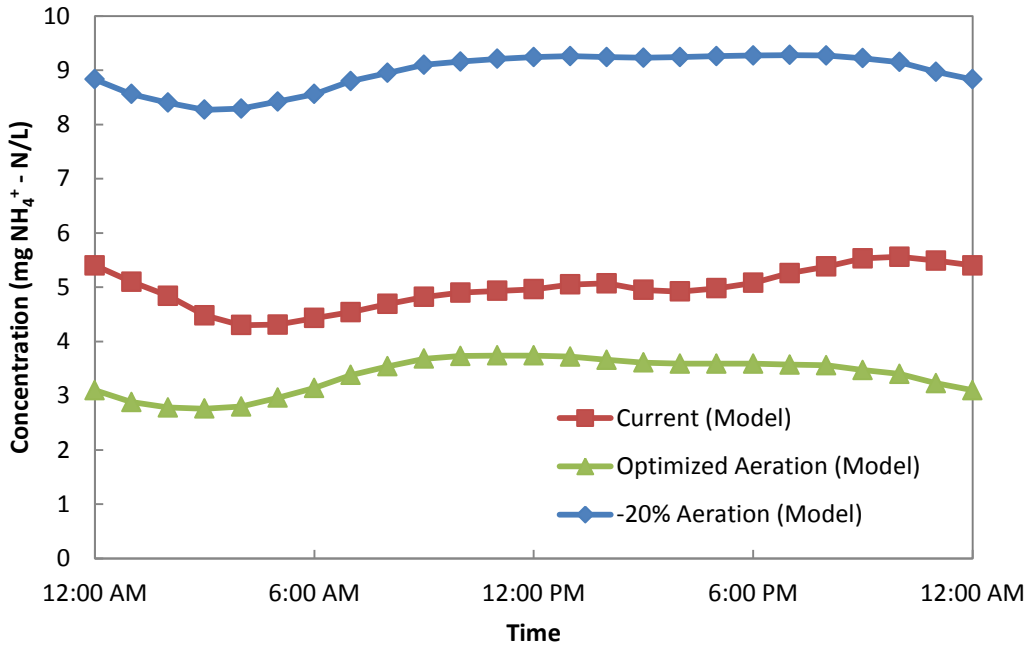

Figure 5-30: Effluent concentration of ammonium including decreased aeration scheme.

Table 5-15: Predicted variations in ammonium discharge using decreased aeration scheme.

Current Mass Discharge (lbs N/day)	-20% Aeration Mass Discharge (lbs N/day)	Change in Mass Discharge
149.6	268.3	+79.3%

5.6.2.2 Impact of Decreased Aeration on Effluent Orthophosphate

In theory, decreasing aeration would be expected to decrease effluent concentrations of orthophosphate, as dissolved oxygen in the aerobic zones would be quickly consumed, promoting the growth of anoxic zones in the oxidation ditches. The larger anoxic zones would be more likely to have insufficient electron acceptors, resulting in anaerobic zones. Anaerobic zones are responsible for conditioning microorganisms to uptake additional phosphorus within biomass, resulting in a decrease of phosphorus in the effluent from the oxidation ditches. Therefore, a decrease in effluent concentrations of orthophosphate was predicted (Figure 5-31). The effluent concentrations of orthophosphate for the decreased aeration alternative maintained an average of 1.4 ± 0.1 mg PO_4^{3-} - P/L, whereas the concentrations using the current aeration strategy were 2.4 ± 0.5 mg PO_4^{3-} - P/L. Additionally, the mass of phosphorus discharged was reduced by 30 pounds per day compared to the current aeration strategy (Table 5-16). It is noteworthy that operation of the secondary clarifier would need to be carefully monitored, to ensure that anaerobic conditions did not occur. If conditions in the secondary clarifiers were allowed to become anaerobic, then it is possible that stored phosphorus would be released, resulting in higher effluent concentrations of phosphorus.

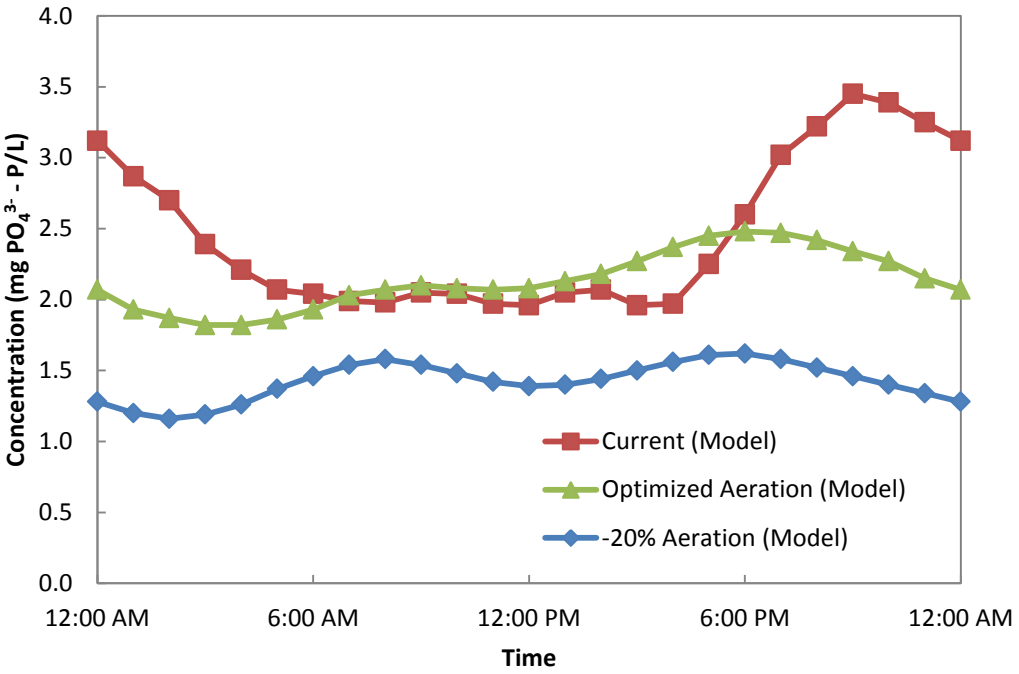

Figure 5-31: Effluent concentration of orthophosphate including decreased aeration scheme.

Table 5-16: Predicted variations in orthophosphate discharge using decreased aeration scheme.

Current Mass Discharge (lbs P/day)	-20% Aeration Mass Discharge (lbs P/day)	Change in Mass Discharge
74.2	42.6	-42.6%

5.6.2.3 Impact of Decreased Aeration on Effluent Nitrate + Nitrite

With the potential for less ammonium being converted to nitrate + nitrite, the total amount of nitrate + nitrite that needs to be removed correspondingly decreases. Anoxic zones also increase in size, as DO levels drop quickly in the aerobic zones due to

the lower oxygen supply. Overall, these system responses to lower aeration result in lower effluent concentrations of nitrate + nitrite. The predicted combined effluent concentrations of nitrate + nitrite with the decreased aeration alternative reached a new low of 0.26 ± 0.0 mg NO_3^--N + NO_2^--N/L, compared with the predicted average concentration of 1.4 ± 0.4 mg NO_3^--N + NO_2^--N/L for the current aeration scenario (Figure 5-32). The mass of nitrate + nitrite in the effluent also decreased to 7.6 pounds of nitrogen a day, a decrease of more than 30 pounds per day of nitrogen (Table 5-17).

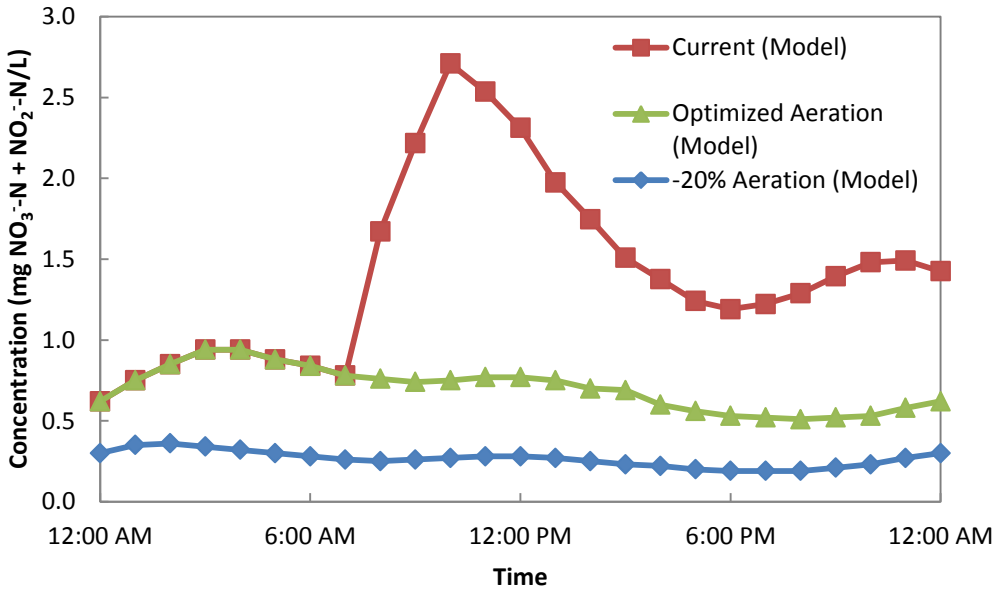

Figure 5-32: Effluent concentration of nitrate + nitrite including decreased aeration scheme.

Table 5-17: Predicted variations in nitrate + nitrite discharge using decreased aeration alternative.

Current Mass Discharge (lbs N/day)	-20% Aeration Mass Discharge (lbs N/day)	Change in Mass Discharge
39.1	7.6	-80.5%

5.6.2.4 Summary of Reduced Aeration Alternative

Whereas the predicted data from the +20% aeration alternative suggested relatively positive results could be achieved at STMWRF, the -20% aeration alternative predicted poorer overall performance. The marked increase in effluent concentrations of ammonium which were predicted make this aeration alternative undesirable. While small decreases in effluent concentrations for both orthophosphate and nitrate + nitrite were generally beneficial, they became less significant when weighed against an increase in the total mass of nitrogen discharged each day of 100 of nitrogen compared to current amount discharged at STMWRF. The only benefit of this aeration scheme would be reduced energy costs; however, the loss of water quality was not consistent with the cost savings.

5.7 Potable Water Reuse at STMWRF

The objective of the second phase of the project was to develop a novel wastewater treatment system with three goals in mind: 1) reduce energy consumption, 2) improve pollutant removal and transformation, and 3) produce a high quality potable effluent. The proposed system incorporated proven technologies, and combined them in such a manner that individual processes could enhance the strengths and minimize

the weaknesses of other processes. This methodology resulted in a system that incorporated the following unit processes: forward osmosis, membrane distillation, an anaerobic membrane bioreactor, SHARON/ANAMMOX, and struvite precipitation. Based on these initial system components, the second phase of the project proceeded in three main parts. Part 1 consisted of research into the chosen technologies (as outlined in the literature review). The purpose of this part was to determine typical operating conditions, flexibility, and expected treatment efficiencies for each unit process. Part 2 involved the use of computational simulations to predict the treatment effectiveness of the system. The wastewater design program *BioWin* was again used for this phase due to its success in modeling STMWRF in the first phase. Part 3 compared the inputs and outputs from the system in comparison with an existing water reuse facility. Using the *BioWin* model from Part 2, the performance of the system could be thoroughly predicted over a wide array of costs, including pumping, heating, aeration, methane harvesting, magnesium addition, and struvite capture.

5.7.1 Design of the Proposed Potable Reuse Treatment System

The design and configuration of the proposed system adapted emerging technologies and combined them such that they can support the requirements of a wastewater treatment facility. The design also took full advantage of osmotic and membrane technologies, especially recent advances in research that have been achieved in these fields. The five individual processes which were proposed included forward osmosis (FO), membrane distillation (MD), an anaerobic membrane bioreactor (AnMBR), SHARON and ANAMMOX, as well as struvite precipitation. These unit

processes were selected based on their relatively low-energy requirements, highly efficient performance, and ability to be integrated together. The original design scenario was based on the idea of complete recycle from the solids circuit (AnMBR, SHARON and ANAMMOX, and struvite precipitation). Based on that scenario, the facility would only have a potable effluent from the membrane distillation unit and no other liquid effluent discharges (Figure 5-33). Conceptually, this implies that all organic and inorganic compounds in the influent wastewater are being removed through production of methane, nitrogen gas, struvite, and sludge in the AnMBR. This original design scenario had to be modified, as it was discovered during initial simulations that concentrations of chloride were predicted to accumulate within the system. Chloride was being introduced into the system from two unit processes, namely forward osmosis and struvite precipitation. During forward osmosis, the draw solute ($MgCl_2$) would diffuse across the membrane from the draw solution into the influent wastewater through reverse solute flux. During struvite precipitation, magnesium chloride ($MgCl_2$) is also added as a source of magnesium for the struvite ($MgNH_4PO_3$). The magnesium would precipitate out as struvite; however, the chloride had no outlet and its concentration would gradually accumulate within the system. The disadvantage of elevated chloride concentrations was enough to modify the design. Primarily, chloride on the feed side of the FO membrane would reduce the osmotic pressure difference between the feed and the draw solution, thereby reducing flux through the membrane. Secondly, elevated concentrations of chloride would likely adversely affect the microorganisms in the AnMBR. Therefore, a non-potable effluent (also referred to as

the #2 effluent – not seen in Figure 5-33) was incorporated into the design after the struvite precipitation unit process in order to regulate concentrations of chloride within the system. The splitter at the non-potable effluent was chosen to split the influent flow from solids handling by half. Therefore, half of the flow would be discharged as a non-potable effluent, and the other half would be recycled back to the influent of the facility. The decision to split the flow by half at the non-potable effluent was based on chloride concentrations in the flow. By choosing a split of 50%, the chloride concentrations in the non-potable effluent would be approximately 304 mg/L Cl^- during the 50% recovery scenario and 374 mg/L Cl^- in the 70% recovery scenario. Even at these concentrations, there is concern that the concentration of chloride would be elevated sufficiently to affect the growth of plants, should the water be used for irrigation and landscaping. Chloride concentrations above 350 mg/L Cl^- may result in “severe” use restrictions on sensitive crops; however, the amount of water discharged from the non-potable effluent can be adjusted to reduce effluent chloride concentrations, such that chloride concentrations are suitable for the chosen applications of the reuse water [93].

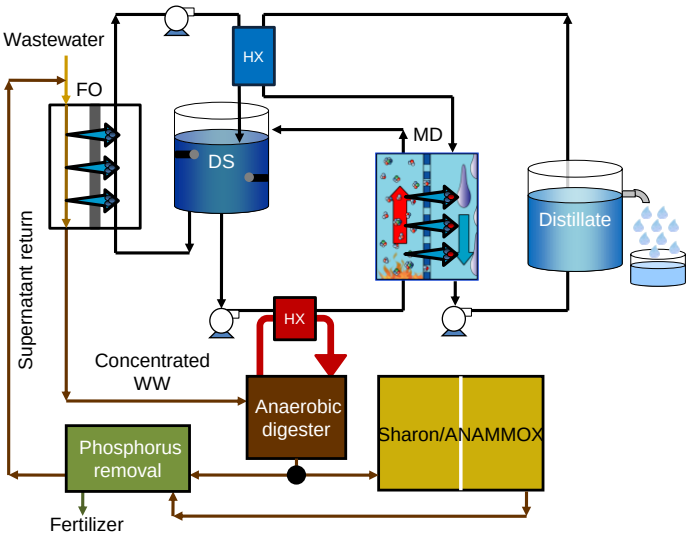

Figure 5-33: Proposed low-energy potable reuse system.

5.7.2 Modeling the Performance of the Proposed Potable Reuse System

The model was configured to simulate the operating conditions found at STMWRF. Using the model, the predicted performance of the proposed reuse system could be compared to the of the current treatment system in place. The model would use the same influent concentrations for the average flow conditions that STMWRF currently experiences (Table 5-18). The influent data were not the same as used for the first phase of the project, since it was desirable to use typical data for water reuse systems. Once completed, the model allowed a comparison between the outputs. Membrane distillation was not included in the model since it is not an available unit process in *BioWin*, and therefore its performance could not be accurately estimated using the software. Forward osmosis was also not specifically included in the model, though the process could be simulated through the use of a membrane bioreactor. By altering the characteristics of the membrane bioreactor, it was possible to simulate the

performance of a forward osmosis system. The final *BioWin* model was able to incorporate all of the other remaining unit processes (Figure 5-34).

Table 5-18: Influent conditions used in the potable reuse model.

Parameter	Value		Parameter	Value
Flow	3 MGD		COD	300 mg COD/L
TKN	20 mg N/L		Total Phosphorus	5 mg P/L
Nitrate	0.3 mg N/L		pH	7.3
Alkalinity	5.5 mmol/L		Calcium	45 mg/L
Magnesium	15 mg/L		Dissolved Oxygen	0 mg/L

The master variable of the model was the water recovery percentage in the forward osmosis sub-system. Based on a literature review, this value typically varies between 50% and 70%. Therefore, two separate models were developed to accommodate the potential range of water recovery scenarios. In the 50% recovery scenario, half of the influent flow would pass through the forward osmosis membrane and continue on to membrane distillation. In the 70% recovery scenario, 70% of the influent flow would pass through forward osmosis and continue to membrane distillation. In both models, half of the flow was diverted at the end of the solids treatment loops (i.e., AnMBR, SHARON and ANAMMOX, struvite precipitation), and discharged as a non-potable effluent. The remaining water was recycled back into the influent of the plant. Due to this recirculation, the amount of water flowing through the initial FO unit is actually greater than the influent flow into the plant. Therefore, the two recovery scenarios were relabeled to incorporate the recycle flow. The 50%

scenario resulted in 67% water recovery (Figure 5-35), and the 70% scenario resulted in 83% water recovery (Figure 5-36).

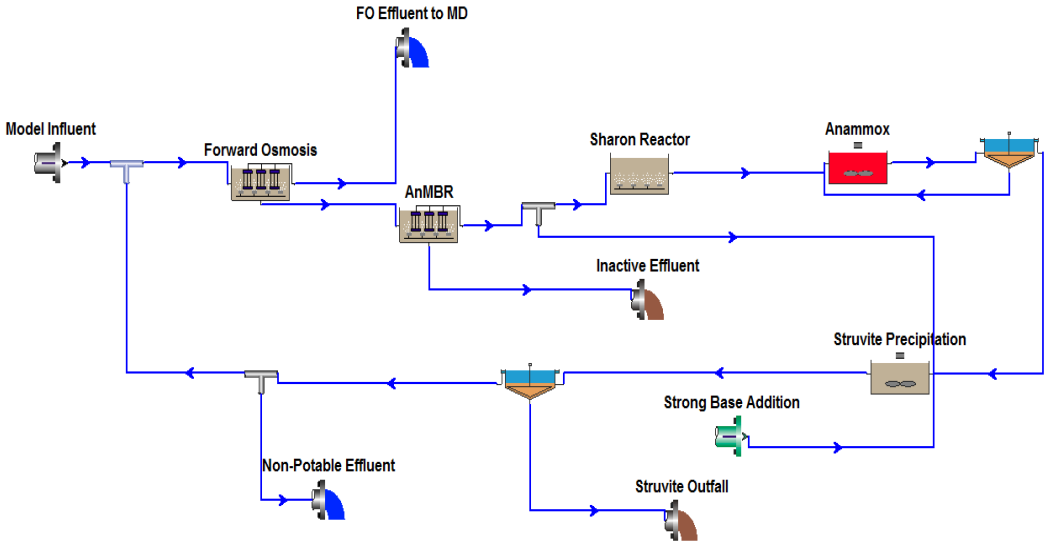

Figure 5-34: Representation of potable reuse system in *BioWin*.

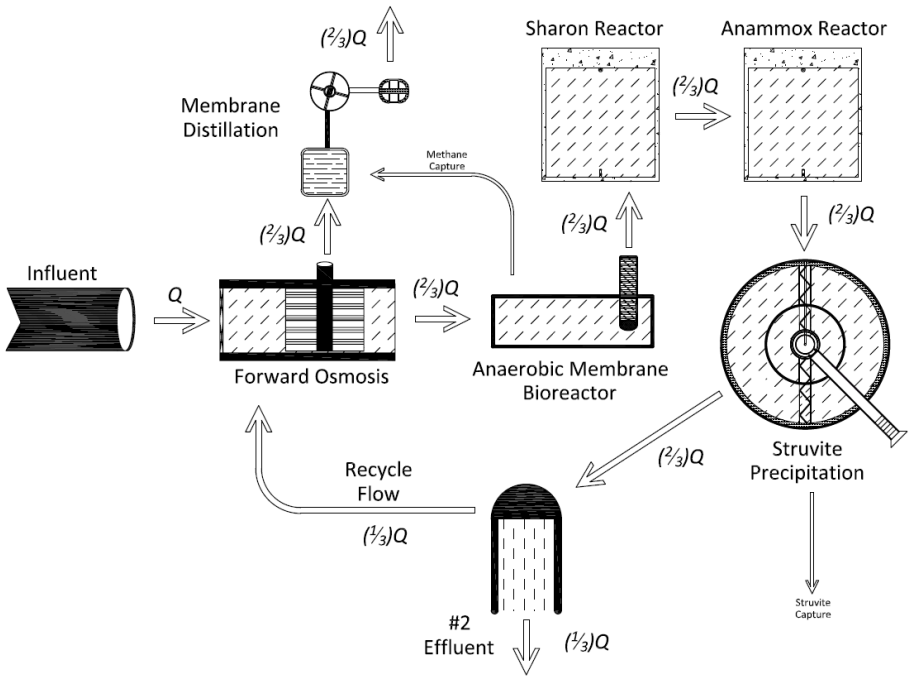

Figure 5-35: Flow diagram of potable reuse system using 67% FO water recovery.

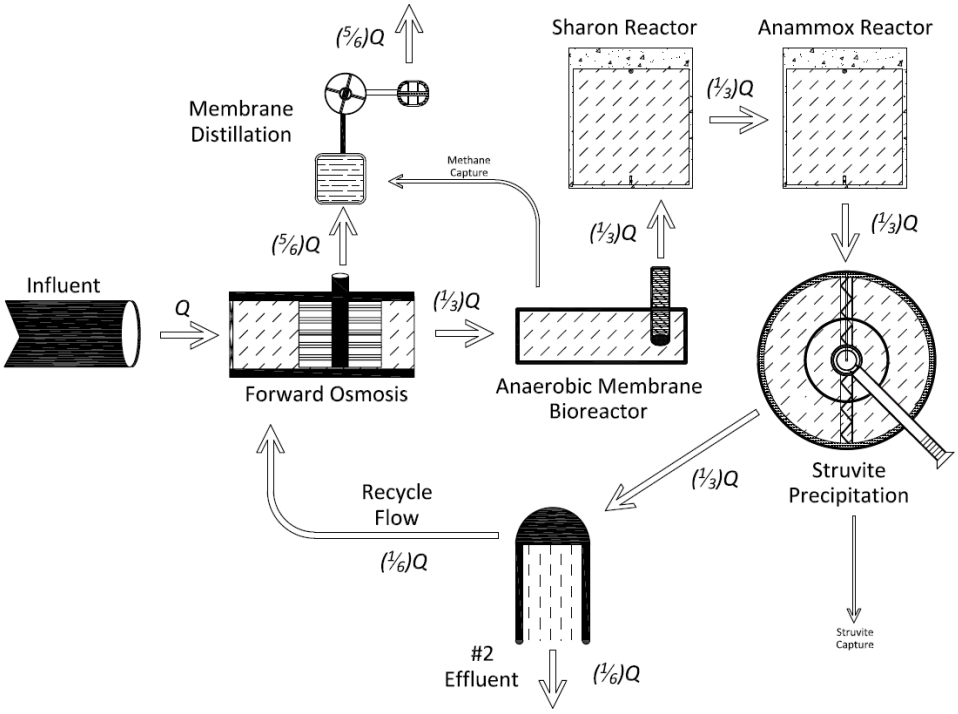

Figure 5-36: Flow diagram of potable reuse system using 83% FO water recovery.

In order to minimize energy costs for the facility, the design incorporated resource recovery. The most important of these pathways was the generation of methane in the AnMBR. As described in the literature review, anaerobic treatment systems can generate methane. This amount of methane produced is combined value; it consists of an off-gas flow and dissolved methane within the reactor. Once harvested, this methane could potentially be used as an energy source to partially power other functions within the facility. It is anticipated that the majority of the methane produced will be used to offset the cost of heating water during the MD step. Since MD is the most energy intensive unit process in the proposed system, any reductions in the cost of MD will improve the overall projected energy profile. The second method of resource

recovery is related to production of struvite. Phosphorus in the treatment process could be precipitated as struvite. Since struvite can be used as a fertilizer for crops, it could potentially be sold to offset operational and maintenance costs.

5.7.3 Comparison of Model Results to Current Practices at STMWRF

After the computer model of the proposed system was developed, it was used to predict effluent concentrations from each of the recovery scenarios (Table 5-19). The model demonstrated that the design of the proposed system effectively in treated influent contaminants, with relatively low effluent concentrations remaining in the non-potable effluent. However, the model was unable to predict any information concerning the quality of the potable water being produced by the membrane distillation module. Previous research has generally suggested that the MD process can produce a high-quality effluent [30,33-52].

Table 5-19: Predicted quality of non-potable effluent compared to actual quality of non-potable effluent[g]

	67% Recovery	83% Recovery	STMWRF
BOD_5 (mg/L)	2.4	2.5	4.3
Total Suspended Solids (mg/L)	0.1	0.1	3.6
Nitrate (mg N/L)	0	0	1.9
Nitrite (mg N/L)	6.2	6.9	0.3
Ammonium (mg N/L)	5.8	5.8	1.4
Total Phosphorus (mg P/L)	1.6	1.9	4.2

[g] Data for STMWRF provided by Washoe County [3].

When comparing the results predicted by the model to the current observed values at STMWRF, a few clear trends became apparent. In terms of the model, the model using 83% recovery slightly underperformed when compared to the model using 67% recovery. However, both models outperformed STMWRF when it came to BOD_5, TSS, nitrate, and total phosphorus. The two parameters that had higher effluent concentrations than STMWRF were nitrite and ammonium. The reason for these elevated values is due to an issue with the ANAMMOX reactor in the model. During the ANAMMOX process, nitrogen in nitrite and ammonium are released as nitrogen gas. This metabolic pathway reportedly releases 80% - 99% of the nitrogen in the system as long as near equal molar concentrations of nitrite and ammonium are entering the reactor [67]. This prerequisite was satisfied in the model, with nearly equal molar concentrations of the two compounds entering the ANAMMOX reactor. The problem was that the ANAMMOX reactor only converted approximately 50% of the influent nitrogen into nitrogen gas, leaving a relatively high residual concentration of the two species. After further research into the issue, it was recommended that the use of a different reactor design could solve the problem. The ANAMMOX reactor in *BioWin* was modeled as a continuously stirred tank reactor (CSTR), whereas other research suggested that alternative reactor designs, such as an upflow anaerobic sludge blanket (UASB) reactor, may be more effective [67,76]. Therefore, future models and should consider using a UASB reactor for the ANAMMOX process.

With the system exercise completed, the result indicated that the proposed design could produce a high quality non-potable effluent. It should be stressed,

however, that this effluent only represents a small portion of the water in the system (17-33%), as the majority of the flow is either being recycled or discharged as potable water from the MD subsystem.

5.7.4 Energy and Chemical Requirements

Part 3 of the second phase of the project examined inputs and outputs from the proposed potable reuse system. After the model of the proposed system was developed, an analysis of anticipated chemical and energy requirements was conducted. Alongside these inputs, the system could also be analyzed for its sustainability measures such as methane harvesting and struvite capture. This would enable annual operating and maintenance costs for the proposed system to be compared to the operating and maintenance costs for more conventional wastewater treatment facilities. More specifically, the performance of the proposed design could be directly compared to the existing conditions and systems used at STMWRF, to assess the feasibility of replacing the existing facility with a similar fully functional water reuse and resource recovery system.

5.7.4.1 Chemical Requirements

Two main chemicals are vital to the operation of the proposed facility: sodium hydroxide and magnesium chloride. Magnesium chloride serves mainly as the draw solute for forward osmosis. It also serves a dual purpose as the magnesium source for struvite precipitation. Model runs suggested that sufficient magnesium will cross the FO membrane (through reverse solute flux) to supply the magnesium needs for the struvite precipitation process. However, conservative cost estimates assumed that this amount

was insufficient and that magnesium had to be separately dosed at the struvite precipitation reactor. Factors affecting the yearly cost of dosing magnesium chloride include the cost of the magnesium chloride itself, which was found to cost $150 to $300 per ton at 85% to 99% purity [94]. Sodium hydroxide serves only to raise the pH of the struvite reactor to the pH range of 8 to 9. Without increasing the pH, struvite would be less likely to form and would greatly reduce the efficiency of the process. Sodium hydroxide was found to cost $320 to $360 per ton. Using these costs, a yearly cost for chemical inputs was developed, with a range between the minimum and maximum expected costs (Table 5-20)

5.7.4.2 Energy Requirements

Energy costs for the facility were comprised of three main categories: pumping, aeration, and heating. In a common wastewater treatment facility, the two main costs are usually pumping and aeration. Aeration is expensive due to the fact that supplying oxygen to wastewater is an inefficient process, with a large percentage of the supplied air being lost to the atmosphere. Most traditional facilities rely on aerobic degradation pathways, and therefore have high aeration energy costs. Pumping is common energy cost in most water treatment facilities, as few plants are situated on an elevation gradient that can be used to move water around the entire facility by gravity. Furthermore, effluent pumping is an unavoidable cost for a system that supports water reuse. Heating costs are usually associated with solids handling using anaerobic digestion, as these processes required elevated temperatures. The proposed design is able to keep heating costs low, though, through its resource recovery processes.

For this design, pumping costs could not be calculated directly from the model. As an actual plant location was not chosen, natural topography could not be considered. Therefore, general pumping costs for the facility were estimated using pipe sizes between 24 and 48 inch diameters, at increments of 6 inches. An assumed length of pipe for the network was 1,000 feet. Using average roughness coefficients and efficiencies for a 24 hour pumping cycle, a minimum and maximum yearly pumping cost were calculated (Table 5-20) [3]. The cost of pumping from the MBR (considered to be a significant cost) was calculated using relationships derived from other actual facilities, which a power requirement between 0.15 and 0.3 kWh/m^3 (Table 5-20) [95]. As the proposed design stressed low-energy systems, the SHARON reactor was the only process that required aeration. The bioreactor used in the SHARON process requires a minimal dissolved oxygen content of near 1 mg/L [67]. The cost of aeration was also correlated from actual plant data, using blowers supplying either 2,210 scfm or 3,400 scfm [96]. By calculating oxygen uptake rates, oxygen transfer efficiencies, and the total required oxygen, a kWh requirement for aeration was calculated for the SHARON process, resulting in a yearly cost (Table 5-20) [2]. Heating costs could be directly calculated from values in the model. All energy values (in kWh) were converted to costs based on the price that STMWRF pays for energy. This average daily cost of energy was $0.087/kWh based on data provided by Washoe County [3]. The heating cost for the reactors was calculated using the specific heat capacity of water (4.18 J/g*K) to generate power costs based on the flow of water being heated (Table 5-20) [2]. The minimum value represents heating using an ideal case, in which no inefficiencies or

losses exist. In application, these costs are expected to be higher. An accurate prediction of losses in the system could not be made at this point in time; however, the maximum cost was calculated using a heating efficiency of 55% [97].

5.7.4.3 Facility Costs

With energy costs calculated, the sustainable elements of the facility could be included in the analysis. This included both methane harvesting and struvite recovery. Unfortunately, a fair market price was difficult to obtain for struvite, so a minimal value of $0.10/kg was assumed. It is likely this value is an underestimate, and therefore the potential energy offset of struvite production would actually be higher. The amount of struvite produced was calculated by the change in phosphorus concentrations in the struvite precipitation reactor. Then, using the assumed cost of struvite, a yearly profit was calculated (Table 5-20). Methane recovery represented a heat source that would likely be used to minimize the costs of heating required for membrane distillation. The amount of heating costs offset depended on which recovery scenario was being used. In the 67% recovery scenario, a larger percentage of heating costs were offset due to less flow passing through membrane distillation. The scenario with 83% recovery had a larger flow through MD, and therefore methane harvesting offset a lower percentage of the cost. The cost offset by methane production was calculated using dissolved methane concentrations in the anaerobic membrane bioreactor, as well as methane concentrations in the biogas produced by the reactor [2]. Using the free energy of the reaction for methane combustion, a yearly kWh total was calculated (Table 5-20) [2]. These values represented an ideal case without losses or inefficiencies; therefore, in

practice the actual savings from methane recovery will likely be less. An accurate prediction of these losses and inefficiencies could not be made at this time. Overall, the 83% recovery scenario resulted in lower overall treatment costs (Table 5-20).

Table 5-20: Comparison of treatment costs between different FO recovery scenarios (Appendix C)

Process	67% Recovery		83% Recovery	
	Minimum	Maximum	Minimum	Maximum
Plant Pumping	$9,806	$48,576	$9,806	$48,576
MBR Pumping[h]	$35,470	$70,940	$18,905	$37,811
Aeration[i]	$135,720	$135,720	$44,109	$44,109
$MgCl_2$ Addition[j]	$146,526	$341,320	$182,742	$425,681
NaOH Addition[j]	$867	$1,007	$365	$424
Heating (MD, SHARON, ANAMMOX)	$16,195	$48,351	$15,749	$47,019
- Methane Recovery	-$14,328	-$14,328	-$8,023	-$8,023
- Struvite Recovery	-$8,066	-$8,066	-$4,668	-$4,668
Costs / year	$322,190	$598,304	$258,986	$566,408
Cost per influent MGD treated / year	$107,397	$236,488	$86,329	$224,068

[h] – Costs calculated using estimates from [95].

i – Costs calculated using estimates from [96].

j – Chemical prices from [94].

5.7.4.4 Cost Comparison

From the data provided by STMWRF, the average annual cost for the current treatment system is $96,290 per MGD treated per year [3]. A direct comparison to the

values generated using both the model and other methods suggested that the proposed design of the potable reuse system is on par or more expensive than the current system in use (Table 5-16). However, it should be noted that the proposed design is a combined potable and irrigation-quality reuse system. Whereas current systems at STMWRF are only producing a non-potable wastewater effluent, the proposed design produces almost exclusively clean water, with a small amount of non-potable effluent. Comparison to high end water reuse systems (such as reverse osmosis) clearly show the proposed design to be far cheaper, with costs exceeding $2,000,000 per MGD treated per year [98].

In addition to the reuse benefits of the proposed system, it is probable that the reported values are still an overestimate of the actual costs. As aeration in the SHARON reactor has to maintain a minimal DO concentration, it is likely the aeration costs would be lower than calculated (as they were based on normal bioreactor data). Furthermore, due to reverse solute flux, it is anticipated the chemical costs for magnesium chloride would be lower in practice. The values generated assumed that no magnesium would be present when the flow reached the struvite reactor; however, in operation it is unlikely additional magnesium would be required as this point, as the unit processes are neither consuming nor reacting with the magnesium in the system. There were additional cost concerns, however, that were not included in the cost analysis. The operational flexibility of the facility is lower than that of a traditional facility, which would require specially-trained operators. The capital costs of the proposed design would also be more expensive than a typical wastewater facility. As the proposed

processes require large reactors, the footprint of the proposed design was estimated to be 40% larger than STMWRF (when designed for the same influent flows). However, these comparisons with STMWRF are relatively inaccurate, as the proposed design includes potable reuse. A better comparison would be with other potable reuse facilities, which include processes including reverse osmosis and advanced oxidation. In such a case, it is expected that the proposed design would be competitive (data for this comparison could not be found). Despite these additional concerns, the data are extremely promising, showing that the proposed design could achieve reuse from a wastewater influent at costs that are similar to current wastewater treatment costs.

Chapter 6 Conclusions and Further Research

With increasing concerns over the quantity and quality of the nation's water supplies, the concepts of non-potable and potable water reuse are becoming increasingly more important. The ability to use non-potable wastewater effluents for landscaping and irrigation offers the potential to significantly reduce the demand for freshwater in urban centers. Potable water reuse offers the ability for areas with severe water limitations to regenerate water supplies. However, both forms of reuse face obstacles. Currently, the non-potable reuse system used at STMWRF is unable to maintain a high quality effluent. Looking to the future, typical high quality potable treatment systems (such as RO or advanced oxidation) are expensive to operate. This study sought to address both the present and potential issues facing water reuse.

The first phase of the study examined the effluent water quality from STMWRF. In order to reduce algae blooms in the adjoining Huffaker Hills Reservoir, nutrient discharges from the system needed to be reduced. Using computer simulations to assess the operation of the oxidation ditches at the facility, it was determined that modifying the aeration cycles would be the cheapest and most effective method to reduce nutrient concentrations in the plant effluent. Two new aeration alternatives were proposed, with the "optimized" aeration alternative reducing effluent mass discharges of ammonium, orthophosphate, and nitrate + nitrite by 32%, 14%, and 48%, respectively. The "+20%" aeration alternative targeted ammonium specifically, reducing effluent mass discharges of ammonium by 69%, while slightly increasing discharges of

orthophosphate and nitrate + nitrite. As nitrogen was determined to be the limiting nutrient in algal growth, the proposed "+20%" aeration cycle may be the best choice for STMWRF, as it had the greatest reduction in nitrogen discharges. Washoe County engineers have discussed an effluent ammonium goal of 2 mg NH_4^+-N/L, and an effluent total nitrogen goal of 5 to 7 mg N/L [3]. Implementation of the +20% aeration cycle would meet this criteria.

It is recommended that the research and monitoring into STMWRF's effluent quality continues. As the model has proposed potential new aeration cycles for the facility, the next step would be to implement these new cycles and test the effluent quality to confirm the predicted results. Furthermore, if nutrient concentrations are reduced as predicted by the model, Huffaker Hills Reservoir could then be observed to determine if the nutrient reductions had the intended effect of reducing algal populations. Additional testing and refinement of the model could continue, until the model has been further calibrated and reached a suitable level of accuracy. Further suggested refinements include optimizing the model seasonally, as the time of year affects process performance and influent wastewater constituency. The model could also be optimized throughout the day to maintain treatment quality while reducing energy costs, based on fluctuations in energy costs throughout the day. However, additional data would be required to make these refinements. After all refinements had been completed, the model could be turned over to facility operators and Washoe County engineers to be used to assist in operation of the treatment plant.

The second phase of the study examined the feasibility of replacing a facility (such as STMWRF) with a potable water reuse system. By integrating forward osmosis, membrane distillation, an anaerobic membrane bioreactor, SHARON and ANAMMOX, and struvite precipitation, the proposed system design was able to operate at nearly the same operating cost as STMWRF. Operating costs were projected to be within the range of $86,000 - $236,000 per MGD treated per year, whereas STMWRF operates at $96,000 per MGD treated per year. The system is more likely to fall on the lower end of the spectrum, as the high end values assumed that the resource recovery systems were functioning at much lower capacities than expected. It is important to note that the proposed system combines both a water treatment facility and a wastewater treatment facility into one design, yet operates at the cost of only one facility. In addition, between 67% - 83% of influent wastewater would be discharged as clean, potable water. The remaining water would be recycled back to the influent, with a small percentage discharged as a non-potable effluent. This non-potable effluent was found to have similar water quality to the current effluent at STMWRF.

As the proposed design returned promising data (low cost and high treatment levels), it is suggested that further research be conducted to confirm the results of the model. Particular attention should be paid to the heating estimations, as the calculations used may underestimate the true cost of the heated unit processes in the proposed design. The construction and testing of a pilot-scale system would be ideal, to ensure the compatibility of the many unit processes, particularly the FO preconcentration step. The pilot-scale system could be located onsite at STMWRF to

allow direct comparison between the two non-potable effluents. Additionally, membrane distillation and forward osmosis should be tested to ensure the production of potable water is without complications. Any additional data to confirm the results of the project would further the possibility of the technology being adopted on a large-scale, and bring about a new future of affordable and sustainable water reuse.

References

1. Randall, C. W., Barnard, L.B., and Stensel, H.D., *Design and Retrofit of Wastewater Treatment Plants for Biological Nutrient Removal*. Technomic Publishing Inc.: Lancaster, PA, 1992.

2. Metcalf, Eddy, *Wastewater Engineering: Treatment and Reuse*. McGraw Hill: New York, NY, 2004; Vol. 4th Edition.

3. Warner, R., Hulett, John, STMWRF Operating Data. Nikkel, C., Ed. Washoe County: Reno, 2013.

4. Rittmann, B. E., McCarty, P.L., *Environmental Biotechnology: Principals and Applications*. McGraw-Hill: New York, NY, 2001.

5. Ho, T. Q., A., The Elemental Composition of Some Marine Phytoplankton. *Journal of Phycology* 2003, *39* (6), 1145-1159.

6. Rhee, G. Y., Gotha, I.J., Optimum N:P Ratios and Coexistence of Planktonic Algae. *Journal of Phycology* 1980, *16* (4), 518-30.

7. Paasche, E., Effect of Ammonium and Nitrate on Growth, Photosynthesis, and Ribulosediphosphate Carboxylase Content on Dunaleilla tertiolecta. *Physiology of Plants* 1971, *25*, 294-99.

8. Raschke, R. L., Algal Periodicity and Waste Reclamation in a Stabilization Pond Ecosystem. *Water Pollution Control Federation* 1970, *42* (4), 518-30.

9. Cath, T. Y.; Childress, A. E.; Elimelech, M., Forward osmosis: Principles, applications, and recent developments. *Journal of Membrane Science* 2006, *281* (1-2), 70-87.

10. Zhao, S.; Zou, L.; Mulcahy, D., Effects of membrane orientation on process performance in forward osmosis applications. *Journal of Membrane Science* 2011, *382* (1-2), 308-315.

11. Shi, L.; Chou, S. R.; Wang, R.; Fang, W. X.; Tang, C. Y.; Fane, A. G., Effect of substrate structure on the performance of thin-film composite forward osmosis hollow fiber membranes. *Journal of Membrane Science* 2011, *382* (1-2), 116-123.

12. Yangali-Quintanilla, V.; Li, Z.; Valladares, R.; Li, Q.; Amy, G., Indirect desalination of Red Sea water with forward osmosis and low pressure reverse osmosis for water reuse. *Desalination* 2011, *280* (1-3), 160-166.

13. Hancock, N. T.; Xu, P.; Heil, D. M.; Bellona, C.; Cath, T. Y., Comprehensive Bench- and Pilot-Scale Investigation of Trace Organic Compounds Rejection by Forward Osmosis. *Environ. Sci. Technol.* 2011, *45* (19), 8483-8490.

14. Zhao, S.; Zou, L., Relating solution physicochemical properties to internal concentration polarization in forward osmosis. *Journal of Membrane Science* 2011, *379* (1-2), 459-467.

15. Zhao, S.; Zou, L., Effects of working temperature on separation performance, membrane scaling and cleaning in forward osmosis desalination. *Desalination* 2011, *278* (1-3), 157-164.

16. Zhang, F.; Brastad, K. S.; He, Z., Integrating Forward Osmosis into Microbial Fuel Cells for Wastewater Treatment, Water Extraction and Bioelectricity Generation. *Environ. Sci. Technol.* 2011, *45* (15), 6690-6696.

17. Xiao, D. Z.; Tang, C. Y. Y.; Zhang, J. S.; Lay, W. C. L.; Wang, R.; Fane, A. G., Modeling salt accumulation in osmotic membrane bioreactors: Implications for FO membrane selection and system operation. *Journal of Membrane Science* 2011, *366* (1-2), 314-324.

18. Achilli, A.; Cath, T. Y.; Childress, A. E., Selection of inorganic-based draw solutions for forward osmosis applications. *Journal of Membrane Science* 2010, *364* (1-2), 233-241.

19. Cath, T. Y.; Hancock, N. T.; Lundin, C. D.; Hoppe-Jones, C.; Drewes, J. r. E., A multi-barrier osmotic dilution process for simultaneous desalination and purification of impaired water. *Journal of Membrane Science* 2010, *362* (1-2), 417-426.

20. Phillip, W. A.; Yong, J. S.; Elimelech, M., Reverse Draw Solute Permeation in Forward Osmosis: Modeling and Experiments. *Environ. Sci. Technol.* 2010, *44* (13), 5170-5176.

21. Wang, R.; Shi, L.; Tang, C. Y. Y.; Chou, S. R.; Qiu, C.; Fane, A. G., Characterization of novel forward osmosis hollow fiber membranes. *Journal of Membrane Science* 2010, *355* (1-2), 158-167.

22. Yip, N. Y.; Tiraferri, A.; Phillip, W. A.; Schiffman, J. D.; Elimelech, M., High Performance Thin-Film Composite Forward Osmosis Membrane. *Environ. Sci. Technol.* 2010, *44* (10), 3812-3818.

23. Tang, C. Y.; She, Q.; Lay, W. C. L.; Wang, R.; Fane, A. G., Coupled effects of internal concentration polarization and fouling on flux behavior of forward osmosis membranes during humic acid filtration. *Journal of Membrane Science* 2010, *354* (1-2), 123-133.

24. Xu, Y.; Peng, X.; Tang, C. Y.; Fu, Q. S.; Nie, S., Effect of draw solution concentration and operating conditions on forward osmosis and pressure retarded osmosis performance in a spiral wound module. *Journal of Membrane Science* 2010, *348* (1-2), 298-309.

25. Hancock, N. T.; Cath, T. Y., Solute Coupled Diffusion in Osmotically Driven Membrane Processes. *Environ. Sci. Technol.* 2009, *43* (17), 6769-6775.

26. Achilli, A.; Cath, T. Y.; Marchand, E. A.; Childress, A. E., The forward osmosis membrane bioreactor: A low fouling alternative to MBR processes. *Desalination* 2009, *239* (1-3), 10-21.

27. Cornelissen, E. R.; Harmsen, D.; de Korte, K. F.; Ruiken, C. J.; Qin, J.-J.; Oo, H.; Wessels, L. P., Membrane fouling and process performance of forward osmosis membranes on activated sludge. *Journal of Membrane Science* 2008, *319* (1-2), 158-168.

28. Holloway, R. W.; Childress, A. E.; Dennett, K. E.; Cath, T. Y., Forward osmosis for concentration of anaerobic digester centrate. *Water Research* 2007, *41* (17), 4005-4014.

29. Lay, W. C. L.; Zhang, Q.; Zhang, J.; McDougald, D.; Tang, C.; Wang, R.; Liu, Y.; Fane, A. G., Study of integration of forward osmosis and biological process: Membrane performance under elevated salt environment. *Desalination* 2011, *283* (0), 123-130.

30. Cartinella, J. L.; Cath, T. Y.; Flynn, M. T.; Miller, G. C.; Hunter, K. W.; Childress, A. E., Removal of natural steroid hormones from wastewater using membrane contactor processes. *Environ. Sci. Technol.* 2006, *40* (23), 7381-7386.

31. Lutchmiah, K.; Cornelissen, E. R.; Harmsen, D. J. H.; Post, J. W.; Lampi, K.; Ramaekers, H.; Rietveld, L. C.; Roest, K., Water recovery from sewage using forward osmosis. *Water Sci. Technol.* 2011, *64* (7), 1443-1449.

32. Bowden, K. S.; Achilli, A.; Childress, A. E., Organic ionic salt draw solutions for osmotic membrane bioreactors. University of Nevada, Reno: 2012.

33. Wang, K. Y.; Teoh, M. M.; Nugroho, A.; Chung, T.-S., Integrated forward osmosis-membrane distillation (FO-MD) hybrid system for the concentration of protein solutions. *Chemical Engineering Science* 2011, *66* (11), 2421-2430.

34. Fang, H.; Gao, J. F.; Wang, H. T.; Chen, C. S., Hydrophobic porous alumina hollow fiber for water desalination via membrane distillation process. *Journal of Membrane Science* 2012, *403-404* (0), 41-46.

35. Tun, C. M.; Groth, A. M., Sustainable integrated membrane contactor process for water reclamation, sodium sulfate salt and energy recovery from industrial effluent. *Desalination* 2011, *283* (0), 187-192.

36. Prince, J. A.; Singh, G.; Rana, D.; Matsuura, T.; Anbharasi, V.; Shanmugasundaram, T. S., Preparation and characterization of highly hydrophobic poly(vinylidene fluoride) - Clay nanocomposite nanofiber membranes (PVDF-clay NNMs) for desalination using direct contact membrane distillation. *Journal of Membrane Science* 2012, *397-398* (0), 80-86.

37. Dumee, L.; Germain, V.; Sears, K.; Schatz, J.; Finn, N.; Duke, M.; Cerneaux, S.; Cornu, D.; Gray, S., Enhanced durability and hydrophobicity of carbon nanotube bucky paper membranes in membrane distillation. *Journal of Membrane Science* 2011, *376* (1-2), 241-246.

38. Dumee, L.; Campbell, J. L.; Sears, K.; Schatz, J.; Finn, N.; Duke, M.; Gray, S., The impact of hydrophobic coating on the performance of carbon nanotube bucky-paper membranes in membrane distillation. *Desalination* 2011, *283* (0), 64-67.

39. Zhang, J.; Dow, N.; Duke, M.; Ostarcevic, E.; Li, J.-D.; Gray, S., Identification of material and physical features of membrane distillation membranes for high performance desalination. *Journal of Membrane Science* 2010, *349* (1-2), 295-303.

40. Singh, D.; Sirkar, K. K., Desalination of brine and produced water by direct contact membrane distillation at high temperatures and pressures. *Journal of Membrane Science* 2012, *389* (0), 380-388.

41. Zhang, J.; Gray, S.; Li, J.-D., Modelling heat and mass transfers in DCMD using compressible membranes. *Journal of Membrane Science* 2012, *387-388* (0), 7-16.

42. Yang, X.; Wang, R.; Fane, A. G., Novel designs for improving the performance of hollow fiber membrane distillation modules. *Journal of Membrane Science* 2011, *384* (1-2), 52-62.

43. Teoh, M. M.; Bonyadi, S.; Chung, T.-S., Investigation of different hollow fiber module designs for flux enhancement in the membrane distillation process. *Journal of Membrane Science* 2008, *311* (1-2), 371-379.

44. Yarlagadda, S.; Gude, V. G.; Camacho, L. M.; Pinappu, S.; Deng, S., Potable water recovery from As, U, and F contaminated ground waters by direct contact membrane distillation process. *Journal of Hazardous Materials* 2011, *192* (3), 1388-1394.

45. Gryta, M.; Barancewicz, M., Influence of morphology of PVDF capillary membranes on the performance of direct contact membrane distillation. *Journal of Membrane Science* 2010, *358* (1-2), 158-167.

46. Khayet, M.; Matsuura, T., Chapter 10 - Direct Contact Membrane Distillation. In *Membrane Distillation*, Elsevier: Amsterdam, 2011; pp 249-293.

47. Teoh, M. M.; Chung, T.-S., Membrane distillation with hydrophobic macrovoid-free PVDF-PTFE hollow fiber membranes. *Separation and Purification Technology* 2009, *66* (2), 229-236.

48. Hou, D.; Wang, J.; Qu, D.; Luan, Z.; Ren, X., Fabrication and characterization of hydrophobic PVDF hollow fiber membranes for desalination through direct contact membrane distillation. *Separation and Purification Technology* 2009, *69* (1), 78-86.

49. Hwang, H. J.; He, K.; Gray, S.; Zhang, J.; Moon, I. S., Direct contact membrane distillation (DCMD): Experimental study on the commercial PTFE membrane and modeling. *Journal of Membrane Science* 2011, *371* (1-2), 90-98.

50. He, K.; Hwang, H. J.; Woo, M. W.; Moon, I. S., Production of drinking water from saline water by direct contact membrane distillation (DCMD). *Journal of Industrial and Engineering Chemistry* 2011, *17* (1), 41-48.

51. Cath, T. Y.; Adams, V. D.; Childress, A. E., Experimental study of desalination using direct contact membrane distillation: a new approach to flux enhancement. *Journal of Membrane Science* 2004, *228* (1), 5-16.

52. Song, L.; Ma, Z.; Liao, X.; Kosaraju, P. B.; Irish, J. R.; Sirkar, K. K., Pilot plant studies of novel membranes and devices for direct contact membrane distillation-based desalination. *Journal of Membrane Science* 2008, *323* (2), 257-270.

53. Lew, B.; Tarre, S.; Beliavski, M.; Dosoretz, C.; Green, M., Anaerobic membrane bioreactor (AnMBR) for domestic wastewater treatment. *Desalination* 2009, *243* (1-3), 251-257.

54. Saddoud, A.; Ellouze, M.; Dhouib, A.; Sayadi, S., Anaerobic membrane bioreactor treatment of domestic wastewater in Tunisia. *Desalination* 2007, *207* (1-3), 205-215.

55. Herrera-Robledo, M.; Morgan-Sagastume, J. M.; Noyola, A., Biofouling and pollutant removal during long-term operation of an anaerobic membrane bioreactor treating municipal wastewater. *Biofouling* 2009, *26* (1), 23-30.

56. Anderson, G. K.; Kasapgil, B.; Ince, O., Microbial kinetics of a membrane anaerobic reactor system. *Environ. Technol.* 1996, *17* (5), 449-464.

57. Huang, Z.; Ong, S. L.; Ng, H. Y., Submerged anaerobic membrane bioreactor for low-strength wastewater treatment: Effect of HRT and SRT on treatment performance and membrane fouling. *Water Research* 2011, *45* (2), 705-713.

58. Hu, A. Y.; Stuckey, D. C., Treatment of dilute wastewaters using a novel submerged anaerobic membrane bioreactor. *J. Environ. Eng.-ASCE* 2006, *132* (2), 190-198.

59. An, Y.; Wang, Z. W.; Wu, Z. C.; Yang, D. H.; Zhou, Q., Characterization of membrane foulants in an anaerobic non-woven fabric membrane bioreactor for municipal wastewater treatment. *Chem. Eng. J.* 2009, *155* (3), 709-715.

60. Gao, W. J.; Leung, K. T.; Qin, W. S.; Liao, B. Q., Effects of temperature and temperature shock on the performance and microbial community structure of a submerged anaerobic membrane bioreactor. *Bioresour. Technol.* 2011, *102* (19), 8733-8740.

61. Lin, H. J.; Chen, J. R.; Wang, F. Y.; Ding, L. X.; Hong, H. C., Feasibility evaluation of submerged anaerobic membrane bioreactor for municipal secondary wastewater treatment. *Desalination* 2011, *280* (1-3), 120-126.

62. Martin-Garcia, I.; Monsalvo, V.; Pidou, M.; Le-Clech, P.; Judd, S. J.; McAdam, E. J.; Jefferson, B., Impact of membrane configuration on fouling in anaerobic membrane bioreactors. *Journal of Membrane Science* 2011, *382* (1-2), 41-49.

63. Liao, B. Q.; Kraemer, J. T.; Bagley, D. M., Anaerobic membrane bioreactors: Applications and research directions. *Crit. Rev. Environ. Sci. Technol.* 2006, *36* (6), 489-530.

64. Van Hulle, S. W. H.; Vandeweyer, H. J. P.; Meesschaert, B. D.; Vanrolleghem, P. A.; Dejans, P.; Dumoulin, A., Engineering aspects and practical application of autotrophic nitrogen removal from nitrogen rich streams. *Chem. Eng. J.* 2010, *162* (1), 1-20.

65. Gala, A.; Dosta, J.; van Loosdrecht, M. C. M.; Mata-Alvarez, J., Two ways to achieve an anammox influent from real reject water treatment at lab-scale: Partial SBR nitrification and SHARON process. *Process Biochemistry* 2007, *42* (4), 715-720.

66. Blackburne, R.; Yuan, Z. G.; Keller, J., Partial nitrification to nitrite using low dissolved oxygen concentration as the main selection factor. *Biodegradation* 2008, *19* (2), 303-312.

67. Van Hulle, S. W. H.; Volcke, E. I. P.; Teruel, J. L.; Donckels, B.; van Loosdrecht, M. C. M.; Vanrolleghem, P. A., Influence of temperature and pH on the kinetics of the Sharon nitritation process. *J. Chem. Technol. Biotechnol.* 2007, *82* (5), 471-480.

68. Gali, A.; Dosta, J.; Mace, S.; Mata-Alvarez, J., Comparison of reject water treatment with nitrification/denitrification via nitrite in SBR and SHARON chemostat process. *Environ. Technol.* 2007, *28* (2), 173-176.

69. Paredes, D.; Kuschk, P.; Mbwette, T. S. A.; Stange, F.; Muller, R. A.; Koser, H., New aspects of microbial nitrogen transformations in the context of wastewater treatment - A review. *Eng. Life Sci.* 2007, *7* (1), 13-25.

70. Yang, J.; Zhang, L.; Hira, D.; Fukuzaki, Y.; Furukawa, K., High-rate nitrogen removal by the Anammox process at ambient temperature. *Bioresour. Technol.* 2011, *102* (2), 672-676.

71. Yang, J.; Zhang, L.; Fukuzaki, Y.; Hira, D.; Furukawa, K., High-rate nitrogen removal by the Anammox process with a sufficient inorganic carbon source. *Bioresour. Technol.* 2010, *101* (24), 9471-9478.

72. Cho, S.; Takahashi, Y.; Fujii, N.; Yamada, Y.; Satoh, H.; Okabe, S., Nitrogen removal performance and microbial community analysis of an anaerobic up-flow granular bed anammox reactor. *Chemosphere* 2010, *78* (9), 1129-1135.

73. Terada, A.; Zhou, S.; Hosomi, M., Presence and detection of anaerobic ammonium-oxidizing (anammox) bacteria and appraisal of anammox process for high-strength nitrogenous wastewater treatment: a review. *Clean Technol. Environ. Policy* 2011, *13* (6), 759-781.

74. Tang, C.-J.; Zheng, P.; Wang, C.-H.; Mahmood, Q.; Zhang, J.-Q.; Chen, X.-G.; Zhang, L.; Chen, J.-W., Performance of high-loaded ANAMMOX UASB reactors containing granular sludge. *Water Research* 2011, *45* (1), 135-144.

75. Isaka, K.; Sumino, T.; Tsuneda, S., High nitrogen removal performance at moderately low temperature utilizing anaerobic ammonium oxidation reactions. *Journal of Bioscience and Bioengineering* 2007, *103* (5), 486-490.

76. Liu, Y.; Kwag, J.-H.; Kim, J.-H.; Ra, C., Recovery of nitrogen and phosphorus by struvite crystallization from swine wastewater. *Desalination* 2011, *277* (1-3), 364-369.

77. Song, Y.-H.; Qiu, G.-L.; Yuan, P.; Cui, X.-Y.; Peng, J.-F.; Zeng, P.; Duan, L.; Xiang, L.-C.; Qian, F., Nutrients removal and recovery from anaerobically digested swine wastewater by struvite crystallization without chemical additions. *Journal of Hazardous Materials* 2011, *190* (1-3), 140-149.

78. Moerman, W.; Carballa, M.; Vandekerckhove, A.; Derycke, D.; Verstraete, W., Phosphate removal in agro-industry: Pilot- and full-scale operational considerations of struvite crystallization. *Water Research* 2009, *43* (7), 1887-1892.

79. Suzuki, K.; Tanaka, Y.; Kuroda, K.; Hanajima, D.; Fukumoto, Y.; Yasuda, T.; Waki, M., Removal and recovery of phosphorous from swine wastewater by demonstration crystallization reactor and struvite accumulation device. *Bioresour. Technol.* 2007, *98* (8), 1573-1578.

80. Ben Moussa, S.; Tlili, M. M.; Batis, N.; Ben Amor, M., Influence of temperature on struvite precipitation by CO(2)-deagassing method. *Cryst. Res. Technol.* 2011, *46* (3), 255-260.

81. Rahman, M. M.; Liu, Y.; Kwag, J.-H.; Ra, C., Recovery of struvite from animal wastewater and its nutrient leaching loss in soil. *Journal of Hazardous Materials* 2011, *186* (2-3), 2026-2030.

82. Korchef, A.; Saidou, H.; Amor, M. B., Phosphate recovery through struvite precipitation by CO2 removal: Effect of magnesium, phosphate and ammonium concentrations. *Journal of Hazardous Materials* 2011, *186* (1), 602-613.

83. Kim, D.; Ryu, H.-D.; Kim, M.-S.; Kim, J.; Lee, S.-I., Enhancing struvite precipitation potential for ammonium nitrogen removal in municipal landfill leachate. *Journal of Hazardous Materials* 2007, *146* (1-2), 81-85.

84. Huang, H.; Xu, C.; Zhang, W., Removal of nutrients from piggery wastewater using struvite precipitation and pyrogenation technology. *Bioresour. Technol.* 2011, *102* (3), 2523-2528.

85. Uysal, A.; Yilmazel, Y. D.; Demirer, G. N., The determination of fertilizer quality of the formed struvite from effluent of a sewage sludge anaerobic digester. *Journal of Hazardous Materials* 2010, *181* (1-3), 248-254.

86. Kim, D.; Kim, J.; Ryu, H.-D.; Lee, S.-I., Effect of mixing on spontaneous struvite precipitation from semiconductor wastewater. *Bioresour. Technol.* 2009, *100* (1), 74-78.

87. Lew, B.; Phalah, S.; Sheindorf, C.; Kummel, M.; Rebhun, M.; Lahav, O., Favorable Operating Conditions for Obtaining High-Value Struvite Product from Sludge Dewatering Filtrate. *Environ. Eng. Sci.* 2010, *27* (9), 733-741.

88. Gadekar, S.; Pullammanappallil, P., Validation and Applications of a Chemical Equilibrium Model for Struvite Precipitation. *Environ. Model. Assess.* 2009, *15* (3), 201-209.

89. Marta, N.; Pastor, L.; Bouzas, A.; Ferrer, J.; Seco, A., Phosphorus recovery by struvite crystallization in WWTPs: Influence of the sludge treatment line operation. *Water Research* 2010, *44* (7), 2371-2379.

90. Pastor, L.; Mangin, D.; Ferrer, J.; Seco, A., Struvite formation from the supernatants of an anaerobic digestion pilot plant. *Bioresour. Technol.* 2010, *101* (1), 118-125.

91. Kannan, S. K.; Krishnamoorthy, R., Isolation of mercury resistant bacteria and influence of abiotic factors on bioavailability of mercury - A case study in Pulicat Lake North of Chennai, South East India. *Science of the Total Environment* 2006, *367* (1), 341-353.

92. *Standard Methods for the Examination of Water and Wastewater*. American Public Health Association: Washington, DC, 1998; Vol. 20 Edition.

93. Herrera, N. Analysis of Centrate Composition and Evaluation of its Applicability as a Nutrient Supplement to Irrigation Water. University of Nevada, Reno, 2009.

94. Alibaba Global Trading. www.alibaba.com (accessed June 6, 2012).

95. Gallagher, P., Tragellis, S., Taking it to the next level: Advanced membrane filtration for water reuse applications. *Water Environment & Technology* August 2009, pp 41-49.

96. Bell, K., Sciandra, J., Wagner, K., Aerate for Less. *Water Environment & Technology* May 2010, pp 42-45.

97. Cengel, Y., Boles, M., *Thermodynamics: An Engineering Approach*. Seventh Edition ed.; McGraw Hill: New York, NY, 2010; Vol. 7th Edition.

98. Kajenthira, A.; Siddiqi, A.; Anadon, L. D., A new case for promoting wastewater reuse in Saudi Arabia: Bringing energy into the water equation. *Journal of Environmental Management 102* (0), 184-192.

Appendix A

Influent and Effluent Data at STMWRF

	Influent First Set			Influent Second Set			Effluent First Set			Effluent Second Set		
	Ortho-P	Ammonia	Nitrate	Ortho-P	Ammonia	Nitrate	Ortho-P	Ammonia	Nitrate	Ortho-P	Ammonia	Nitrate
12:00 AM	1.97	11.00	0.16	2.29	18.30	0.00	1.37	5.83	0.00	5.67	7.42	0.00
1:00 AM	2.55	9.70	0.08	2.13	19.20	0.00	3.72	7.71	0.00	7.68	7.06	0.00
2:00 AM	*2.69*	*6.84*	*0.04*	2.15	18.40	0.00	5.92	7.52	0.00	8.55	8.23	0.00
3:00 AM	2.83	3.98	0.00	1.94	13.80	0.15	5.75	6.86	0.00	7.94	7.98	0.00
4:00 AM	2.28	1.70	0.00	1.70	14.70	0.16	5.22	7.08	0.00	9.00	8.33	0.00
5:00 AM	1.90	10.80	0.02	1.75	12.70	0.09	6.47	7.09	0.00	3.66	7.47	0.00
6:00 AM	1.97	12.90	0.00	1.69	11.70	0.13	3.51	7.08	0.00	0.54	5.81	0.73
7:00 AM	2.02	8.95	0.14	2.28	14.40	0.21	0.77	5.18	0.39	0.20	3.41	2.37
8:00 AM	3.98	15.30	1.37	4.02	23.90	1.41	2.65	5.10	2.14	1.33	3.49	4.52
9:00 AM	3.49	17.40	0.14	3.96	26.60	0.20	0.70	4.74	1.72	1.00	3.04	5.47
10:00 AM	3.34	18.00	0.42	3.76	23.60	0.39	0.65	5.33	2.20	0.73	2.71	6.15
11:00 AM	2.96	13.80	0.28	3.02	18.10	0.42	0.62	5.11	2.43	0.62	3.11	6.08
12:00 PM	2.68	13.20	0.33	2.94	25.50	0.14	0.58	4.84	1.98	0.75	3.98	3.80
1:00 PM	2.35	9.09	0.55	2.83	25.30	0.00	0.63	6.05	0.33	1.49	5.13	1.44
2:00 PM	2.17	10.50	0.58	2.48	18.40	0.47	0.75	4.92	0.00	0.93	4.93	1.28
3:00 PM	1.94	10.80	0.72	2.40	17.80	0.45	0.50	4.68	0.38	0.63	4.47	1.78
4:00 PM	2.23	10.00	0.49	2.03	12.90	0.64	0.60	6.39	0.98	0.75	3.92	1.44
5:00 PM	2.55	12.80	0.46	2.37	17.70	0.97	0.51	4.62	0.60	1.19	4.63	0.29
6:00 PM	2.56	13.00	0.54	2.71	23.80	1.04	0.74	6.49	0.00	0.80	4.58	0.62
7:00 PM	2.55	10.60	2.65	2.53	18.60	1.03	0.63	4.82	0.00	0.53	3.52	0.90
8:00 PM	2.41	14.20	0.77	2.53	15.40	1.63	0.56	6.30	0.00	2.03	4.39	0.03
9:00 PM	2.16	11.70	0.33	1.93	13.20	0.69	3.11	5.74	0.00	4.20	5.71	0.00
10:00 PM	1.65	9.21	0.57	1.97	13.60	0.45	4.54	7.30	0.00	3.00	5.81	0.00
11:00 PM	2.07	14.50	0.12	2.39	18.20	0.22	2.87	6.47	0.00	3.08	6.31	0.00
Average =	2.47	11.25	0.45	2.49	18.16	0.45	2.22	5.97	0.55	2.76	5.23	1.54
St. Dev. =	0.55	3.73	0.57	0.66	4.52	0.46	2.06	1.02	0.85	2.87	1.77	2.08

	COD Testing			
	First Set		Second Set	
Time	Influent	Effluent	Influent	Effluent
8:30 AM	118	55	152	49
9:30 AM	63	39	156	45
10:30 AM	74	50	233	52
11:30 AM	86	57	160	49
12:30 PM	87	45	258	87
1:30 PM	82	46	199	53
2:30 PM	179	41	194	39
3:30 PM	150	42	184	47
4:30 PM	318	47	162	58
5:30 PM	236	42	216	57
6:30 PM	121	74	220	38
7:30 PM	147	42	269	40
8:30 PM	162	51	301	39
9:30 PM	120	40	224	37
10:30 PM	66	43	228	38
11:30 PM	133	64	258	50
12:30 AM	152	41	305	43
1:30 AM	172	47	179	36
2:30 AM	188	44	175	38
3:30 AM	203	45	158	36
4:30 AM	94	64	128	48
5:30 AM	104	40	135	36
6:30 AM	785	82	160	37
7:30 AM	433	48	224	44
AVG	178	49	203	46
STDEV	154	11	50	11

Appendix B

SCADA Data from STMWRF for Second Data Set

Time	Total INF flow rate (15 min average gpm)	Total INF Flow in MGD	Total net INF previous day MGD	Total net INF flow gpm	Ditch 1 air flow scfm	Ditch 1 Oper. Air Flow (scfm)	Ditch 1 DO east	Ditch 1 DO west	Ditch 2 air flow scfm	Ditch 2 Oper. Air Flow (scfm)	Ditch 2 DO east	Ditch 2 DO west	RAS comb. Recyc. previous day MGD	Clarifier 1 RAS return MGD	Clarifier 1 RAS return gpm	Clarifier 2 RAS return MGD	Clarifier 2 RAS return gpm	Clarifier 3 RAS return MGD	Clarifier 3 RAS return gpm	Clarifier 4 RAS return MGD	Clarifier 4 RAS return gpm	WAS total previous day mgd	WAS flow gpm
8:30 AM	2168	3.1	3.4	2470	1736	391	1.8	3.9	3291	411	5.9	4.1	1.7	0.38	293	0.37	288	0.61	426	0.38	305	Null	362.9849
9:30 AM	2967	4.3	3.4	1989	1676	377	1.3	3.9	3284	410	5.7	3.9	1.7	0.38	375	0.37	392	0.61	414	0.38	372	Null	359.9511
10:30 AM	3302	4.8	3.4	2367	1636	368	1.4	3.9	3149	394	5.7	3.9	1.7	0.38	329	0.37	331	0.61	426	0.38	321	Null	0
11:30 AM	3208	4.6	3.4	2852	1591	358	1.5	3.9	3073	384	5.6	4.0	1.7	0.38	334	0.37	331	0.61	420	0.38	331	Null	0
12:30 PM	3080	4.4	3.4	2844	0	0	0.1	3.9	0	0	3.9	3.9	1.7	0.38	305	0.37	305	0.61	417	0.38	300	Null	0
1:30 PM	2880	4.1	3.4	3243	0	0	0.1	3.9	0	0	3.9	3.9	1.7	0.38	288	0.37	303	0.61	420	0.38	288	Null	0
2:30 PM	2727	3.9	3.4	2344	1620	364	1.1	3.9	2856	357	5.2	3.9	1.7	0.38	284	0.37	272	0.61	426	0.38	284	Null	0
3:30 PM	2554	3.7	3.4	2401	1591	358	1.5	3.9	2856	357	5.4	3.9	1.7	0.38	252	0.37	243	0.61	423	0.38	266	Null	0
4:30 PM	2455	3.5	3.4	2111	0	0	0.1	3.9	0	0	3.9	3.9	1.7	0.38	249	0.37	243	0.61	419	0.38	254	Null	0
5:30 PM	2407	3.5	3.4	2453	1602	360	0.9	3.9	2768	346	5.0	3.9	1.7	0.38	248	0.37	243	0.61	427	0.38	254	Null	0
6:30 PM	2452	3.5	3.4	2020	1593	358	1.1	3.9	2829	354	5.1	3.9	1.7	0.38	246	0.37	243	0.61	423	0.38	263	Null	0
7:30 PM	2654	3.8	3.4	3026	1622	365	0.8	3.9	2930	366	4.9	3.9	1.7	0.38	270	0.37	267	0.61	413	0.38	279	Null	0
8:30 PM	2960	4.3	3.4	1238	0	0	0.1	3.9	3	0	3.9	3.9	1.7	0.38	284	0.37	295	0.61	408	0.38	281	Null	0
9:30 PM	3239	4.7	3.4	2487	1723	388	0.2	3.9	2952	369	4.1	3.9	1.7	0.38	312	0.37	317	0.61	415	0.38	318	Null	0
10:30 PM	3402	4.9	3.4	2615	1689	380	0.1	3.9	3073	384	4.1	3.9	1.7	0.38	342	0.37	345	0.61	430	0.38	333	Null	0
11:30 PM	3276	4.7	3.4	3010	1705	384	0.2	3.9	3104	388	4.2	3.9	1.7	0.38	327	0.37	345	0.61	427	0.38	322	Null	0
12:30 AM	2849	4.1	3.3	2169	0	0	0.1	3.9	3	0	3.9	3.9	1.7	0.38	290	0.37	279	0.61	425	0.37	282	Null	0
1:30 AM	2333	3.4	3.3	728	0	0	0.1	3.9	0	0	3.9	3.9	1.7	0.38	240	0.37	251	0.61	430	0.37	221	Null	0
2:30 AM	1910	2.8	3.3	1047	990	223	0.1	3.9	1178	147	4.0	3.9	1.7	0.38	210	0.37	191	0.61	423	0.37	189	Null	0
3:30 AM	1572	2.3	3.3	1135	0	0	0.1	3.9	0	0	3.9	3.9	1.7	0.38	158	0.37	162	0.61	423	0.37	159	Null	0
4:30 AM	1404	2.0	3.3	488	1012	228	0.2	3.9	1185	148	4.0	3.9	1.7	0.38	144	0.37	144	0.61	430	0.37	126	Null	0
5:30 AM	1326	1.9	3.3	1618	1842	414	1.3	3.9	3409	426	5.4	3.9	1.7	0.38	146	0.37	140	0.61	432	0.37	126	Null	0
6:30 AM	1327	1.9	3.3	1664	1821	410	1.8	3.9	3432	429	5.9	3.9	1.7	0.38	144	0.37	122	0.61	429	0.37	126	Null	0
7:30 AM	1610	2.3	3.3	1879	1781	401	1.8	3.9	3405	426	6.1	3.9	1.7	0.38	144	0.37	143	0.61	429	0.37	144	Null	0

Appendix C

Calculations for Yearly Costs of Proposed Design

	Model completed under 50% water recovery, final concentrations:							
		Outflow from struvite clarifier						
	Soluble PO4 - P		3.63	mg/L				
		Total P	3.63	mg/L				
	Nitrite + Nitrate		4.43	mg/L				
		Total N	12.6	mg/L				
	Bicarbonate		3.85	mg/L				
	Magnesium		32.3	mg/L				
		Calcium	79.4	mg/L				
	PO4-P (Sol. + Me Complex.)		3.62	mg/L				
		Nitrate N	0	mg/L				
		Nitrite N	4.42	mg/L				
	Ammonia N		6.66	mg/L				
		Total COD	31.93	mg/L				
		BOD5	2.28	mg/L				
		TKN	8.16	mg/L				
		Total P	3.63	mg/L				
		VSS	0.01	mg/L				
		TSS	0.05	mg/L				
	Magnesium Chloride =		150-300	$/ton	85-99% purity		From alibaba.com	
		Flow =	5,000	gallons/day				
			18,910	liters/day				
	Mg Concentration =		500	mg/L				
			9,455,000	mg/day				
			9,455	grams/day				
		$MgCl_2$ =	95.21	g/mol				
		Need:	389.0	moles of mg/day				
			37,038	g of $MgCl_2$ / day				
	1 metric ton =		1000	kg				
	@ 85% purity, $300 / ton =		44	kg/day				
			13.1	$/day				
	@99% purity, $150		37	kg/day				
			5.6	$/day				
	Yearly Costs -		4,771	$ (maximum)				
			2,048	$ (minimum)				

	Effluent Concentrations at 70% Recovery							
	Example Flow -		3	MGD				
	Water Recovery @ FO -		70	%				
	Flow to Solids Units -		0.9	MGD				
	Run 2 - Concentrations will increase more due to FO at 70% recovery							
		Flow	3	MGD				
		COD	1,000	mg COD / L				
		TKN	67	mg N / L				
		Total P	17	mg P / L				
		Nitrate	1	mg N/ L				
		pH	7.3					
		Alkalinity	9	mmol/L				
		Calcium	150	mg/L				
	Magnesium		50	mg/L				
		DO	0	mg/L				
Effluent Filtered COD			50	mg COD / L				
Influent Filtered COD (GFC)			345	mg COD / L				
	Influent FF COD		167	mg COD / L				
	Influent Acetate		33	mg COD / L				
	Influent Ammonia		67	mg N / L				
Influent Ortho-phosphate			13	mg P / L				
	Influent $CBOD_5$		493	mg O_2 / L				
Influent Filtered $CBOD_5$			210	mg O_2 / L				
		Total VSS	417	mg VSS / L				
		Total TSS	833	mg TSS / L				

	Effluent Concentrations at 70% Recovery (continued)							
	Model completed under 70% water recovery, final concentrations:							
		Outflow from struvite clarifier						
	Soluble PO4 - P		3.56	mg/L				
		Total P	3.58	mg/L				
	Nitrite + Nitrate		11.60	mg/L				
		Total N	23.0	mg/L				
	Bicarbonate		4.45	mg/L				
	Magnesium		20.28	mg/L				
		Calcium	25.4	mg/L				
PO4-P (Sol. + Me Complex.)			3.56	mg/L				
		Nitrate N	0	mg/L				
		Nitrite N	11.6	mg/L				
	Ammonia N		9.37	mg/L				
		Total COD	52.3	mg/L				
		BOD5	3.23	mg/L				
		TKN	11.36	mg/L				
		Total P	3.58	mg/L				
		VSS	0.02	mg/L				
		TSS	0.12	mg/L				
Magnesium Chloride =			150-300	$/ton	85-99% purity		From alibaba.com	
		Flow =	5,000	gallons/day				
			18,910	liters/day				
	Mg Concentration =		750	mg/L				
			1.42E+07	mg/day				
			14,183	grams/day				
		$MgCl_2$ =	95.21	g/mol				
		Need:	583.5	moles of mg/day				
			55,558	g of $MgCl_2$ / day				
	1 metric ton =		1000	kg				
@ 85% purity, $300 / ton =			65	kg/day				
			19.6	$/day				
	@99% purity, $150		56	kg/day				
			8.4	$/day				
	Yearly Costs -		7,157	$ (maximum)				
			3,073	$ (minimum)				

Dissolved Oxygen Requirements								
	@ 50% Water Recovery					1.41		
	DO in Sharon =		1	mg/L		9.99		
Total Oxygen Uptake Rate =			2.92	mg O/L/hr		1235.16	411.72	
Oxygen Transfer Efficiency =			0.42			8751.24	2917.08	
Total Oxygen Supply =			6.95	mg O/L/hr				
		Volume =	1.5	MG / day				
			1,500,000	gallons/day				
			5,670,000	liters/day				
			0.115873	mg O/L/min				
			657,000	mg O/min				
		Volume =	20,405	L O/min				
			721	ft^3 O/min				
			3,133	ft^3 of air/min		Maximum, likely ~50% lower		
		Use:	3,400	ft^3/min blower				
	Avg Power Draw:		89	kW				
Avg. Annual Power Consump.			780,000	kWh/yr				
Cost @ $ 0.10 / kWh -			78,000	$/yr		=		
	@ 70% Water Recovery							
	DO in Sharon =		0.27	mg/L				
Total Oxygen Uptake Rate =			3.43	mg O/L/hr				
Oxygen Transfer Efficiency =			0.43					
Total Oxygen Supply =			7.98	mg O/L/hr				
		Volume =	0.89	MG / day				
			890,000	gallons/day				
			3,364,200	liters/day				
			0.1329457	mg O/L/min				
			447,256	mg O/min				
		Volume =	13,891	L O/min				
			491	ft^3 O/min				
			2,133	ft^3 of air/min		Maximum		
		Use:	2,210	ft^3/min blower				
	Avg Power Draw:		57.85	kW		Linearly correlated		
Avg. Annual Power Consump.			507,000	kWh/yr				
Cost @ $ 0.10 / kWh -			50,700	$/yr		16900	= / 3	
		Page 42-45 WE&T May 2010						

	Calculating Effluent Chloride Concentrations							
			Mil Gal	ft^2				
		AnMBR =	5.3	17,712				
		Sharon =	1.5	8,020				
		Anammmox =	2.5	8,355				
		An. 2° =	1.5	15,280				
		Strv. Prec. =	0.25	3,342				
		Strv. 2° =	0.5	4,774				
		Total	11.55	57,483				
		@ 50% recovery, chloride levels						
		Flow in MGD		Split 50% of solids flow off				
	Influent	Solids L	Clean L	Outflow (WW)				
	3	1.5	1.5	0.75				
	3.75	1.875	1.875	0.9375				
	3.94	1.97	1.97	0.98				
	3.98	1.99	1.99	1.00				
	4.00	2.00	2.00	1.00				
	4.00	2.00	2.00	1.00				
	4.00	2.00	2.00	1.00				
	4.00	2.00	2.00	1.00				
	50% Recovery, 50% solids split, Chloride concentrations (no FO RS Flux)							
		Add (g Cl)	Split	Concentration (mg/L)				
		27,582	13,791	2				
		27,582	20,687	3				
		27,582	24,135	3				
		27,582	25,859	3				
		27,582	26,720	4				
		27,582	27,151	4				
		27,582	27,367	4				
		27,582	27,475	4				
		27,582	27,529	4				
		27,582	27,555	4				
		27,582	27,569	4				
		27,582	27,576	4				
		27,582	27,579	4				
		27,582	27,581	4				
		27,582	27,582	4				

	Calculating Effluent Chloride Concentrations (continued)							
	Reverse Salt Flux through FO Membrane							
	Flux:	2.7	L/m^2hr		Minimum			
		12.9	L/m^2hr		Maximum			
	Reverse Flux = 0.15 * Flux							
		0.41	g/m^2hr		Minimum			
		1.94	g/m^2hr		Maximum			
	Flow through membrane @ 50% Recovery (steady state)							
		2	MGD					
		2,000,000	gpd					
		7,560,000	liters per day					
		315,000	liters per hour					
		116,667	m^2 of membrane		Using minimum flux			
		24,419	m^2 of membrane		Using maximum flux			
		2,268,000	g Cl^- / day		Using min/max flux			
	50% Recovery, 50% solids split, Chloride concentrations (w/ FO RS Flux)							
		Add (g Cl)	Split	Concentration (mg/L)				
		2,295,582	1,147,791	152				
		2,295,582	1,721,687	228				
		2,295,582	2,008,635	266				
		2,295,582	2,152,109	285				
		2,295,582	2,223,845	294				
		2,295,582	2,259,714	299				
		2,295,582	2,277,648	301				
		2,295,582	2,286,615	302				
		2,295,582	2,291,099	303				
		2,295,582	2,293,341	303				
		2,295,582	2,294,462	304				
		2,295,582	2,295,022	304				
		2,295,582	2,295,302	304				
		2,295,582	2,295,442	304				
		2,295,582	2,295,512	304				

	Calculating Effluent Chloride Concentrations (continued)							
		50% Recovery						
		Flow in MGD		Split 25% of solids flow off				
	Influent	Solids L	Clean L	Outflow (WW)				
	3	1.5	1.5	0.38				
	4.13	2.0625	2.0625	0.52				
	4.55	2.27	2.27	0.57				
	4.71	2.35	2.35	0.59				
	4.76	2.38	2.38	0.60				
	4.79	2.39	2.39	0.60				
	4.79	2.40	2.40	0.60				
	4.80	2.40	2.40	0.60				
	Flow through membrane @ 50% Recovery (steady state)							
		2.4	MGD					
		2,400,000	gpd					
		9,072,000	liters per day					
		378,000	liters per hour					
		140,000	m^2 of membrane		Using minimum flux			
		29,302	m^2 of membrane		Using maximum flux			
		2,721,600	g Cl^- / day		Using min/max flux			
50% Recovery, 25% solids split, Chloride concentrations								
Add (g Cl)	Split	Conc (mg/L)			Add (g Cl)	Split	Conc (mg/L)	
2,749,182	2,061,887	227			2,749,182	8,185,551	902	
2,749,182	3,608,302	398			2,749,182	8,201,050	904	
2,749,182	4,768,113	526			2,749,182	8,212,674	905	
2,749,182	5,637,972	621			2,749,182	8,221,393	906	
2,749,182	6,290,366	693			2,749,182	8,227,931	907	
2,749,182	6,779,661	747			2,749,182	8,232,835	907	
2,749,182	7,146,633	788			2,749,182	8,236,513	908	
2,749,182	7,421,861	818			2,749,182	8,239,272	908	
2,749,182	7,628,283	841			2,749,182	8,241,341	908	
2,749,182	7,783,099	858			2,749,182	8,242,892	909	
2,749,182	7,899,211	871			2,749,182	8,244,056	909	
2,749,182	7,986,295	880			2,749,182	8,244,929	909	
2,749,182	8,051,608	888			2,749,182	8,245,583	909	
2,749,182	8,100,593	893			2,749,182	8,246,074	909	
2,749,182	8,137,332	897						
2,749,182	8,164,885	900						

Calculating Effluent Chloride Concentrations (continued)

	50% Recovery				
	Flow in MGD		Split 5% of solids flow off		
Influent	Solids L	Clean L	Outflow (WW)		
3	1.5	1.5	0.08		
4.43	2.2125	2.2125	0.11		
5.10	2.55	2.55	0.13		
5.42	2.71	2.71	0.14		
5.58	2.79	2.79	0.14		
5.65	2.82	2.82	0.14		
5.68	2.84	2.84	0.14		
5.70	2.85	2.85	0.14		
5.71	2.85	2.85	0.14		
5.71	2.86	2.86	0.14		

Flow through membrane @ 50% Recovery (steady state)

2.9	MGD		
2,860,000	gpd		
1.08E+07	liters per day		
450,450	liters per hour		
166,833	m^2 of membrane	Using minimum flux	
34,919	m^2 of membrane	Using maximum flux	
3,243,240	g Cl^- / day	Using min/max flux	

50% Recovery, 5% solids split, Chloride concentrations

Add (g Cl)	Split	Concentration (mg/L)
3,270,822	3.11E+06	287
3,270,822	6.06E+06	560
3,270,822	8.86E+06	820
3,270,822	1.15E+07	1,066
3,270,822	1.41E+07	1,300
3,270,822	1.65E+07	1,523
3,270,822	1.87E+07	1,734
3,270,822	2.09E+07	1,935
3,270,822	2.30E+07	2,126
3,270,822	2.49E+07	2,307
3,270,822	2.68E+07	2,479
…	…	…
3,270,822	6.21E+07	5,742

Calculating Effluent Chloride Concentrations (continued)

70% Recovery

	Flow in MGD		Split 50% of solids flow off
Influent	Solids L	Clean L	Outflow (WW)
3	0.9	2.1	0.45
3.45	1.04	2.42	0.52
3.52	1.06	2.46	0.53
3.53	1.06	2.47	0.53
3.53	1.06	2.47	0.53
3.53	1.06	2.47	0.53
3.53	1.06	2.47	0.53
3.53	1.06	2.47	0.53

Flow through membrane @ 70% Recovery (steady state)

2.47	MGD	
2,470,000	gpd	
9.34E+06	liters per day	
389,025	liters per hour	
144,083	m^2 of membrane	Using minimum flux
30,157	m^2 of membrane	Using maximum flux
2,800,980	g Cl^- / day	Using min/max flux

70% Recovery, 50% solids split, Chloride concentrations

Add (g Cl)	Split	Concentration (mg/L)
2,828,562	1,414,281	187
2,828,562	2,121,422	281
2,828,562	2,474,992	327
2,828,562	2,651,777	351
2,828,562	2,740,170	362
2,828,562	2,784,366	368
2,828,562	2,806,464	371
2,828,562	2,817,513	373
2,828,562	2,823,038	373
2,828,562	2,825,800	374
2,828,562	2,827,181	374
2,828,562	2,827,872	374
2,828,562	2,828,217	374
2,828,562	2,828,390	374
2,828,562	2,828,476	374

	Calculating Effluent Chloride Concentrations (continued)							
		70% Recovery						
		Flow in MGD		Split 25% of solids flow off				
	Influent	Solids L	Clean L	Outflow (WW)				
	3	0.9	2.1	0.23				
	3.68	1.10	2.57	0.28				
	3.83	1.15	2.68	0.29				
	3.86	1.16	2.70	0.29				
	3.87	1.16	2.71	0.29				
	3.87	1.16	2.71	0.29				
	3.87	1.16	2.71	0.29				
	3.87	1.16	2.71	0.29				
	Flow through membrane @ 70% Recovery (steady state)							
		2.71	MGD					
		2,710,000	gpd					
		1.02E+07	liters per day					
		426,825	liters per hour					
		158,083	m^2 of membrane		Using minimum flux			
		33,087	m^2 of membrane		Using maximum flux			
		3,073,140	g Cl^- / day		Using min/max flux			
	70% Recovery, 25% solids split, Chloride concentrations							
Add (g Cl)	Split	Conc (mg/L)		Add (g Cl)	Split	Concentration (mg/L)		
3,100,722	2,325,542	530		3,100,722	9,232,243	2,106		
3,100,722	4,069,698	928		3,100,722	9,249,724	2,109		
3,100,722	5,377,815	1,226		3,100,722	9,262,835	2,112		
3,100,722	6,358,903	1,450		3,100,722	9,272,668	2,115		
3,100,722	7,094,719	1,618		3,100,722	9,280,043	2,116		
3,100,722	7,646,581	1,744		3,100,722	9,285,574	2,118		
3,100,722	8,060,478	1,838		3,100,722	9,289,722	2,119		
3,100,722	8,370,900	1,909		3,100,722	9,292,834	2,119		
3,100,722	8,603,717	1,962		3,100,722	9,295,167	2,120		
3,100,722	8,778,330	2,002		3,100,722	9,296,917	2,120		
3,100,722	8,909,289	2,032		3,100,722	9,298,230	2,121		
3,100,722	9,007,509	2,054		3,100,722	9,299,214	2,121		
3,100,722	9,081,173	2,071		3,100,722	9,299,952	2,121		
3,100,722	9,136,422	2,084						
3,100,722	9,177,858	2,093						
3,100,722	9,208,935	2,100						

	Calculating Effluent Chloride Concentrations (continued)							
		70% Recovery						
		Flow in MGD		Split 5% of solids flow off				
	Influent	Solids L	Clean L	Outflow (WW)				
	3	0.9	2.1	0.05				
	3.86	1.16	2.70	0.06				
	4.10	1.23	2.87	0.06				
	4.17	1.25	2.92	0.06				
	4.19	1.26	2.93	0.06				
	4.19	1.26	2.94	0.06				
	4.20	1.26	2.94	0.06				
	4.20	1.26	2.94	0.06				
	4.20	1.26	2.94	0.06				
	4.20	1.26	2.94	0.06				
	Flow through membrane @ 70% Recovery (steady state)							
		2.94	MGD					
		2,940,000	gpd					
		1.11E+07	liters per day					
		463,050	liters per hour					
		171,500	m^2 of membrane		Using minimum flux			
		35,895	m^2 of membrane		Using maximum flux			
		3,333,960	g Cl^- / day		Using min/max flux			
		70% Recovery, 5% solids split, Chloride concentrations						
			Add (g Cl)	Split	Concentration (mg/L)			
			3,361,542	3.19E+06	671			
			3,361,542	6.23E+06	1,307			
			3,361,542	9.11E+06	1,913			
			3,361,542	1.18E+07	2,487			
			3,361,542	1.44E+07	3,034			
			3,361,542	1.69E+07	3,552			
			3,361,542	1.93E+07	4,045			
			3,361,542	2.15E+07	4,514			
			3,361,542	2.36E+07	4,958			
			3,361,542	2.56E+07	5,381			
			3,361,542	2.75E+07	5,782			
			…	…	…			
			3,361,542	6.39E+07	13,409			

	Estimation of Pumping Costs						
	24 Hour Pumping						
			Size [in]	24	30	36	42	48
			Length [ft]	1,000	1,000	1,000	1,000	1,000
			Cost [$/ft] (1987)	102	123	158	200	217
			Cost [$/ft] (2010)	178	215	277	351	381
			Total Pipe Cost [$]	1.78E+05	2.15E+05	2.77E+05	3.51E+05	3.81E+05
			Annual Pipe Cost over 25 years [$]	10,827	13,043	16,811	21,282	23,115
			Roughness [C]	120	120	120	120	120
			Total H_L [ft]	160	153	151	151	150
			Required [PSI]	69	67	66	65	65
			Pump Station Costs [$]	807,022	786,339	780,143	777,856	776,878
			Annual Pump Station Cost (25 years) [$]	48,986	47,731	47,355	47,216	47,156
			WHP	70	67	66	66	66
			Efficiency	77%	77%	77%	77%	77%
			MHP Req.	91	87	86	86	85
			Power [kW]	68	65	64	64	64
			Power Cost [$/kWhr]	0.1	0.1	0.1	0.1	0.1
			Power Cost [$/day] 24 hours	163	156	154	153	153
			Power Cost [$/year] 24 hour Pumping	59,515	56,990	56,233	55,954	55,835
			Yearly Operating Cost 24 hour [$]	108,501	104,721	103,588	103,170	102,991
			Minimum Annual Pumping	14,952	12,426	11,670	11,391	11,271
			Maximum Annual Pumping	59,515	56,990	56,233	55,954	55,835

	Aeration							
	@ 50% Water Recovery							
	DO in Sharon =		1	mg/L				
	Total Oxygen Uptake Rate =		4.44	mg O/L/hr				
	Oxygen Transfer Efficiency =		0.4					
	Total Oxygen Supply =		11.10	mg O/L/hr				
		Volume =	1.87	MG / day				
			1,870,000	gallons/day				
			7,068,600	liters/day				
			0.19	mg O/L/min				
			1,307,691	mg O/min				
		Volume =	40,614	L O/min				
			1434	ft^3 O/min				
			6,235	ft^3 of air/min		Maximum, likely ~50% lower		
		Use:	3,400	ft^3/min blower x2				
	Avg Power Draw:		178	kW				
	Avg. Annual Power Consump.		1,560,000	kWh/yr				
	Cost @ $ 0.10 / kWh -		156,000	$/yr		=		
	@ 70% Water Recovery							
	DO in Sharon =		0.5	mg/L				
	Total Oxygen Uptake Rate =		2.73	mg O/L/hr				
	Oxygen Transfer Efficiency =		0.47					
	Total Oxygen Supply =		5.81	mg O/L/hr				
		Volume =	1	MG / day				
			1,000,000	gallons/day				
			3,780,000	liters/day				
			0.096809	mg O/L/min				
			365,936	mg O/min				
		Volume =	11,365	L O/min				
			401	ft^3 O/min				
			1,745	ft^3 of air/min		Maximum		
		Use:	2,210	ft^3/min blower				
	Avg Power Draw:		57.85	kW		Linearly correlated		
	Avg. Annual Power Consump.		507,000	kWh/yr				
	Cost @ $ 0.10 / kWh -		50,700	$/yr		16900	= / 3	
		Page 42-45 WE&T May 2010						

	Magnesium Addition						
	Magnesium Addition - Assume reverse salt flux insufficient for struvite prec.						
		Amount of $MgCl_2$ added for DS = amount of $MgCl_2$ lost to RSF					
	@50% Water Recovery						
			2,268,000	g of Cl^- per day			
			63,972	moles of Cl^- per day			
			31,986	moles of $MgCl_2$ per day			
			3,045,420	g of $MgCl_2$ per day			
			1.11E+09	g $MgCl_2$ per year			
	Magnesium Chloride =		150-300	$/ton	85-99% purity	From alibaba.com	
			3,045,420	g of $MgCl_2$ / day			
	1 metric ton =		1000	kg			
	@ 85% purity, $300 / ton =		3,583	kg/day			
			1074.9	$/day			
	@99% purity, $150		3,076	kg/day			
			461.4	$/day			
	Yearly Costs -		392,322	$ (maximum)			
			168,421	$ (minimum)			

	Magnesium Addition (continued)							
	Magnesium Addition - Assume reverse salt flux insufficient for struvite prec.							
		Amount of $MgCl_2$ added for DS = amount of $MgCl_2$ lost to RSF						
	@70% Water Recovery							
			2,828,562	g of Cl^- per day				
			79,783	moles of Cl^- per day				
			39,892	moles of $MgCl_2$ per day				
			3,798,131	g of $MgCl_2$ per day				
			1.39E+09	g $MgCl_2$ per year				
	Magnesium Chloride =		150-300	$/ton	85-99% purity		From alibaba.com	
			3,798,131	g of $MgCl_2$ / day				
	1 metric ton =		1000	kg				
	@ 85% purity, $300 / ton =		4,468	kg/day				
			1340.5	$/day				
	@99% purity, $150		3,836	kg/day				
			575.5	$/day				
	Yearly Costs -		489,289	$ (maximum)				
			210,048	$ (minimum)				

		50% Recovery - Strong Base Addition - NaOH						
	Sodium Hydroxide -		320 - 360	$/metric ton				
		Flow =	5,000	gallons/day				
			18,910	liters/day				
	Strong Base Conc =		190	meq/L				
			190	mg/L				
			3,592,900	mg/day				
			3,593	g/day				
		NaOH =	40.0	g/mol				
		Need :	211.3	moles of NaOH a day				
			8,452	g of NaOH / day				
	1 metric ton =		1000	kg				
	@ 96% purity, $360 / ton =		8.8	kg / day				
			3.2	$ / day				
	@99% purity, $320/ ton =		8.5	kg / day				
			2.7	$ / day				
	Yearly Costs -		1157	$ (maximum)				
			997	$ (minimum)				

		50% Recovery - Strong Base Addition - NaOH						
	Sodium Hydroxide -		320 - 360	$/metric ton				
		Flow =	5,000	gallons/day				
			18,910	liters/day				
	Strong Base Conc =		80	meq/L				
			80	mg/L				
			1,512,800	mg/day				
			1,513	g/day				
		NaOH =	40.0	g/mol				
		Need :	89.0	moles of NaOH a day				
			3,559	g of NaOH / day				
	1 metric ton =		1000	kg				
	@ 96% purity, $360 / ton =		3.7	kg / day				
			1.3	$ / day				
	@99% purity, $320/ ton =		3.6	kg / day				
			1.2	$ / day				
	Yearly Costs -		487	$ (maximum)				
			420	$ (minimum)				

	50% Recovery - Heating:							
		H20 (l) -	4.18	J / g K		Specific Heat Capacity		
	For Sharon Process							
		Volume =	1.87	MG / day				
			1,870,000	gallons				
			7,068,600	liters				
			7,069	kg				
	Initial WW Temp -		20	C°				
	Final Temp -		35	C°				
			4.43E+08	Joules / day				
			5,130	J/sec = watts				
			5.13	KW				
	For MD Process							
		Volume =	1.97	MG / day				
			1970000	gallons				
			7446600	liters				
			7446.6	kg				
	Initial WW Temp -		20	C°				
	Final Temp -		60	C°				
			1.25E+09	Joules / day				
			14,411	J/sec = watts				
			14.41	KW				
	For Anammox Process							
		Volume =	1.87	MG / day				
			1,870,000	gallons				
			7,068,600	liters				
			7,069	kg				
	Initial WW Temp -		20	C°				
	Final Temp -		25	C°				
			1.48E+08	Joules / day				
			1,710	J/sec = watts				
			1.71	KW				
	Maximums calculated using 55% efficiency							

	70% Recovery - Heating:							
		H20 (l) -	4.18	J / g K		Specific Heat Capacity		
	For Sharon Process							
		Volume =	1	MG / day				
			1,000,000	gallons				
			3,780,000	liters				
			3,780	kg				
	Initial WW Temp -		20	C°				
	Final Temp -		30	C°				
			1.58E+08	Joules / day				
			1,829	J/sec = watts				
			1.83	KW				
	For MD Process							
		Volume =	2.45	MG / day				
			2450000	gallons				
			9261000	liters				
			9261	kg				
	Initial WW Temp -		20	C°				
	Final Temp -		60	C°				
			1.55E+09	Joules / day				
			17,922	J/sec = watts				
			17.92	KW				
	For Anammox Process							
		Volume =	1	MG / day				
			1,000,000	gallons				
			3,780,000	liters				
			3,780	kg				
	Initial WW Temp -		20	C°				
	Final Temp -		25	C°				
			7.90E+07	Joules / day				
			914	J/sec = watts				
			0.91	KW				
	Maximums calculated using 55% efficiency							

	Methane - at 50% recovery							
	Methane in AnMBR -			1.5	mg/L			
	Gibbs Free Energy							
		ΔG = G(products) - G(reactants)						
		CH_4 (g) + $2O_2$ (g) -> CO_2 (g) + $2H_2O$						
		CH_4 =	-50.74	kJ/mol				
		O_2 =	0	kJ/mol				
		CO_2 =	-394.37	kJ/mol				
		H_2O =	-237.18	kJ/mol				
		ΔG =	-817.99	kJ/mol CH_4		(exothermic)		
		Flow =	1.97	MGD				
			1,970,000	gallons				
			7,446,600	liters				
			1.12E+07	mg of methane /day				
			11,170	g of methane /day				
	1 mol methane =		18	g				
			620.6	mol of methane /day				
			507,604	kJ/day				
			5,875	watts				
			5.9	KW		At 100% efficiency		
	Including off-gas flow rate:							
	In AnMBR -		4.95	ft^3/min				
	Estimated % Methane -		65%		Metcalf & Eddy			
			3.2	ft^3/min				
			546	moles of CH_4 /day				
			446,710	kJ/day				
			1.29E+04	watts				
			12.9	KW				

	Methane - at 70% recovery							
	Methane in AnMBR -			1.04	mg/L			
	Gibbs Free Energy							
		ΔG = G(products) - G(reactants)						
		CH_4 (g) + $2O_2$ (g) -> CO_2 (g) + $2H_2O$						
		CH_4 =	-50.74	kJ/mol				
		O_2 =	0	kJ/mol				
		CO_2 =	-394.37	kJ/mol				
		H_2O =	-237.18	kJ/mol				
		ΔG =	-817.99	kJ/mol CH_4		(exothermic)		
		Flow =	1.05	MGD				
			1,050,000	gallons				
			3,969,000	liters				
			4.13E+06	mg of methane /day				
			4,128	g of methane /day				
	1 mol methane =		18	g				
			229.3	mol of methane /day				
			187,581	kJ/day				
			2,171	watts				
			2.2	KW		At 100% efficiency		
	Including off-gas flow rate:							
	In AnMBR -		3.2	ft^3/min				
	Estimated % Methane -		65%		Metcalf & Eddy			
			2.1	ft^3/min				
			353	moles of CH_4 /day				
			288,782	kJ/day				
			8.36E+03	watts				
			8.4	KW				

	50% Recovery - Estimated Struvite Recovery							
	Initial Phosphate Conc -		6.12	mg P / L	Assume all PO_4 losses to struvite			
	Final Phosphate Conc -		1.56	mg P / L				
		Change -	4.56	mg P / L				
			0.00456	g P / L				
		1 mol P =	1 mol Struvite ($MgPO_4NH_4*6H_2O$)					
		P =	1.47E-04	mol/L	Same molar conc. as struvite			
		Struvite =	244	g/mol				
			0.036	g/L				
		Volume =	1.87	MG / day				
			1,870,000	gallons				
			7,068,600	liters				
			254	kg struvite/day				
			84.6	kg struvite produced / MG treated each day				
	70% Recovery - Estimated Struvite Recovery							
	Initial Phosphate Conc -		6.81	mg P / L	Assume all PO_4 losses to struvite			
	Final Phosphate Conc -		1.86	mg P / L				
		Change -	4.95	mg P / L				
			0.00495	g P / L				
		1 mol P =	1 mol Struvite ($MgPO_4NH_4*6H_2O$)					
		P =	1.60E-04	mol/L	Same molar conc. as struvite			
		Struvite =	244	g/mol				
			0.039	g/L				
		Volume =	1	MG / day				
			1,000,000	gallons				
			3,780,000	liters				
			147	kg struvite/day				
			49.1	kg struvite produced / MG treated each day				

MBR Power Usage @ 50% Water Recovery								
Surface Water Treatment -			0.15	kWh/m^3		Minimum		
			0.3	kWh/m^3		Maximum		
		Flow =	1.97	MGD				
			1,970,000	gallons				
			7,446,600	liters				
			7,447	m^3/day				
			407,701	kWh/yr		Minimum		
			815,403	kWh/yr		Maximum		
Cost @ $ 0.10 / kWh -			40,770	$/yr		Minimum		
			81,540	$/yr		Maximum		
MBR Power Usage @ 70% Water Recovery								
Surface Water Treatment -			0.15	kWh/m^3		Minimum		
			0.3	kWh/m^3		Maximum		
		Flow =	1.05	MGD				
			1,050,000	gallons				
			3,969,000	liters				
			3,969	m^3/day				
			217,303	kWh/yr		Minimum		
			434,606	kWh/yr		Maximum		
Cost @ $ 0.10 / kWh -			21,730	$/yr		Minimum		
			43,461	$/yr		Maximum		
		From WE&T pg 42 August 2009						

Summation of Costs - Yearly							
		50% Recovery			70% Recovery		
		Min.	Max.		Min.	Max.	
+	Pipe Costs	10,827	23,115		10,827	23,115	
+	Pump Infrastructure	256,672	254,853		256,672	254,853	
+	Plant Pumping	11,271	55,834		11,271	55,834	
+	MBR Pumping	40,770	81,540		21,730	43,461	
+	Aeration	156,000	156,000		50,700	50,700	
+	$MgCl_2$ Addition	168,421	392,322		210,048	489,289	
+	NaOH Addition	997	1,157		420	487	
+	Heating	18,615	48,351		18,102	47,019	
-	Methane Recovery	16,469	16,469		9,222	9,222	
-	Struvite Recovery	9,271	9,271		5,366	5,366	
	Costs / year	370,334	709,464		297,685	672,203	
	Costs / year per MGD	123,445	236,488		99,228	224,068	
	Assumptions						
	0.1 per kg for struvite						
	Does not include non-pumping infrastructure						
	Does not include mixing						